

**PONTIFICIA UNIVERSIDAD**

**CATÓLICA DEL PERÚ**

**Escuela de Posgrado**



**Prediction of failure of sands under constant volume  
general cyclic simple shear loading using specific  
dissipated energy**

Tesis para obtener el grado académico  
de Doctor en Ingeniería que presenta:

***Guillermo José Zavala Rosell***

Asesor:

***Rafael Aguilar Vélez***

Co-asesor:

***Miguel Ángel Pando López***


Lima, 2023

## Informe de Similitud

Yo, **Rafael Aguilar Vélez**, docente de la Escuela de Posgrado de la Pontificia Universidad Católica del Perú, asesor de la tesis titulada **Prediction of failure of sands under constant volume general cyclic simple shear loading using specific dissipated energy**, del autor Guillermo José Zavala Rosell, dejo constancia de lo siguiente:

- El mencionado documento tiene un índice de puntuación de similitud de 19%. Así lo consigna el reporte de similitud emitido por el software *Turnitin* el 16-01-2023. Este reporte se realizó considerando el retiro de las referencias a trabajos del mismo autor y las fuentes que tenían resúmenes de los artículos y el resultado muestra que todas las citas refieren trabajos con menos del 1% de similitud.
- He revisado con detalle dicho reporte y la Tesis y no se advierte indicios de plagio.
- Las citas a otros autores y sus respectivas referencias cumplen con las pautas académicas.

Lima, 17 de enero de 2023.

Apellidos y nombres del asesor / de la asesora: <b>Aguilar Vélez, Rafael</b>	
DNI: 40591707	Firma
ORCID: <b>0000-0002-8175-8950</b>	

## ACKNOWLEDGEMENTS

I would like to thank my advisors, Prof. Rafael Aguilar, from Pontificia Universidad Católica del Perú, and Prof. Miguel Pando, from Drexel University, for all the guidance and supervision given during the period this endeavor lasted. Their advice has been invaluable in the development of this thesis work and the journal articles.

I would like to thank Dr. Youngjin Park, for his support and advice during experimental program at University of North Carolina at Charlotte, and the graduate students who gave me advice and support at UNC Charlotte.

I would like to express my gratitude to the Pontificia Universidad Católica del Peru, for the funding provided to spend a sabbatical year and two summer periods at UNC Charlotte performing most of the experimental tests required for this research.

I would like to express my gratitude to the CEE department of UNC Charlotte, and Prof. Miguel Pando, for providing office space and access to the testing and computing facilities during my visiting scholar periods.

I would like to thank Miguel, Sandra, Diego, Maya, Pachi and Luna, for making me feel at home while I was away from home in Charlotte for more than a year.

I would like to thank my colleagues at Pontificia Universidad Católica del Peru who have encouraged me to pursue this degree, particularly Prof. Jorge Zegarra, who first encouraged me to pursue graduate studies over 20 years ago and has continued to do so extensively, always helping me to get the support I needed from the university.

I would like to thank my parents, sister, nieces, extended family and friends who have encouraged and given me support to pursue my doctoral degree, particularly Dennys and Alejandro, for their support in the final stages of this work.

## ABSTRACT

Seismic soil liquefaction is a recurring phenomenon that may cause significant damage to infrastructure during earthquakes and that in turn may also cause injuries and even fatalities. This phenomenon has been widely studied by researchers, and for its study the laboratory characterization of behavior of sands when subjected to cyclic loading is very important. One of the approaches for this kind of studies is through the calculation of the energy that is dissipated by the soil when it is subjected to cyclic loading. One of the hypotheses for utilizing these energy methods states that the cumulative dissipated energy required in a soil to reach failure only depends on the initial state of the sample (relative density and initial vertical effective stress) and should be reasonably constant and independent of the loading amplitude and waveform applied to the sample. This thesis work seeks to evaluate the validity of this hypothesis. Also, based on this hypothesis, it seeks to develop a simplified methodology to predict failure of sands when subjected to general cyclic loading, performing only simple harmonic tests. The hypothesis for the development of this methodology is that there is a relationship between the initial state of the sample and the cumulative dissipated energy to failure in cyclic simple shear test. To reach these goals, over 250 uniform and non-uniform constant volume cyclic simple shear tests were performed on Ottawa 20/30 sand, and the dissipated energy to failure was measured in each of these tests. The experimental program showed that the measured cumulative dissipated energy to failure was reasonably constant for the same initial sample conditions, but with some variability inherent to geotechnical laboratory testing. As expected, the cumulative dissipated energy increased with increasing initial stress level and relative density. Also, a simplified method to predict the dissipated energy to failure of a sample subjected to general cyclic loading, based on a multivariable regression performed on a simplified set of laboratory results, is presented, and it is next validated with two independent data sets. In both cases the method was found to yield reasonable predictions of failure of sands when subjected to complex and irregular cyclic shear loading.

## RESUMEN

La licuefacción sísmica del suelo es un fenómeno recurrente que puede causar daños significativos a la infraestructura durante los terremotos, y que también puede causar lesiones e incluso muertes. Este fenómeno ha sido ampliamente estudiado por los investigadores, y para su estudio es muy importante la caracterización del comportamiento de las arenas en el laboratorio, cuando se someten a esfuerzos cíclicos. Este tipo de estudios se pueden realizar calculando la energía disipada por el suelo cuando éste es sometido a cargas cíclicas. Una de las hipótesis para utilizar estos métodos de energía establece que la energía disipada acumulada requerida para alcanzar la falla en un suelo solo depende del estado inicial de la muestra (densidad relativa y esfuerzo efectivo vertical inicial) y que debe ser razonablemente constante e independiente de la carga, amplitud y forma de onda aplicada a la muestra. Este trabajo de tesis busca evaluar la validez de esta hipótesis. Asimismo, con base en esta hipótesis, se busca desarrollar una metodología simplificada para predecir la falla de arenas cuando se someten a cargas cíclicas generales, realizando únicamente ensayos armónicos simples. La hipótesis para el desarrollo de esta metodología es que existe una relación entre el estado inicial de la muestra y la energía disipada acumulada hasta la falla en el ensayo cíclico de corte simple. Para alcanzar estos objetivos, se realizaron más de 250 ensayos de corte simple cíclico a volumen constante, uniformes y no uniformes, en arena Ottawa 20/30, y se midió la energía disipada hasta la falla en cada uno de estos ensayos. El programa experimental mostró que la energía disipada acumulada medida hasta la falla fue razonablemente constante para las mismas condiciones iniciales de la muestra, pero con cierta variabilidad inherente a las pruebas geotécnicas de laboratorio. Como se esperaba, la energía disipada acumulada aumentó con el aumento del nivel de esfuerzo inicial y la densidad relativa. Además, se presenta un método simplificado para predecir la energía disipada hasta la falla de una muestra sujeta a carga cíclica general, basado en una regresión multivariable realizada en un juego simplificado de resultados de laboratorio, y luego se valida con dos juegos de datos independientes. En ambos casos, se encontró que el método proporcionaba predicciones razonables de falla de arenas cuando se sometían a cargas cíclicas de corte irregulares y complejas.

# Table of Contents

<b>ACKNOWLEDGEMENTS</b>	<b>ii</b>
<b>ABSTRACT</b>	<b>iii</b>
<b>RESUMEN</b>	<b>iv</b>
<b>1. Introduction</b>	<b>1</b>
1.1. General Introduction	1
1.2. Problem Statement	2
1.3. Research Objectives	3
1.4. Thesis Structure and published articles	4
1.4.1. Thesis Structure	4
1.4.2. List of published articles	4
<b>2. Theoretical framework</b>	<b>5</b>
2.1. Soil liquefaction	5
2.2. Cyclic simple shear tests	8
2.2.1. Representation of an irregular load by an equivalent sinusoidal load	8
2.2.2. Palmgren-Miner cumulative damage hypothesis	10
2.2.3. Dissipated Energy Approach	18
2.2.4. Constant volume testing	21
<b>3. Experimental Methodology</b>	<b>23</b>
3.1. Equipment	23
3.2. Materials	27
3.3. Testing program	28
3.4. Sample preparation	30
3.5. Testing Procedures	34
3.6. Test results and analysis	37
<b>4. Manuscript #1: Specific Dissipated Energy as a Failure Predictor for Uniform Sands under Constant Volume Cyclic Simple Shear Loading</b>	<b>47</b>
4.1. Introduction	47
4.2. Background and literature review	48
4.3. Experimental program	51
4.3.1. Test sand	52
4.3.2. Cyclic simple shear testing program	54
4.4. Results	56
<b>5. Manuscript #2: A simplified method for predicting failure of sands under general cyclic simple shear loading</b>	<b>65</b>
5.1. Introduction	65
5.2. The Proposed Simplified Method	70
5.3. Application of the simplified method to two experimental datasets	71
5.3.1. Application of simplified method to the first experimental dataset	72
5.3.2. Application of simplified method to the Lasley (2015) experimental dataset	82
5.3.3. Summary of comparison between simplified method and whole dataset predictions	86
<b>6. Summary, conclusions and recommendations for future work</b>	<b>87</b>
6.1. Summary of findings	87
6.2. Manuscript #1 conclusions	88
6.3. Manuscript #2 conclusions	89
6.4. Recommendations for further studies	91
<b>References</b>	<b>93</b>
<b>Appendix: Influence of irregular loading and frequency on the cumulative damage and dissipated energy of dry loose sand under cyclic simple shear</b>	<b>96</b>

## List of Figures

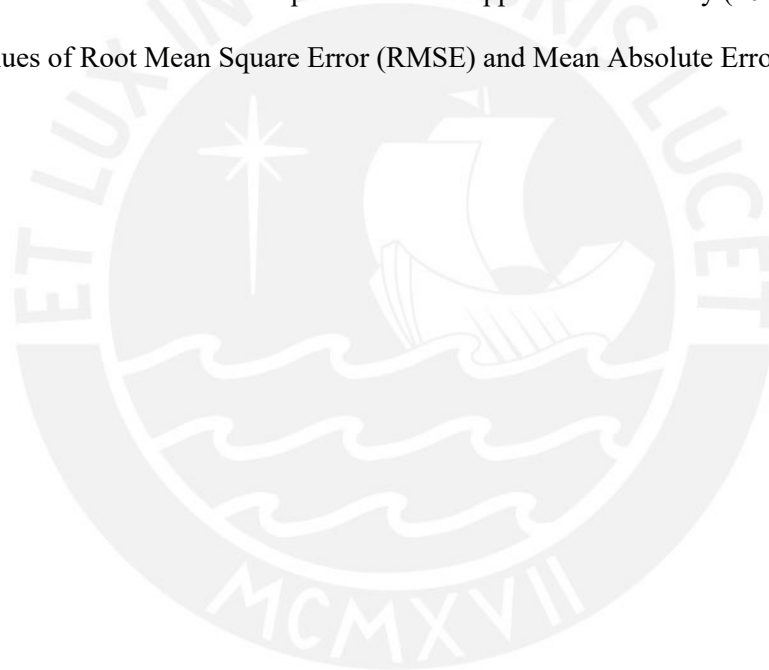
Figure 2-1. Schematic graph showing a cyclic resistance curve indicating the number of cycles to failure corresponding to two values of CSRs .....	12
Figure 2-2: Cumulative damage against number of cycles assuming linearly proportional damage....	13
Figure 2-3: Schematic showing progression of damage due to non-uniform loading (a) Non-uniform stress-time history and (b) Progression of damage due to applied stress time history shown in (a). .....	14
Figure 2-4. Sequence of steps used by Seed et al. (1975) to normalize cyclic stress ratio – $N_{liq}$ curve. Step1: designate the cyclic stress ratio required to induce liquefaction as $CSR_1$ ; Step2: normalize ordinates values by dividing cyclic stress ratio by $CSR_1$ ; Step3: apply safety factor to $CSR_1$ (divide $CSR_1$ by a safety factor) and determine the number of cycles required to induce liquefaction ( $N_{ref}$ ) corresponding to the normalized peak amplitude ( $\alpha$ ) of uniform cyclic load; and step4: normalize abscissa as $N_{ref}/N_{liq}$ (adapted from Green and Terri, 2005).....	15
Figure 2-5. Cumulative damage and equivalent cycle concepts (adapted from Annaki & Lee, 1977).	17
Figure 2-6: Example of dissipated energy calculations for different cycles of an individual CSS test (a) Cycles 1 and 2; (b) Cycles 31 to 34; (c) to (f) Cycles 1, 31, 32 and 34 with area defined to calculate dissipated energy .....	20
Figure 2-7. Liquefaction resistance of Ottawa sand in constant volume and undrained simple shear (adapted from Finn and Vaid, 1977) .....	22
Figure 3-1: General View of ADVDCSS System .....	24
Figure 3-2: Sample box used for shear tests in the ADVDCSS .....	25
Figure 3-3: Data Acquisition boxes: From top to bottom: Bender Element controller, DCS and LVDT signal conditioner .....	25
Figure 3-4: Cell pressure controller and back pressure controller.....	26
Figure 3-5: Microscope photographs of Ottawa 20/30 sand used in this study .....	27
Figure 3-6: Grain size distribution of Ottawa 20/30 sand used in this study .....	28
Figure 3-7: Graphical representation of dynamic load patterns used in this study (a) Uniform; (b) Non-uniform Type 1 (varying CSR); (c) Non-uniform Type 2 (varying frequency); (d) Non-uniform Type 3 (varying frequency and CSR); and (e) Non-uniform Type 4 (Spike load).....	29
Figure 3-8: Sample preparation procedure for loose samples: (a) Placement of pipe, (b) Placement of sand, (c) Sand in place, (d) Sand in sample box after pulling pipe out, (e) Placement of calibrated cylinder, (f) Measurement of sand height.....	31
Figure 3-9: Sample preparation procedure for dense samples: (a) Materials used to prepare the sample, (b) Initial assembly of sample box, (c) Final assembly of sample box, (d) Beaker with sand, (e) Placement of sand in sample box using the beaker, (f) Finished sample .....	32
Figure 3-10: Sample preparation procedure for very dense samples: (a) Sample box, tamper and sand split in 3 parts, (b) First layer of sand placed, (c) Compaction of first layer, (d) Compaction of second layer, (e) Finished sample with calibrated cylinder, (f) Measurement of sample height .....	33
Figure 3-11: Sample box pedestal in ADVDCSS machine: (a) Placing and start of bolt installation, (b) Bolts being tightened with Allen wrench .....	34
Figure 3-12: Application of seating load on a sand sample: (a) Top cap is lowered to the edge of the rings to check alignment, (b) Top cap is lowered until it touches the surface of the sample, (c) Ring guides are removed, (d) Membrane and O-ring are put in their place for testing. ....	35
Figure 3-13: Tested sample after failure.....	37
Figure 3-14: Results of Uniform Constant Volume CSS Test in Loose Sand, $\sigma'_{vo} = 100$ kPa, CSR = 0.05 .....	39
Figure 3-15: Results of Uniform Constant Volume CSS Test in Dense Sand, $\sigma'_{vo} = 200$ kPa, CSR = 0.065 .....	39
Figure 3-16: Results of Uniform Constant Volume CSS Test in Very Dense Sand, $\sigma'_{vo} = 100$ kPa, CSR = 0.05 .....	40
Figure 3-17: Results of Uniform Constant Volume CSS Test in Loose Sand, $\sigma'_{vo} = 200$ kPa, CSR = 0.09 .....	40

Figure 3-18: Results of Uniform Constant Volume CSS Test in Dense Sand, $\sigma'_{vo} = 200$ kPa, CSR = 0.1	41
Figure 3-19: Results of Uniform Constant Volume CSS Test in Very Dense Sand, $\sigma'_{vo} = 400$ kPa, CSR = 0.12	41
Figure 3-20: Cyclic resistance curve for loose sand with $\sigma'_{vo} = 100$ kPa	43
Figure 3-21: Cyclic resistance curve for loose sand with $\sigma'_{vo} = 200$ kPa	43
Figure 3-22: Cyclic resistance curve for loose sand with $\sigma'_{vo} = 400$ kPa	44
Figure 3-23: Cyclic resistance curve for dense sand with $\sigma'_{vo} = 100$ kPa	44
Figure 3-24: Cyclic resistance curve for dense sand with $\sigma'_{vo} = 200$ kPa	45
Figure 3-25: Cyclic resistance curve for dense sand with $\sigma'_{vo} = 400$ kPa	45
Figure 4-1. Example of Different Stress-Strain Load Cycles from a Representative CSS Test from the Present Study: (a) Stress-Strain Cycles 1 and 2, (b) Stress-Strain Cycles 31 to 34, (c) Hysteresis Loop Used in the Dissipated Energy Calculation for Cycle 1, (d) Hysteresis Loop Used in the Dissipated Energy Calculation for Cycle 31, (e) Hysteresis Loop Used in the Dissipated Energy Calculation for Cycle 32, (f) Hysteresis Loop Used in the Dissipated Energy Calculation for Cycle 34	50
Figure 4-2. General View of ADVDCSS System	52
Figure 4-3: Results of Uniform Constant Volume CSS Test in Very Dense Sand, $\sigma'_{vo} = 200$ kPa, CSR = 0.08, $f = 0.1$ Hz: (a) Norm. Effective Vert. Stress (NEVS) vs Normalized Shear Stress, (b) Shear Strain (%) vs Normalized Shear Stress, (c) $1 - \text{NEVS}$ vs number of cycles, (d) Shear Strain (%) vs Number of Cycles	57
Figure 4-4. Specif. diss. energy to failure - Loose sand. (a) $\sigma'_{vo} = 100$ kPa, (b) $\sigma'_{vo} = 200$ kPa, and (c) $\sigma'_{vo} = 400$ kPa	61
Figure 4-5. Specif. diss. energy to failure – Very dense sand. (a) $\sigma'_{vo} = 100$ kPa, (b) $\sigma'_{vo} = 200$ kPa, (c) $\sigma'_{vo} = 400$ kPa	62
Figure 4-6. Variation of the Mean Specific Dissipated Energy to Failure as a Function of (a) Initial Vertical Effective Stress ( $\sigma'_{vo}$ ), and (b) Average Initial Relative Density ( $D_r$ )	64
Figure 5-1. (a) Schematic CSS test setup; (b) Sinusoidal load cycles and dissipated energy in the $i^{\text{th}}$ load cycle in a CV stress-controlled CSS test	67
Figure 5-2. Flow chart depicting the proposed simplified method	70
Figure 5-3. 3D mesh plot showing the regression obtained using the selected reduced dataset from Zavala et al. (2022)	74
Figure 5-4. Comparison of the multivariable regression using the simplified method with the full dataset of 258 values of normalized cumulative specific dissipated energy reported by Zavala et al. (2022)	76
Figure 5-5. Comparison plot of predicted versus measured normalized cumulative specific dissipated energy to failure using Equation 2 regression (simplified method) for Zavala et al. (2022) ( $n = 258$ )	77
Figure 5-6. Comparison plot of predicted versus measured cumulative specific dissipated energy to failure using Equation 3 regression (whole dataset) for Zavala et al. (2022) ( $n = 258$ )	78
Figure 5-7. Comparison of estimated cumulative specific dissipated energies to failure using the simplified method regression (Equation 3-2) and the whole dataset regression (Equation 3-3)	79
Figure 5-8. Shear stress time history used in a CV CSS test under earthquake-like loading	80
Figure 5-9. Results of a CV CSS Test under irregular loading of Figure 5-8 on an Ottawa sand sample at a very dense sand state an initial $\sigma'_{vo} = 200$ kPa	81
Figure 5-10. 3D mesh plot showing the regression obtained using the selected reduced dataset from Lasley (2015)	83
Figure 5-11. Comparison of the multivariable regression using the simplified method with the full dataset of 74 values of normalized cumulative specific dissipated energy reported by Lasley (2015)	84
Figure 5-12. Comparison of normalized cumulative specific dissipated energy to failure calculated with the regression obtained using the reduced set of data, and points of normalized specific dissipated energy of all tests reported by Lasley (2015)	85



## List of Tables

Table 3-1: Example of uniform test results .....	37
Table 4-1. Initial states of CSS samples and direct shear monotonic shear strength. ....	53
Table 4-2. Loading patterns used in this study.....	55
Table 4-3. Cumulative Specific Dissipated Energy .....	60
Table 5-1. Main features of test programs by Zavala et al. (2022) and Lasley (2015).....	72
Table 5-2. Data subset used for the simplified method applied to the Zavala et al. (2022) dataset.	73
Table 5-3. Summary of cumulative specific dissipated energy to failure in Zavala et al. (2022)....	75
Table 5-4. Data subset used for the simplified method applied to the Lasley (2015) dataset.....	82
Table 5-5. Values of Root Mean Square Error (RMSE) and Mean Absolute Error (MAE).....	86



# *1. Introduction*

## 1.1. General Introduction

Seismic soil liquefaction is a recurring phenomenon that may cause significant damage to infrastructure during earthquakes and that in turn may also cause injuries and even fatalities. This study of liquefaction involves field and laboratory studies. Among the laboratory studies, the cyclic simple shear is one of the tests that are used the most for studying the cyclic behavior of sands. This test consists of applying a vertical load to a sand specimen, which is confined by rigid Teflon coated rings, and then applying cyclic shear stresses, which reduce the effective confining stress as the cycles progress until the point that failure occurs. Historically, laboratory studies have been performed using uniform sinusoidal loading, mainly due to limitations of the equipment, and researchers have found ways to convert the random loading of an earthquake into equivalent uniform (harmonic) loading cycles. Even though newer advanced equipment permits the application of random loads, the equipment that runs uniform loads are simpler, more common and less expensive. Regarding pore pressure development during testing, simple shear laboratory testing has been done in two ways. One of them is performing a truly undrained test, in which the total vertical stress is maintained constant during cyclic loading, with the pore pressure rising and the effective stress decreasing during each cycle of loading; this is a true representation of the behavior of saturated soil when subjected to cyclic loads. Other way to run a test is performing a constant volume test, where the sample does not need to be saturated, but it can be moist or even dry. After the initial vertical effective stress is applied, the cyclic shearing load is applied under constant height (constant volume) condition, and the vertical stress (total and effective) starts decreasing as cyclic loading progresses, until the sample reaches failure. Even though some studies affirm that the reduction of vertical stress under constant volume conditions is equivalent to the pore water pressure, have the test been run in the truly undrained manner, the results are not completely conclusive. However, it is very common for studies of cyclic behavior of sands to be performed in dry sands under constant volume conditions, as it is much easier to perform a large number of tests under these

conditions. This study will look at the cyclic behavior of dry sands under constant volume simple shear, as this behavior is very similar to the cyclic behavior of saturated sands, though it will not state that it is equivalent to pore water pressure in saturated sands.

The characterization of this cyclic behavior has been studied in several ways, such as using the cumulative damage hypothesis initially developed by Miner (1945), which is explained with more details in the sections below. This hypothesis is more applicable to high-cycle fatigue, such as fatigue that occurs in metals, and it is usually applied to the number of cycles in which failure occur. The initial cumulative damage definition by Miner (1945) suggests that failure of a material when subjected to cyclic loading occurs after an amount of work is absorbed at failure by the material, which is equivalent to say that a certain amount of energy is dissipated by the material. This approach is used in this study, validating that this hypothesis can be applied when the sand is subjected to a general type of loading, by utilizing several different types of uniform and non-uniform loadings. Subsequently, and based on the validity of this hypothesis, a simplified method to calculate a multivariable regression to predict the dissipated energy by a sand sample to failure will be presented, which will be useful to reduce the amount of testing required to perform those predictions.

## 1.2. Problem Statement

Seismic soil liquefaction is a phenomenon that might occur in saturated sands, depending their behavior when they are subjected to cyclic loads. Laboratory studies, particularly those done utilizing simple shear tests, are very important for the characterization of that behavior. Researchers have used energy methods to develop regressions to predict dissipated energy to failure using large number of laboratory tests, including tests with complex loading (e.g. Figueroa et al., 1994; S. Lasley, 2015; L. Liang et al., 1995). However, running a large number of cyclic simple shear tests can be costly and time consuming. Therefore, the development of a methodology to predict failure of sands under random cyclic loading, based on the results of a small number of uniform cyclic simple shear tests, will be very useful to the scientific community.

### 1.3. Research Objectives

The main objectives of this thesis work are to evaluate the cumulative energy hypothesis which states that dissipated energy required by a sand sample to reach failure depends only on its initial state and to develop a simplified methodology to predict failure of sands when subjected to general cyclic loading based on uniform cyclic simple shear tests. To accomplish this objective, the following tasks were required:

- Task 1: Perform constant volume shear tests on dry sand, with different relative densities and initial effective stresses, utilizing several regular and irregular waveforms, with varying frequencies and CSRs
- Task 2: Process the data calculating the cumulative dissipated energy to failure in each of the cases
- Task 3: Utilizing the calculated dissipated energy data, evaluate the cumulative energy hypothesis
- Task 4: Evaluate if the dissipated energy to failure in a constant volume simple shear test on dry sand varies with frequency or applied cyclic stress ratio (CSR).
- Task 5: Evaluate the relationship of the dissipated energy to failure in a constant volume simple shear tests on dry sand to parameters of the initial sample state , such as relative density and initial effective vertical stress.
- Task 6: Evaluate regressions to predict the dissipated energy to failure in a constant volume simple shear tests on dry sand based on the parameters of the sample initial state

## 1.4. Thesis Structure and published articles

### 1.4.1. Thesis Structure

The main body of this thesis consists of the theoretical framework, the experimental methodology, two manuscripts, and a conclusions chapter that presents a summary of key findings from this study. A related conference paper is included in the appendix.

**Chapter 2** contains the theoretical framework of this work

**Chapter 3** contains the experimental methodology

**Chapter 4** contains the first manuscript, which presents a study performed to evaluate the validity of the cumulative specific dissipated energy hypothesis of sand samples subjected to uniform and non-uniform load cycles.

**Chapter 5** contains the second manuscript, presents the development of a methodology to predict failure of sands under general cyclic loading, based on creating a multivariable regression developed utilizing a reduced data set of simple harmonic tests.

**Chapter 6** presents a summary of key findings of this work, the conclusions and recommendations for future work.

### 1.4.2. List of published articles

Zavala GJ, Pando MA, Park Y and Aguilar R. (2022). Specific Dissipated Energy as a Failure Predictor for Uniform Sands under Constant Volume Cyclic Simple Shear Loading. *KSCE Journal of Civil Engineering*, 26(2), 703–714. <https://doi.org/10.1007/s12205-021-1205-4>

Zavala GJ, Pando MA, Park Y and Aguilar R (2022). A simplified method for predicting failure of sands under general cyclic simple shear loading. *Geotechnical Research XX(XXXX): 1–XX*, <https://doi.org/10.1680/jgere.22.00011>

Zavala GJ, Pando MA and Aguilar R (2017). Influence of irregular loading and frequency on the cumulative damage and dissipated energy of dry loose sand under cyclic simple shear. *ICSMGE 2017 - 19th International Conference on Soil Mechanics and Geotechnical Engineering 2017*. (pp. 537-541) SEÚL: Southeast Asian Geotechnical Society, c/o Asian Institute of Technology

## 2. *Theoretical framework*

### 2.1. Soil liquefaction

Seismic soil liquefaction is a recurring phenomenon that occurs in most medium to large earthquakes, which can generate an enormous quantity of infrastructure damage, large economic losses and personal injuries that can possibly turn into fatalities. The 1964 earthquakes of Alaska, USA (Mw=8.4) and Niigata, Japan (Mw=7.5), caused a large amount of damage associated to soil liquefaction (National Academies of Sciences, Engineering, 2021) . These two earthquakes helped the geotechnical and earthquake engineering community realize the importance of studying this phenomenon.

In general, this phenomenon occurs when an external force, such as a large earthquake, causes a rapid of pore water pressure in the soil which can reach a value equal to the geostatic total stress. When this happens, the effective stress in the soil reaches a value of zero, and given that the shear strength of the soil directly depends on the effective stress, the shear strength decreases dramatically, which causes the soil to behave as a liquid, and liquefaction failure to occur (National Academies of Sciences, Engineering, 2021). A liquefaction failure is also associated with large strains occurring in the soil and very large settlements occurring in structures founded over the liquefied soils. During soil liquefaction some distinct features can appear in the terrain, such sand boils, which also serve to identify soil liquefaction in areas where there are no structures.

Over the years, multiple researchers (particularly in regions close to active earthquake zones) have been developing methods to predict liquefaction occurrence based on the soil properties and the design earthquake characteristics, in an effort to identify liquefiable areas that should be avoided for construction of infrastructure or treated to mitigate liquefaction effects. These methods usually involve testing the soil in-situ with field tests such as Cone Penetration Tests (CPTs), Standard Penetration Tests (SPTs) and geophysical methods such as seismic refraction or MASW. However, laboratory studies can also be very important to understand the behavior of soils when subjected to cyclic loads,

as the soil can be tested under controlled conditions. The laboratory tests that are more commonly used to study the behavior of soils when subjected to dynamic loads are the Cyclic Triaxial Test, Cyclic Simple Shear Test (which is the test used in this study) and Cyclic Torsional Shear Test.

There are multiple complexities involved in its study. Among these complexities, one important concept to discuss is the criteria that define soil liquefaction. Another concept that is crucial to study is the critical state of the soil, because it defines its behavior when subjected to shear loading. From this point of view, the behavior of the soil depends on the void ratio and confining pressure that the soil is subjected to. Both concepts will be discussed in the following subsections.

Several definitions of soil liquefaction have been proposed by different researchers (Wu et al., 2004). This phenomenon can be characterized mainly by three factors: Excess pore water pressure, soil strength reduction and shear strain/ deformation of the soil . Even though these three factors are closely related, many liquefaction definitions are based solely on one of those factors, which may lead to some confusion among the geotechnical community. UC Berkeley, adopted a broad definition of liquefaction such as: “significant reduction of strength and stiffness of a soil, principally as a result of pore pressure increase and corresponding reduction in effective stress”, which deliberately does not quantify the threshold of strength or stiffness reduction necessary for liquefaction. While there are multiple ways to describe liquefaction, the majority of academic definitions are based in one of the three following criteria (Wu et al., 2004):

- Pore Pressure

This criterion establishes that liquefaction occurs when the excess pore water pressure ratio reaches a value of 1 ( $r_u=1$ ). The value of  $r_u$  is the ratio between the excess pore water pressure and the vertical effective overburden stress ( $r_u=\Delta u/\sigma'_{vo}$ ) in the case of field conditions, the ratio between the excess pore water pressure and the initial effective vertical stress ( $r_u=\Delta u/\sigma'_{vo}$ ) in the case of the simple shear tests, or the ratio between the excess pore water pressure and the minimum principal stress ( $r_u=\Delta u/\sigma'_{3c}$ ) in the case of triaxial tests. This definition of liquefaction has some drawbacks, however, such as some soils not being able to achieve exactly  $r_u=1$ , despite behaving as a liquefied soil for all practical purposes. This has been shown by Ishihara (1993) in sandy silts and silty sands, and by Wu (2002) in Monterey

0/30 sands. Other drawback is that this criterion may not reflect the seismic performance of denser soils. In loose soils, the  $r_u=1$  condition is immediately accompanied by large shear strains, but dense soils, which may achieve high excess pore water pressures under severe cyclic loading, may have limited strain because of their strong dilatant behavior. Also, it is very difficult to measure pore water pressures in the center of the sample, where most of the shearing occurs. Equipment usually measures pore water pressures in the boundaries, which may result in a pore pressure lag in low permeability specimens.

- Strength

One of the major concerns of soil liquefaction is the loss of shear strength of a soil, especially when the soil behaving as a viscous fluid, because it jeopardizes the overall stability of structures, earth slopes or embankments. As mentioned before, a total loss of shear strength occurs if the effective confining stress reaches zero, product of a rise of pore water pressure that make makes the  $r_u$  reach a value of 1, which theoretically makes this criterion identical to the pore water pressure criterion. However, in real conditions, some differences may arise between both criteria.

- Strain/Deformation

These criteria are associated with the development of shear strains or shear deformations in the soil. Initially these criteria were not very popular as many tend to consider the shear strains a consequence of liquefaction. However, the development of pore water pressures and shear strains are closely interrelated (Wu, 2002). Dobry et al. (1982) suggested the existence of a threshold strain below which no permanent excess pore water pressure will occur, and could be used for liquefaction assessment, though it may be too conservative for engineering applications. Due to the strong correlation of seismic performance of soils and structures built over them or out of them, shear strain and deformation of the soils serve as good criteria for seismic performance assessment (Wu et al., 2004). One of the drawbacks of using shear strain as a liquefaction criterion is that the measurement of shear strain depends on the deformation mode. Therefore, different criteria must be used for different deformation modes (i.e., triaxial, simple shear or others). Other drawback of this criterion is the non-uniqueness of the selected level of strain to define liquefaction. Different researchers have used levels between 2% and 10%. The influence of the selection of strain level for liquefaction varies from insignificant in loose soils to very



significant in dense soils. Ishihara (1996) proposed the use of 5% double amplitude (DA) axial strain in cyclic triaxial testing as a criterion to define liquefaction and cyclic triaxial testing for clean sands and sands with fines. He also proposed (Ishihara, 1985) the use to 3% single amplitude (SA) strain as criterion to define liquefaction in simple shear tests and in field studies (level ground), which is equivalent to 6% double amplitude strain.

One of the first attempts to delineate condition under which a soil might liquefy was done by Casagrande in the 1930s (Casagrande, 1936), when he coined the term “critical void ratio” for cohesionless soils. It was noted that during the application of a shearing load, dense sands tend to increase volume (dilate) and loose sands tend to decrease in volume (contract). If the soil is tested under drained shear, the indicated volume changes take place. If the soil is tested under undrained conditions, the soil generates either positive pore water pressure (if it is contractive) or negative pore pressure (if it is dilative). The “critical void ratio” is the term for the initial void ratio for which a sand neither dilates nor contracts during drained shear or does not generate any kind of pore water pressure during undrained shear. However, according to critical state soil mechanics concepts, the stress state of the soil is also a parameter that determines if a soil is contractive or dilative (Jefferies & Been, 2016). Therefore, the critical void ratio of a soil is not a sole property of a soil itself, but it is also dependent on the stress state of the soil.

## 2.2. Cyclic simple shear tests

### 2.2.1. Representation of an irregular load by an equivalent sinusoidal load

The analytical evaluation of liquefaction potential invariably has two independent components: The evaluation of the cyclic stress induced by an earthquake and a laboratory investigation in which the cyclic stresses for which a deposit of soil (at certain depth) will cause liquefaction or certain amount of cyclic strain are determined (National Academies of Sciences, Engineering, 2021). The evaluation itself consists on comparing the stresses in the field with the stresses that cause liquefaction or more than an acceptable amount of strain in the laboratory. This comparison results in a fundamental problem. While

the earthquake loads usually are comprised by relatively erratic movement with varying amplitudes and frequencies, which induce an equally irregular set of stresses in the soil, most of the laboratory test data involves the application of uniform cyclic stresses to the soils being tested. Therefore, in order to perform an adequate comparison of the field and laboratory stresses, there are two options that could be followed. The first option is to subject specimens to the exact loading series induced by the earthquake. Even though equipment is available to perform these tests, there are major disadvantages, such as a requirement that for every earthquake motion being investigated multiple series of tests must be run, leading to a large number of tests, and if the design earthquake is changed, tests would need to be run again. The second option would be to represent or convert the irregular earthquake series in an equivalent series of uniform stresses. This equivalent series consists of a stress selected by the user, applied a certain number of times (equivalent number of cycles at the selected stress level). This last method has the advantage of allowing one set of data to be used in several earthquake evaluations. However, a rational method of converting the irregular series into uniform stress series is necessary.

Nowadays equipment to impose random loading to a soil is available, but the “equivalent number of cycles” concept is still an integral part of cyclic liquefaction evaluations. The idea is to convert a random load into a simpler “equivalent damaging” load, such as a sinusoid. This concept can be used in field evaluations or directly in laboratory evaluations. Even though the evaluation of liquefaction potential has switched from laboratory testing to in situ testing, the number of equivalent cycles concept is still important because it underlies the derivation of Magnitude Scaling Factors (MSF) used in the field evaluations .

Converting or finding equivalence between a non-uniform loading, like experienced by soil samples during an earthquake, and a uniform sinusoidal load as applied by early experimental studies has involved the concept of equivalent number of uniform cycles that has been studied since the 1970s (e.g., Annaki & Lee, 1977; Seed et al., 1975). Finding an equivalent number of uniform sinusoidal load cycles, as applied by most early geotechnical cyclic load devices, was based on the goal of achieving the same level of damage or a failure state as compared to the more complex irregular earthquake loading that the researchers wanted to capture. The approach of converting an irregular, complex load signal to an equivalent uniform signal had several advantages, such as being able to analyze the effect

of a different earthquake on a soil by using a single set of data and facilitating laboratory testing as simpler machines are required to perform uniform sinusoidal loading patterns.

The concept on converting a random load to an “equivalent damaging” load has long been used to study metal fatigue. The Palmgren-Miner (P-M) cumulative damage hypothesis (initially proposed by Palmgren in 1924) is commonly used because of its simplicity and relatively good agreement with experimental data for various metals. The problem is that this implementation applies to high cycle fatigue conditions, (low amplitude and a large number of cycles), where the amplitude of loading is constrained to the elastic range, which is usually not the case of soils in liquefaction.

In the early 1970s, Professor H.B. Seed and others adopted Miner’s procedure for evaluating cyclic liquefaction of the soil, with slight modifications, even though the plastic strain in the soil is more characteristic of low cycle fatigue. The method of implementation should consider the nonlinear strain stress properties of the soil.

### 2.2.2. Palmgren-Miner cumulative damage hypothesis

Fatigue evaluations in metals can be performed creating an S-N curve, which is a plot of the number of cycles required to cause failure as a function of peak amplitudes of a uniform cyclic stress. However, these curves do not describe how the damage progresses in the material. Therefore, cumulative damage hypotheses have been developed to quantify the accumulation of component damage as the loading progresses.

The Palmgren-Miner damage hypothesis was initially proposed by Palmgren in 1924 and outlined by Miner in 1945, and it is known as the Cumulative Damage Hypothesis. Cumulative damage was defined by Miner (Miner, 1945) as the ratio of the absorbed work ( $w_i$ ) after  $n_i$  load cycles to the total absorbed work at failure ( $W$ ). He also proposed an alternative definition of damage as the ratio of the number of cycles ( $n_i$ ) in the load history having an amplitude  $S_i$  and the total number of cycles ( $N_i$ ) of this same amplitude  $S_i$  required to cause failure.

The basic form of Miner's damage hypothesis is as follows:

$$\frac{\omega_1}{W} = \frac{n_1}{N_1} \quad (2-1)$$

where:  
 $N_1$  : number of stress cycles to failure at stress level  $S_1$   
 $n_1$  : number of cycles having peak stress amplitude  $S_1$   
 $\omega_1$  : absorbed work after  $n_1$  cycles

If different stress levels are applied, then the equation gets modified as follows:

$$\frac{\omega_1}{W} + \frac{\omega_2}{W} + \frac{\omega_3}{W} + \dots + \frac{\omega_m}{W} = \frac{n_1}{N_1} + \frac{n_2}{N_2} + \frac{n_3}{N_3} + \dots + \frac{n_m}{N_m} \quad \text{or} \quad \sum_{i=1}^m \frac{\omega_i}{W} = \sum_{i=1}^m \frac{n_i}{N_i} \quad (2-2)$$

The sum of the ratios is defined by Miner as the "Cumulative component damage" and it is represented by a "D". Both these definitions of D, are presented in Equation (2-3), as follows:

$$D = \sum_{i=1}^m \frac{\omega_i}{W} \quad D = \sum_{i=1}^m \frac{n_i}{N_i} \quad (2-3)$$

where:  
D = cumulative damage  
 $w_i$  = absorbed work in cycle  $i$ ;  
W = total absorbed work at failure;  
 $n_i$  = number of cycles in the load history with an amplitude  $S_i$ ;  
 $N_i$  = total number of cycles of amplitude  $S_i$  required to cause failure

It is important to note that  $D = 0$  corresponds to the initial state of the sample before cyclic loads have been applied,  $D = 1$  corresponds to the damage state of the sample at failure, and D values between 0 and 1 correspond to the damage state of a sample that has been subjected to a certain loading but has not yet failed.

In order to compute an equivalent number of cycles, a reference stress needs to be selected. Being  $N_{ref}$  the number of cycles that cause failure at the reference stress of  $S_{ref}$ , then the number of equivalent cycles at that reference stress is  $n_{eq}$  and it is given by the following equation 2-4:

$$\frac{n_{eq}}{N_{ref}} = \sum_i \frac{n_i}{N_i} \Rightarrow n_{eq} = \sum_i \frac{N_{ref}}{N_i} n_i \quad (2-4)$$

However, as mentioned before, this approach is only valid when the material response is constrained to the elastic range.

In soil mechanics (especially when working with sands), and because of the nature of this particulate material whose resistance depends greatly on the applied normal stress, the applied maximum cyclic

shear stress is usually represented by the Cyclic Stress Ratio (CSR), which is the ratio between the maximum applied cyclic shear stress (horizontal) and the initial normal stress (vertical). The CSR concept is used in the field when evaluating liquefaction resistance and in the laboratory when performing shear tests. Figure 2-1 shows a typical cyclic resistance curve (analog to S-N curves in classical fatigue evaluation), developed after performing uniform loading cyclic simple shear tests on soils. These curves plot the “Number of cycles to failure”, ( $N_i$  in Equation 2-1) vs the applied CSR (amplitude  $S_i$  described in Equation 2-1) in a particular soil placement and testing condition. This specific graph indicates two values of applied CSRs with the corresponding values of number of cycles to failure. Note that due to the logarithmic scale in the “number of cycles” axis, a sample subjected to lower CSR needs a much greater number of cycles to reach failure.

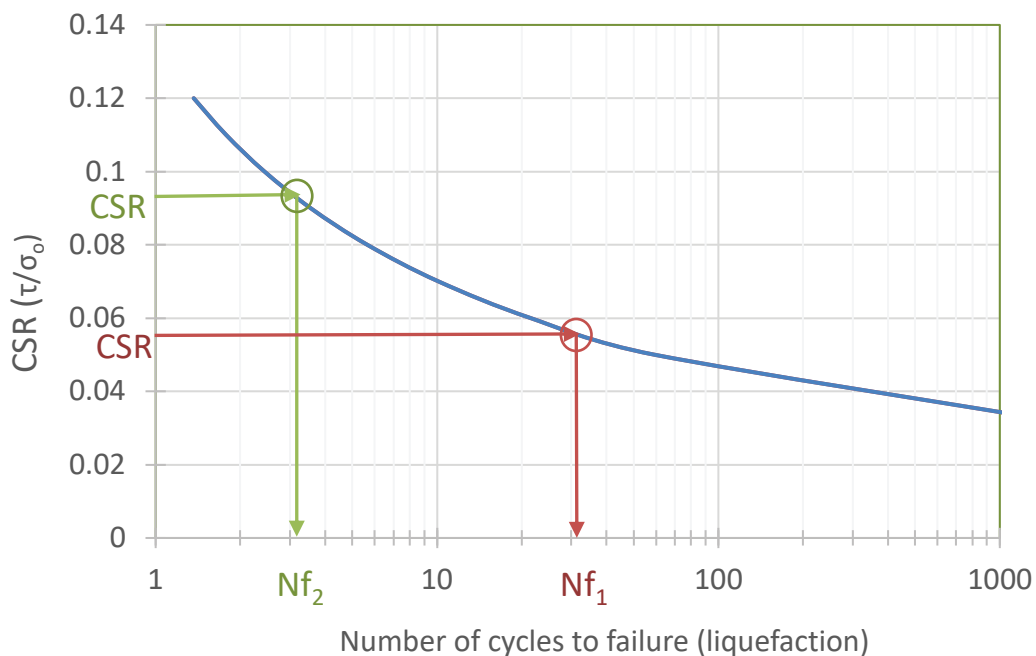


Figure 2-1. Schematic graph showing a cyclic resistance curve indicating the number of cycles to failure corresponding to two values of CSRs

One of the first applications of the P-M hypothesis to attempt to represent irregular earthquake time histories as equivalent stress series for liquefaction evaluations was done by Seed et al. (1975). This study used data from DeAlba et al. (1975), who performed large scale liquefaction tests using a shaking table and saturated sand under a constant normal stress. The authors developed cyclic resistance curves

(S-N curves), which plot number of cycles to cause initial liquefaction versus cyclic stress ratio (CSR) used in their tests, for Monterey #0 Sand at four different relative densities.

Annaki & Lee (1977) performed an experimental program to check the validity of Seed's implementation of the P-M hypothesis using triaxial tests under uniform and irregular deviatoric load cycles. The authors stated that their data generally confirmed the validity of the P-M based equivalent uniform cycles, or the cumulative damage method of dealing with irregular loading effects on soil, and support the analysis presented by Seed et al. (1975).

An equivalent number of uniform cycles at any stress level would be the value that causes the same amount of damage. A detailed description of the P-M hypothesis can be found in Green & Terri (2005).

According to the P-M cumulative damage hypothesis (based on number of cycles), applied to soils subjected to cyclic loading, each loading cycle produces a fraction of damage to the soil, and the soil reaches failure when the accumulated damage reaches a value of 100%. The simplest representation of this condition is shown in Figure 2-2. This figure shows the progression of the damage with the applied loading cycles if the distribution of damage in time is linear with each cycle. In this case  $CSR_1$  is smaller than  $CSR_2$ , and thus the number of cycles to failure is much larger.

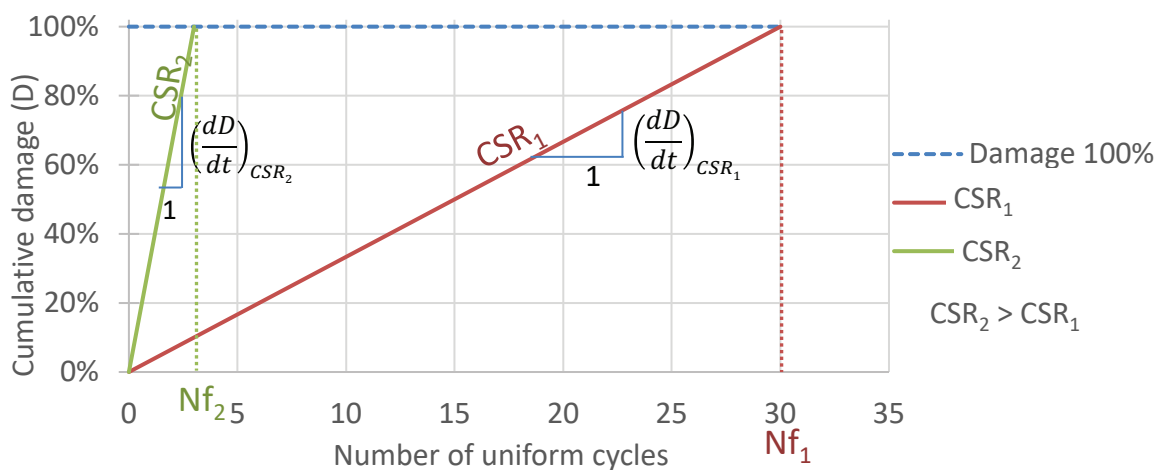
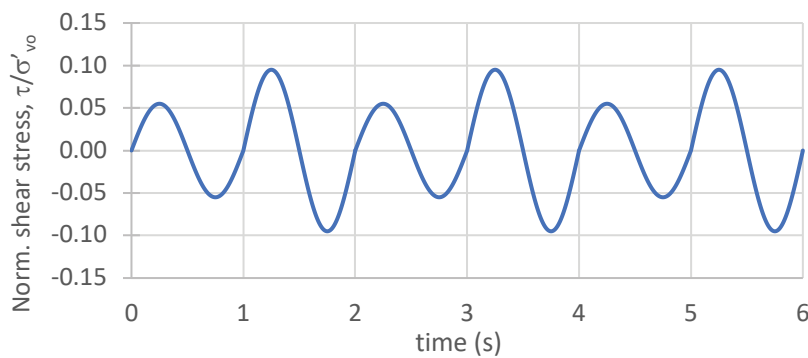


Figure 2-2: Cumulative damage against number of cycles assuming linearly proportional damage

Following the cumulative damage theory, when a soil is subjected to a non-uniform load, the damage produced is a fraction of unity. Figure 2-3 shows an example of how the damage would occur with a

non-uniform load, considering two values of CSR (CSR1 and CSR2) from Figure 2-2. Applying the P-M based cumulative damage theory as described before, when a soil is subjected to a non-uniform load, the damage produced is a fraction of unity that depends on the number of cycles to failure associated to the CSR of that particular cycle. Figure 2-3 shows an example of how the damage would occur up to failure in a sample subjected to a non-uniform load, considering two values of CSR, which match the values of CSR (CSR<sub>1</sub> and CSR<sub>2</sub>) shown in Figure 2-2. As CSR<sub>1</sub> is smaller, the damage caused by cycles at this stress level is much smaller.

(a)



(b)

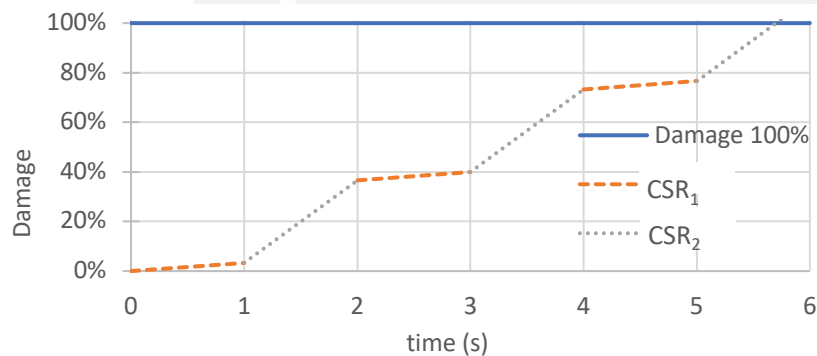


Figure 2-3: Schematic showing progression of damage due to non-uniform loading (a) Non-uniform stress-time history and (b) Progression of damage due to applied stress time history shown in (a).

One of the first attempts to represent irregular time histories as equivalent stress series for liquefaction evaluations was done by Seed et al. (1975). They used data from DeAlba et al. (1975), who performed large scale liquefaction tests in a shaking table, developing S-N curves (which plot number

of cycles to cause initial liquefaction versus cyclic stress ratio used in the tests) for Monterey #0 Sand at relative densities of 54%, 68%, 82% and 90%.

Seed then selects a single curve for 65% relative density to be representative of all sands and normalizes the curve to  $\tau_{\max}$  for 1 cycle to liquefaction. Then a standard weighting curve is developed where the stress required to cause failure in 1 cycle is equal to 1.5 times the maximum stress developed during an earthquake (that is a factor of safety but varies from 1.5 at 1 cycle to about 1.0 at a large number of cycles). A table is created to obtain the equivalence of # of cycles for different cyclic stresses. Then we can count the peaks in the earthquake time histories and calculate the equivalent number of cycles at a predetermined cyclic stress level. Figure 2-4 summarizes the sequence used by Seed in his normalization.

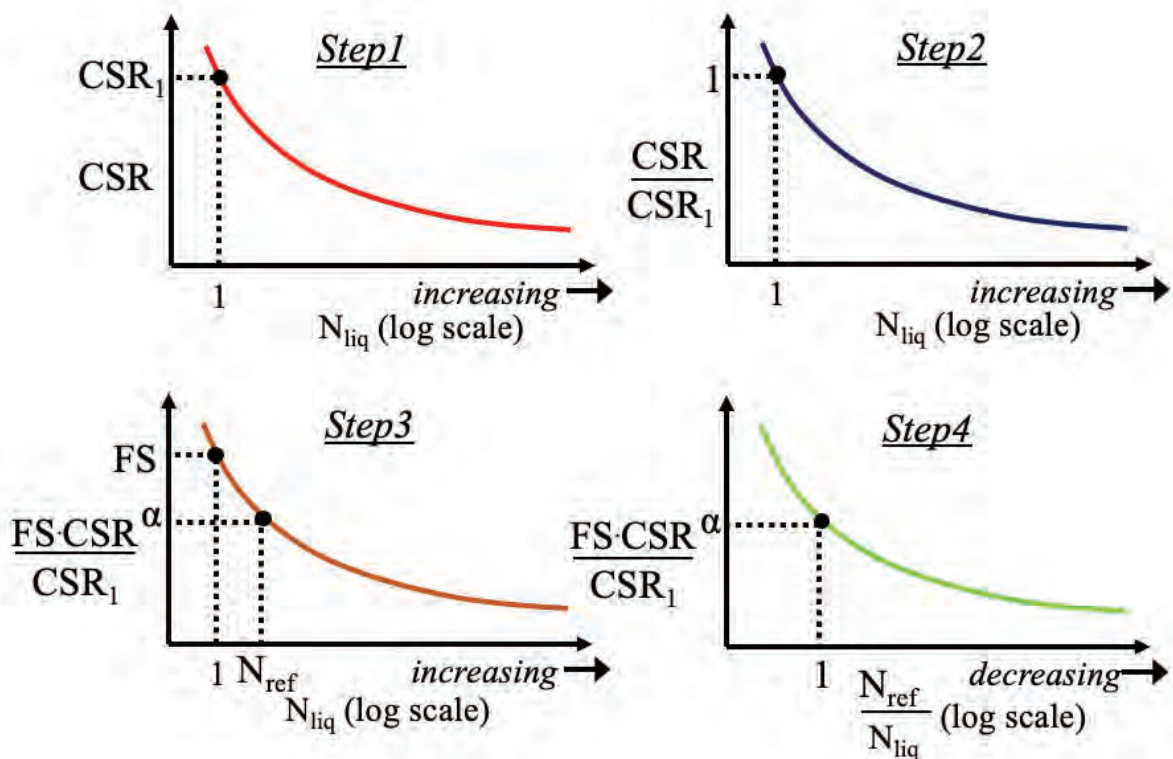


Figure 2-4. Sequence of steps used by Seed et al. (1975) to normalize cyclic stress ratio –  $N_{liq}$  curve. Step1: designate the cyclic stress ratio required to induce liquefaction as  $CSR_1$ ; Step2: normalize ordinate values by dividing cyclic stress ratio by  $CSR_1$ ; Step3: apply safety factor to  $CSR_1$  (divide  $CSR_1$  by a safety factor) and determine the number of cycles required to induce liquefaction ( $N_{ref}$ ) corresponding to the normalized peak amplitude ( $\alpha$ ) of uniform cyclic load; and step4: normalize abscissa as  $N_{ref}/N_{liq}$  (adapted from Green and Terri, 2005)



Annaki & Lee (1977) perform an experimental program to check the validity of Seed's implementation of Palmgren-Miner hypothesis using triaxial tests. They used Los Angeles Harbor Sand and Lake Arrowhead Decomposed granite. Due to the characteristics of the triaxial test and soils in general, the extension part of a cycle generates much more damage than the compression part. Therefore, their program included uniform cycles, extension cycles with a small compression component (to ensure stress reversal) and compression cycles with a small extension component (also to ensure stress reversal). Also, their experimental program included a pattern with increasing stresses, a pattern with decreasing stresses, a pattern with increasing and then decreasing stresses, and a random pattern, all of which were repeated until sample failure. Due to the great difference in the amount of damage inflicted by extension vs compression cycles, the authors consider separately the damage from each of those parts of the cycle. The authors conclude that their data generally confirm the validity of the equivalent cycle or the cumulative damage method to deal with irregular cycles, though direction independent tests (such as cyclic simple shear, torsion shear, or shaking table). Figure 2-5 below shows a linear relationship in the S-N data when plotted on a log-log scale, based on Seed et al. (1975)

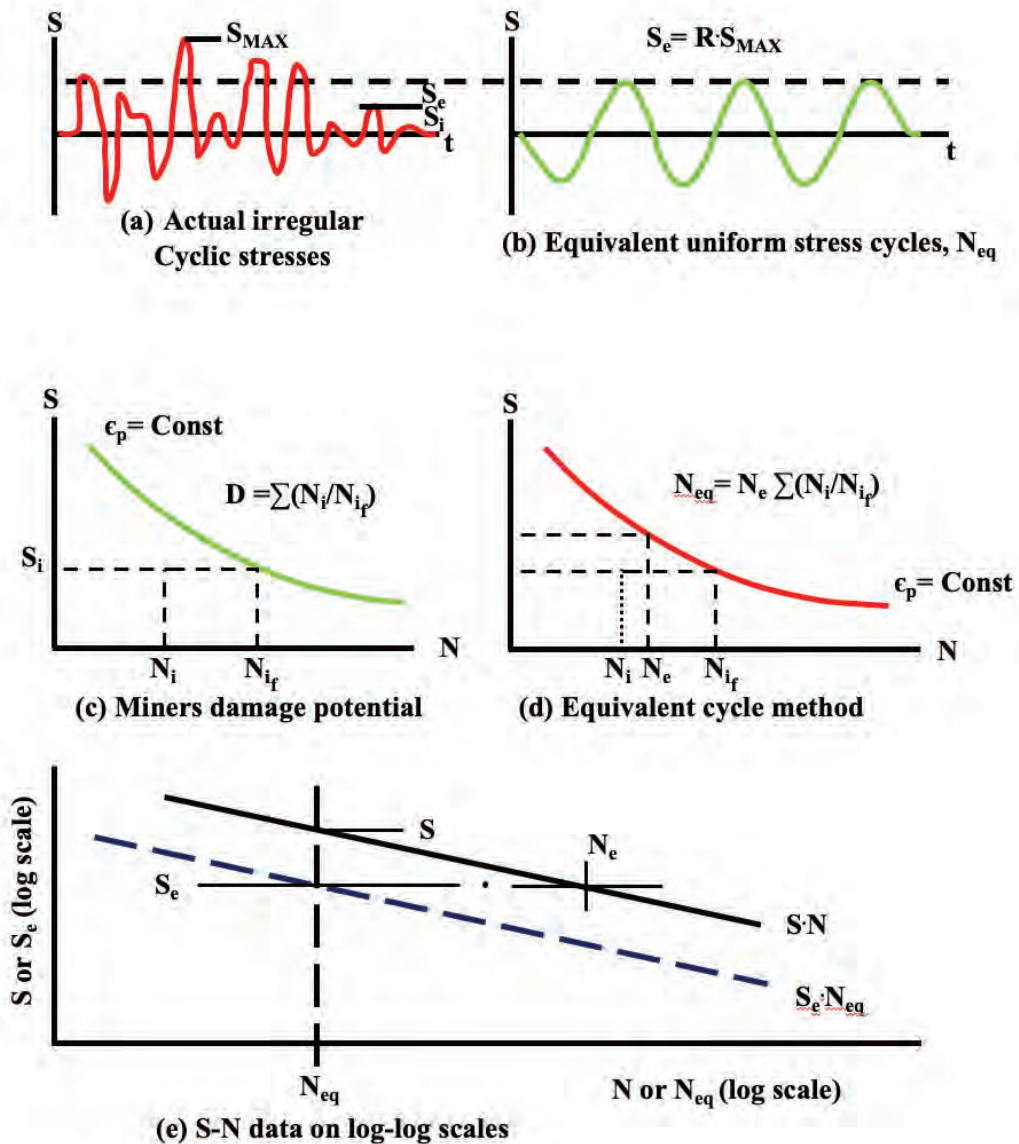


Figure 2-5. Cumulative damage and equivalent cycle concepts (adapted from Annaki & Lee, 1977)

Tatsuoka & Silver (1981) performed a theoretical and laboratory investigation, developing a procedure to predict the behavior of cohesionless soils under irregular cyclic loading patterns. Even though the authors conclude that the cumulative damage hypothesis can be used to predict the maximum shear strain amplitude induced in a sand subjected to irregular loads, they say that the hypothesis cannot predict the strain-time history, so a new analytical method is developed. The authors used wet tamped Monterey No. 0 sand for their experimental work. Unlike many other studies that include cyclic simple shear tests, the authors use an unreinforced membrane, which allow to maintain a constant (and known)

horizontal stress. They run saturated tests with no allowance to volumetric and vertical strain. From uniform cyclic simple shear tests, the authors formulate a relationship between double amplitude shear strain, stress ratio for uniform loading, number of loading cycles and relative density, finding that the equations they develop are better representation of their test results than the linear relationship on a log-log scale suggested by Annaki & Lee (1977).

Other studies including irregular loadings was performed by several researchers, such as professor Ishihara, Nagase and Yasuda (Ishihara & Yasuda, 1975; Ishihara & Nagase, 1988). Many researchers also make a calculation of the equivalent number of cycles from earthquake records considering the magnitude, duration, distance to fault, etc. These conversions are outside the scope of this work.

### 2.2.3. Dissipated Energy Approach

Other approach to perform an equivalence of irregular cycles in order to evaluate soil liquefaction involves the use of energy-based methods. Several researchers have developed methods to evaluate liquefaction potential based on the energy dissipated by the soil movements.

Energy based models that explain densification and liquefaction of cohesionless soils, such as the one developed Nemat-Nasser & Shokoh (1979) are based on the premise that certain amount of energy is involved in changing the void ratio from one value to another one, the amount of energy increasing as the void ratio approaches  $e_{min}$ . However, in the case of undrained loading in sand, the result will be an increase of pore water pressure, which decreases the intergranular forces, so the incremental energy will decrease with increasing pore water pressure.

Figuroa et al. (1994) use the energy concept to define liquefaction potential, and validate it using laboratory tests on Reid Bedford sand specimens of different relative densities. In this case the authors use hollow cylinder (torsional) tests, with strain control. They measure the energy per unit volume required to liquefaction, varying the relative density of the samples, the shear strain amplitude, and the confining pressure. The authors conclude that the amount of energy per unit volume required to liquefy is higher as the relative density of the sand increases, is higher as the confining pressure increases, and varies very little with a different shear strain amplitude. Based on their tests, the authors formulated a relationship between the energy required for the sand to liquefy and the mentioned parameters. Also,

according to the authors, their data confirms the conclusion that the energy per unit volume needed to induce liquefaction is not dependent on the loading form and can be used to evaluate the liquefaction potential under earthquake loads.

Green & Terri (2005b) present an overview the methods based on the Palmgren-Miner hypothesis (described above) in order to calculate an equivalent number of cycles of uniform stress, particularly the method by . However, they emphasize the fact that the Palmgren-Miner hypothesis applies to high-cycle fatigue conditions (low amplitude, large number of cycles), which is usually the case in metal fatigue applications, but is not directly applicable to low-cycle fatigue conditions (large amplitude and low number of cycle), which is mostly the case for liquefaction analyses due to the plastic strain accumulated after each cycle of loading. They also remark that the method of implementation needs to consider the nonlinear stress-strain response of the material. The authors propose an alternative implementation of the Palmgren-Miner hypothesis using energy principles to calculate an equivalent number of cycles at a uniform stress. Also, recognizing that the change of stiffness that occurs as the normal effective stress is reduced, the authors propose an expression to “convert” the energy dissipated at a  $j^{\text{th}}$  cycle to energy that would have been dissipated using the first cycle with the initial confining stress, which allows to calculate an equivalent number of “initial” cycles from a non-uniform applied loading. Green (2001) describes with more detail the implementation of the Green-Mitchel energy-based liquefaction evaluation procedure. This procedure takes directly into account the non-linear stress-strain behavior of the soil.

An alternative approach to equivalent cycles that is commonly used to study the cyclic behavior of sands under uniform and irregular loading is based on the energy dissipated by the soil during the loading event until reaching failure. Several researchers have used energy dissipation to evaluate liquefaction potential (e.g., (Azeiteiro et al., 2017; Fardad Amini & Noorzad, 2018; Figueroa et al., 1994; Green & Terri, 2005b; Ishac & Heidebrecht, 1982; Kokusho, 2017; Kokusho & Mimori, 2015)). The dissipated energy per unit volume for each load cycle of a CSS tests is equal to the area of the hysteresis loops in the shear stress versus strain plots. Figure 2-6 shows an example of the dissipated energy per unit of volume for different cycles of a CSS test. The cumulative dissipated energy can be

computed by the summation of the different areas of the hysteresis loops of the different load cycles until failure is reached.

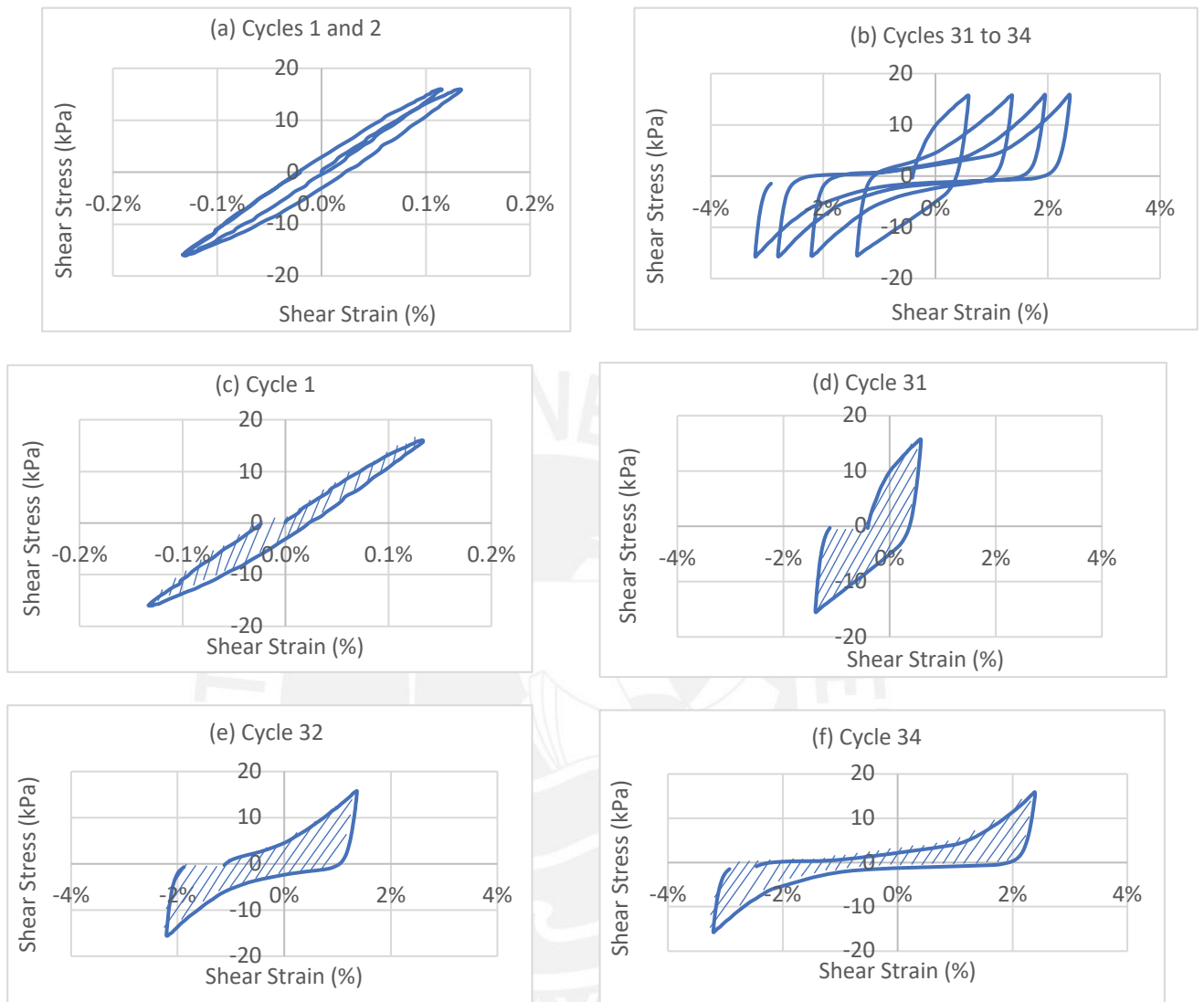


Figure 2-6: Example of dissipated energy calculations for different cycles of an individual CSS test (a) Cycles 1 and 2; (b) Cycles 31 to 34; (c) to (f) Cycles 1, 31, 32 and 34 with area defined to calculate dissipated energy

The cumulative dissipated energy has been found to explain densification of drained tests and liquefaction of sands under undrained loading. Figueroa et al. (1994) and Liang et al. (1995) used the energy concept to define liquefaction potential, and validated it using undrained hollow cylinder torsional shear tests on saturated sand specimens. According to these authors, the energy per unit volume needed to induce liquefaction is not dependent on the loading form and can thus be used to evaluate the liquefaction potential under general earthquake loads.

Green & Terri (2005) and Lasley et al. (2016) emphasized the fact that the P-M hypothesis applies to high-cycle fatigue conditions (low amplitude, large number of cycles), which is usually the case in metal fatigue applications, but is not directly applicable to low-cycle fatigue conditions (large amplitude and low number of cycles). These authors also point out that damage predictions using the P-M hypothesis are load-path independent. Thus, these authors propose an alternative implementation to the P-M hypothesis using energy principles that can be used to calculate an equivalent number of cycles at a uniform stress and to predict liquefaction.

#### 2.2.4. Constant volume testing

Constant volume CSS testing on dry sands has been used by several researchers to study liquefaction and cyclic behavior of sands (e.g. Finn et al., 1979; Lasley et al., 2016). This testing approach involves maintaining the height of a dry CSS specimen constant by using an active control of the applied vertical normal stress during the cyclic simple shearing. At any instance during the CSS test the difference between this variable applied vertical normal stress, required to maintain constant the sample height, and the initial applied vertical normal stress has been approximated by many researchers as equivalent to the excess pore water pressure that would have been developed in an undrained CSS test carried out on saturated sand samples prepared to the same initial relative density and with the same initial effective stress state. The advantages of constant volume testing are that it reduces compliance issues of the testing box and that the sample does not need to be saturated (it could be dry or moist). A comparison of pseudo-drained and truly undrained CSS tests was performed by Pickering (1973) using Ottawa sand samples at an average initial void ratio of about 0.65 and at a shear loading frequency of 2 Hz. The results reported in this study suggest these two test approaches are similar, but the pseudo-drained tests were on the conservative side in terms of number of cycles required to reach failure. The equivalency between the constant volume CSS test on a dry sand sample and a truly undrained CSS test on a saturated sand was further reported by W.D.L. Finn (Pickering's advisor) and co-workers at the University of British Columbia (Finn, 1985; Finn et al., 1979; Finn & Vaid, 1977). Figure 2-7, from Finn & Vaid (1977), shows the number of cycles to liquefaction from dry constant volume CSS are lower compared to the number of cycles recorded from undrained CSS on saturated samples of uniform

medium dense sands. This figure, often cited in references that have used dry, constant volume CSS, suggests that constant volume CSS on dry samples is on the conservative side compared to equivalent undrained CSS on saturated samples. This experimental evidence although useful, seems to be scarce and warrants further evaluation of the validity of this equivalency of these two CSS tests types. However, this was outside the scope of this research. This study will use constant volume testing on dry sands for all the tests run. Even though the behavior of sands when subjected to cyclic loads is similar under truly undrained testing and under constant volume testing, as stated above, the study will state that the results are equivalent to one running truly undrained tests.

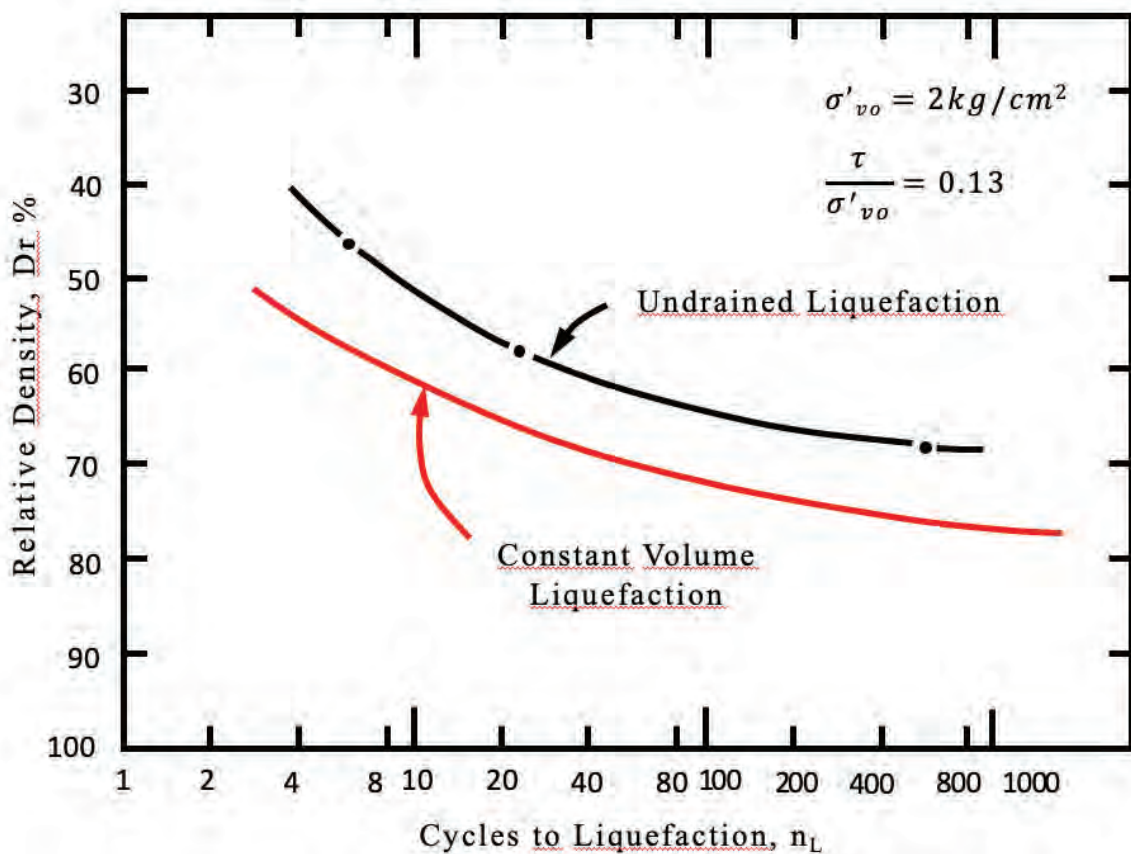


Figure 2-7. Liquefaction resistance of Ottawa sand in constant volume and undrained simple shear (adapted from Finn and Vaid, 1977)

### 3. *Experimental Methodology*

The test program for this research consisted of a series of uniform and non-uniform cyclic simple shear tests performed in an Advanced Dynamic Simple Shear testing system. This system can apply any kind of cyclic shear loading to the sample. The tests were performed in Ottawa 20/30 sand, at three relative density levels. The tests results were plotted, and several test parameters were calculated, such as the number of cycles to failure and cumulative dissipated energy to failure. Details on the testing methodology and analyses are shown below. Based on these results, conclusions were obtained respect to the validity of the cumulative energy hypothesis applied to constant volume simple shear testing (details are shown in Chapter 2). Also based on the test results, regressions were tested and a methodology to obtain a regression to predict the dissipated energy to failure, based on a limited number of harmonic simple shear tests, was developed (details are shown in Chapter 3).

#### 3.1. Equipment

All the tests for this research work were performed using a GDS Advanced Dynamic Simple Shear (ADVDCSS) testing system, in the simple shear configuration. This system is capable of applying axial and shear loads or displacements using GDS electromechanical force actuators, with axial and shear load and displacement readings controlled under closed loop conditions. Shear tests can be performed under displacement or load control, and active axial control permits the tests to be performed at a constant load or at a constant height (constant volume test). The system has the capability of performing static tests and dynamic tests, up to a maximum frequency of 5 Hz (at small strains), and it can apply either uniform or non-uniform loads. The system also has the capability of applying an all-around confining pressure to the sample (including the top cap), using either with air or water, which makes possible to perform saturated tests with backpressure saturation. A general view of the system is shown in Figure 3-1.





Figure 3-1: General View of ADVDCSS System

- **Sample box**

The sample box used in the tests has a circular cross-section, with a nominal diameter of 70mm and an approximate height of 21mm (depending on the amount of sand that is placed in the box). The sample lateral confinement is provided by an unreinforced membrane which is surrounded by 30 stacked Teflon-coated steel rings of approximately 1 mm height each. These rings do not permit relative in the horizontal direction, therefore keeping a constant sample diameter, but allowing the sample to attain significant shear strains, as shown in Figure 3-2. The pedestal and top cap have steel porous disks with teeth for a better transfer of shear load to the sample. The system also has the option of installing a pedestal and top cap which include bender elements that are capable of measuring the shear wave and compression wave velocities of the sample (this option is shown in Figure 3-2).

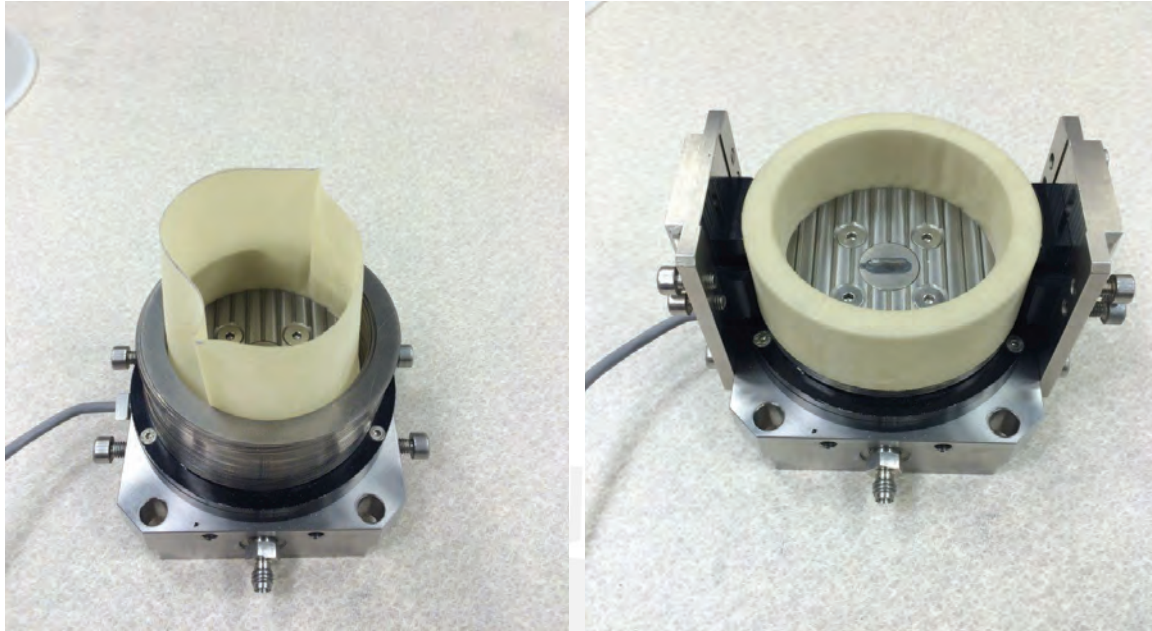


Figure 3-2: Sample box used for shear tests in the ADVDCSS

- **Data Acquisition box**

The data acquisition box (DCS) has 8 channels input (as shown in Figure 3-3), which record the readings of two displacement transducers for each direction (shear and axial), the two load cells, pore pressure transducer, and barometric pressure transducer. The DCS is an analog to digital converter and is connected to the data acquisition computer via a USB port.



Figure 3-3: Data Acquisition boxes: From top to bottom: Bender Element controller, DCS and LVDT signal conditioner

- **Pressure Controllers**

Additionally, separate components called pressure controllers can measure and apply the cell pressure and the back pressure and are also connected to the data acquisition computer directly via Serial and USB ports. The cell pressure controller/actuator is pneumatic and uses house pressure to apply the desired pressure to the cell chamber. The backpressure controller consists of an electrically actuated piston in a cylinder with a capacity of 200 cm<sup>3</sup> (see Figure 3-4). Volume differential is measured with a precision of 1mm<sup>3</sup> and pressure is measured with a precision of 1 kPa.



Figure 3-4: Cell pressure controller and back pressure controller

The data acquisition computer runs Windows 7.0, and has the program GDS Lab installed, which is the interface to control the characteristics and parameters of all the tests that are run in the system.

### 3.2. Materials

The test sand used in this experimental program was Ottawa 20/30 silica sand. This is a uniform, poorly graded silica sand with sub-rounded to rounded grains. Figure 3-5 shows microscope photographs of the sand. The mean particle size ( $D_{50}$ ) of this sand is 0.71 mm, and the 20/30 designation is based on having 95 % retained between the ASTM standard sieves #20 and #30. The grain size distribution of the sand is shown in Figure 3-6. The average maximum and minimum void ratio values obtained for the test sand were 0.644 and 0.503, respectively. Statistics of relative density of the sand used in the tests, and the sand shear strength are shown in section 4.3.1.

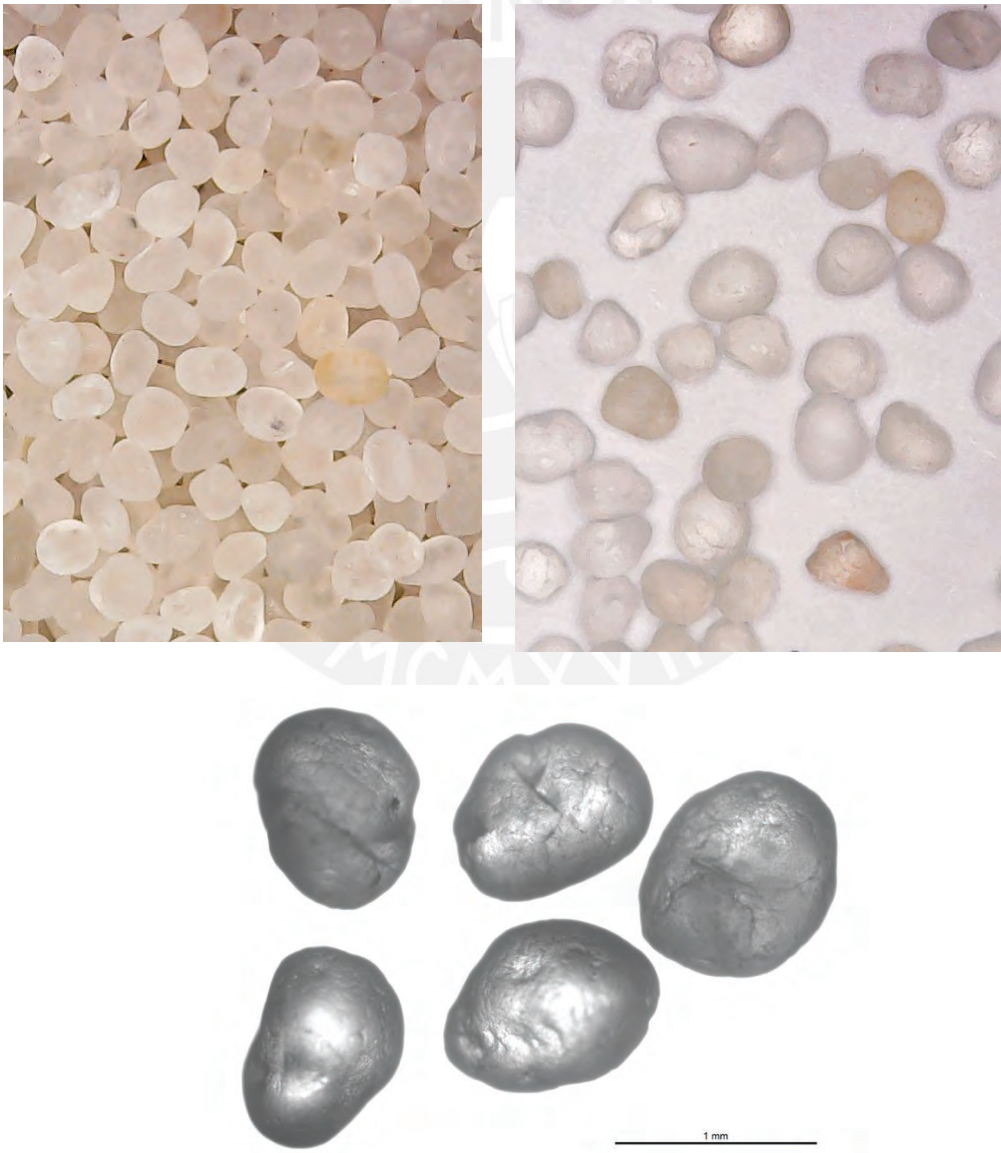


Figure 3-5: Microscope photographs of Ottawa 20/30 sand used in this study

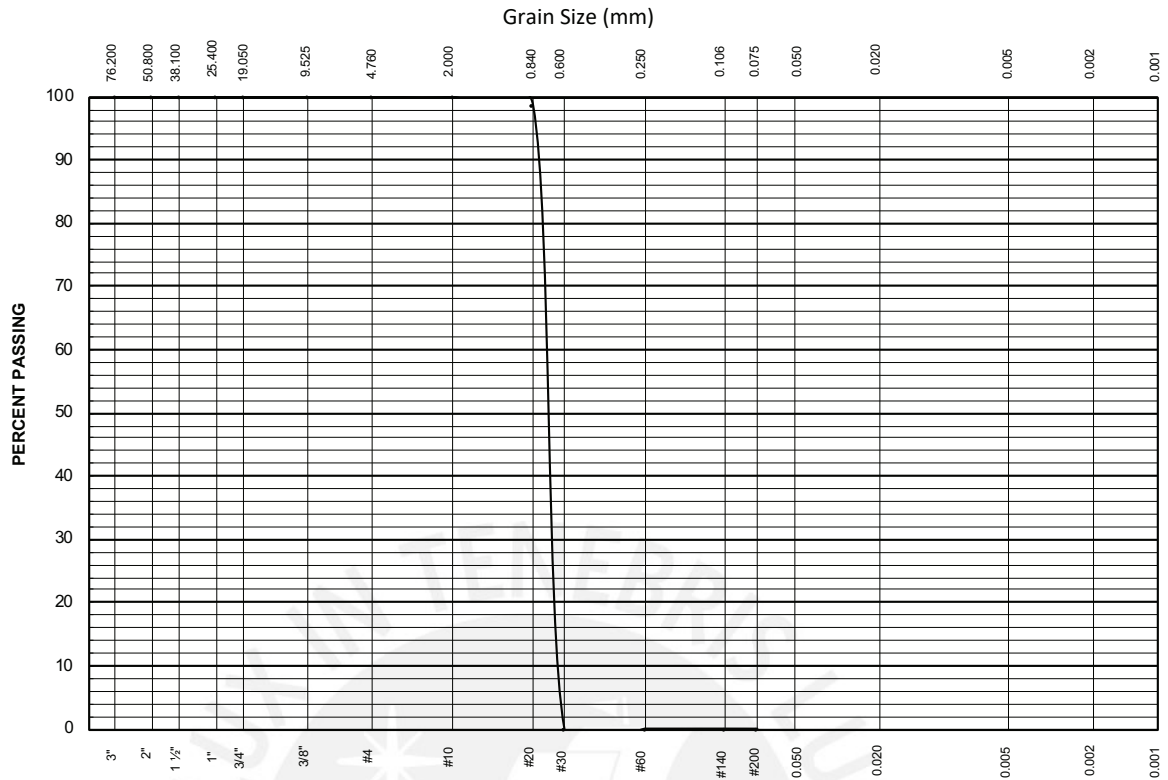
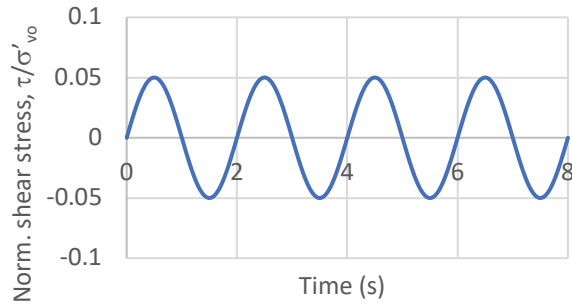


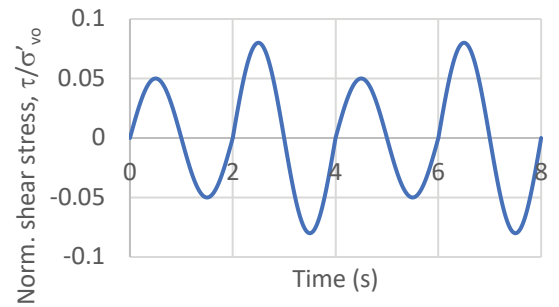
Figure 3-6: Grain size distribution of Ottawa 20/30 sand used in this study

### 3.3. Testing program

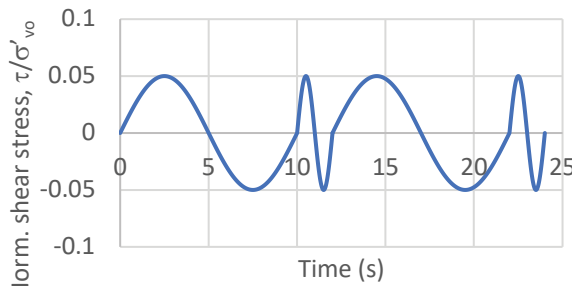
The cyclic simple shear testing program involved 269 tests conducted with the ADVDCSS system. The cyclic shearing phase for all tests was stress controlled and the applied normal stress was actively controlled to ensure constant volume conditions. The test program involved 9 possible sample initial states corresponding to 3 initial relative densities (loose, dense, or very dense) and 3 initial normal stresses (100, 200, or 400 kPa). A full description of the testing loading patterns performed for the test program is show in section 4.3.2 and summarized in Table 4-2. Graphical representations of examples of all the different types of loading types are shown in Figure 3-7.



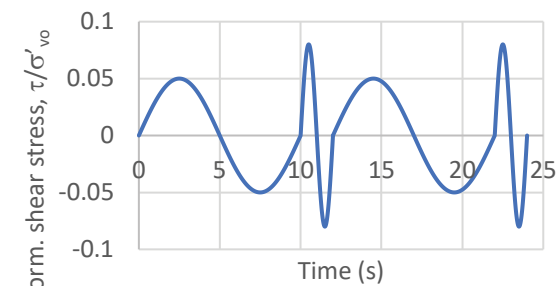
(a) Uniform cycles  
(CSR = 0.05,  $f = 0.5\text{Hz}$ )



(b) Non-uniform CSR (amplitude)  
(CSR = 0.05&0.08,  $f = 0.5\text{Hz}$ )



(c) Non-uniform frequency  
(CSR = 0.05,  $f = 0.1\&0.5\text{Hz}$ )



(d) Non-uniform frequency and CSR (CSR = 0.05&0.08,  $f = 0.1\&0.5\text{Hz}$ )

(e) Spike load (50xCSR=0.05 + 1xCSR=0.1,  $f = 0.5\text{Hz}$ )

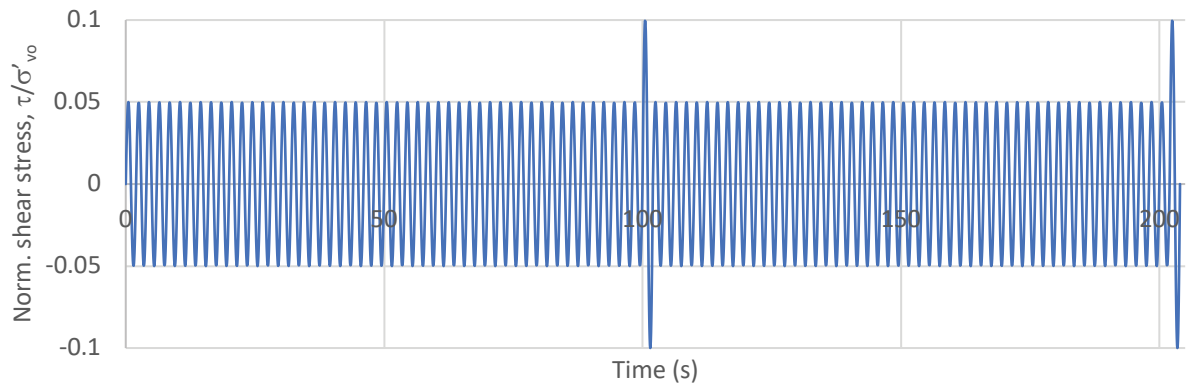


Figure 3-7: Graphical representation of dynamic load patterns used in this study (a) Uniform; (b) Non-uniform Type 1 (varying CSR); (c) Non-uniform Type 2 (varying frequency); (d) Non-uniform Type 3 (varying frequency and CSR); and (e) Non-uniform Type 4 (Spike load).

### 3.4. Sample preparation

As mentioned in the testing program section, the sand samples used in this investigation were prepared at three relative density levels: loose, dense and very dense. The cylindrical CSS sample box had a diameter of approximately 70 mm and an approximate height of 20 mm. The sample preparation methods used for each of the three relative density levels are listed below.

Loose samples were conformed in a dry state using a short pipe of 50mm of diameter that was placed in the sample box and filled with a predetermined weight of sand (130g). The pipe was quickly pulled up leaving the sample in a loose condition. Next the sample was carefully leveled, and the initial sample height measured using a caliper and a calibrated cylinder before normal stress application. Figure 3-8 shows the sample preparation procedure for these samples.

Dense samples were prepared using with a glass beaker, a stopper and a steel tube inserted in the stopper. A predetermined weight of sand (131.7g) was placed in the beaker, and then the sand was poured in the sample box using the dry pluviation technique. The height of the sample was then measured and noted. Figure 3-9 shows the sample preparation procedure for these samples.

Very dense samples were prepared in the following way: a predetermined weight of sand (141g) was split into three equal portions, and the sample box was marked at three levels with equal height. The first third of the soil was placed in the sample box and tamped with a tamper weighing 125 g until the soil level reached the first mark. The second and third layer were conformed the same way. A final measurement of the sample height was taken using a caliper and a calibrated plastic cylinder.

In all cases, the sample height was then measured in the ADVCSS machine using the calibrated displacement sensor. The first measurement in the machine was taken after the application of the seating load. The second measurement was made after the application of the normal stress. The latter one was used in the calculation of the relative density reported in the test data.

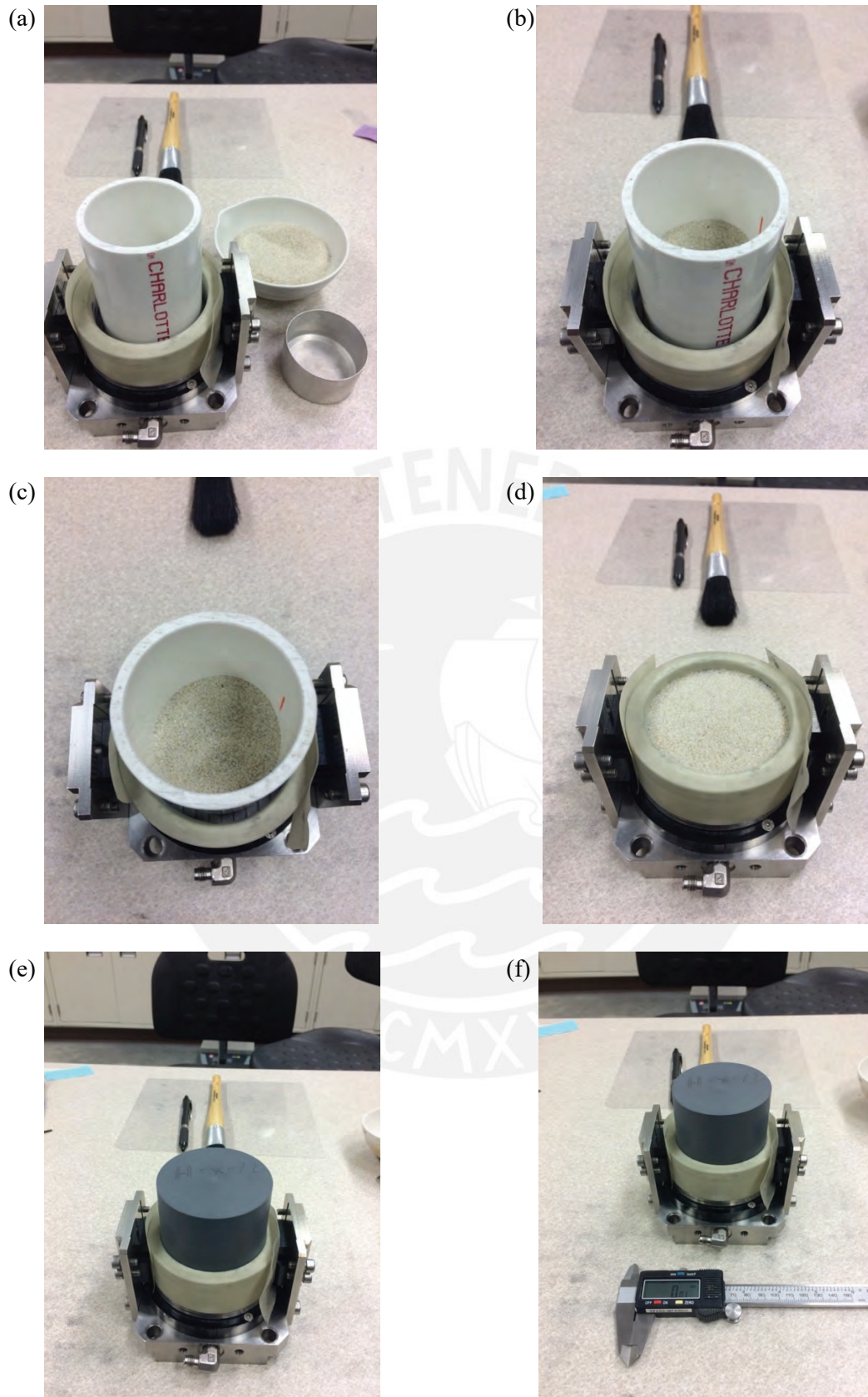


Figure 3-8: Sample preparation procedure for loose samples: (a) Placement of pipe, (b) Placement of sand, (c) Sand in place, (d) Sand in sample box after pulling pipe out, (e) Placement of calibrated cylinder, (f) Measurement of sand height



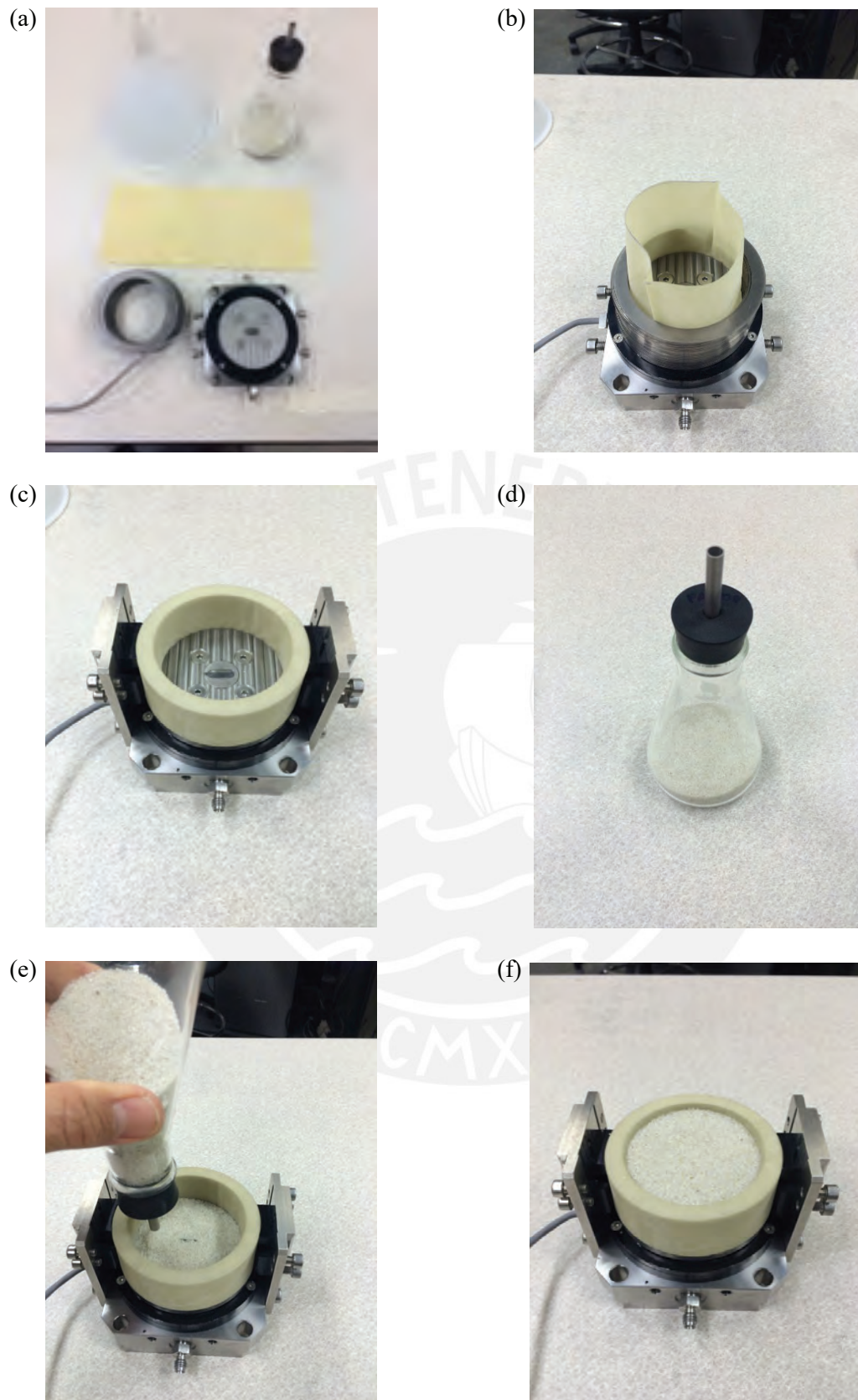


Figure 3-9: Sample preparation procedure for dense samples: (a) Materials used to prepare the sample, (b) Initial assembly of sample box, (c) Final assembly of sample box, (d) Beaker with sand, (e) Placement of sand in sample box using the beaker, (f) Finished sample

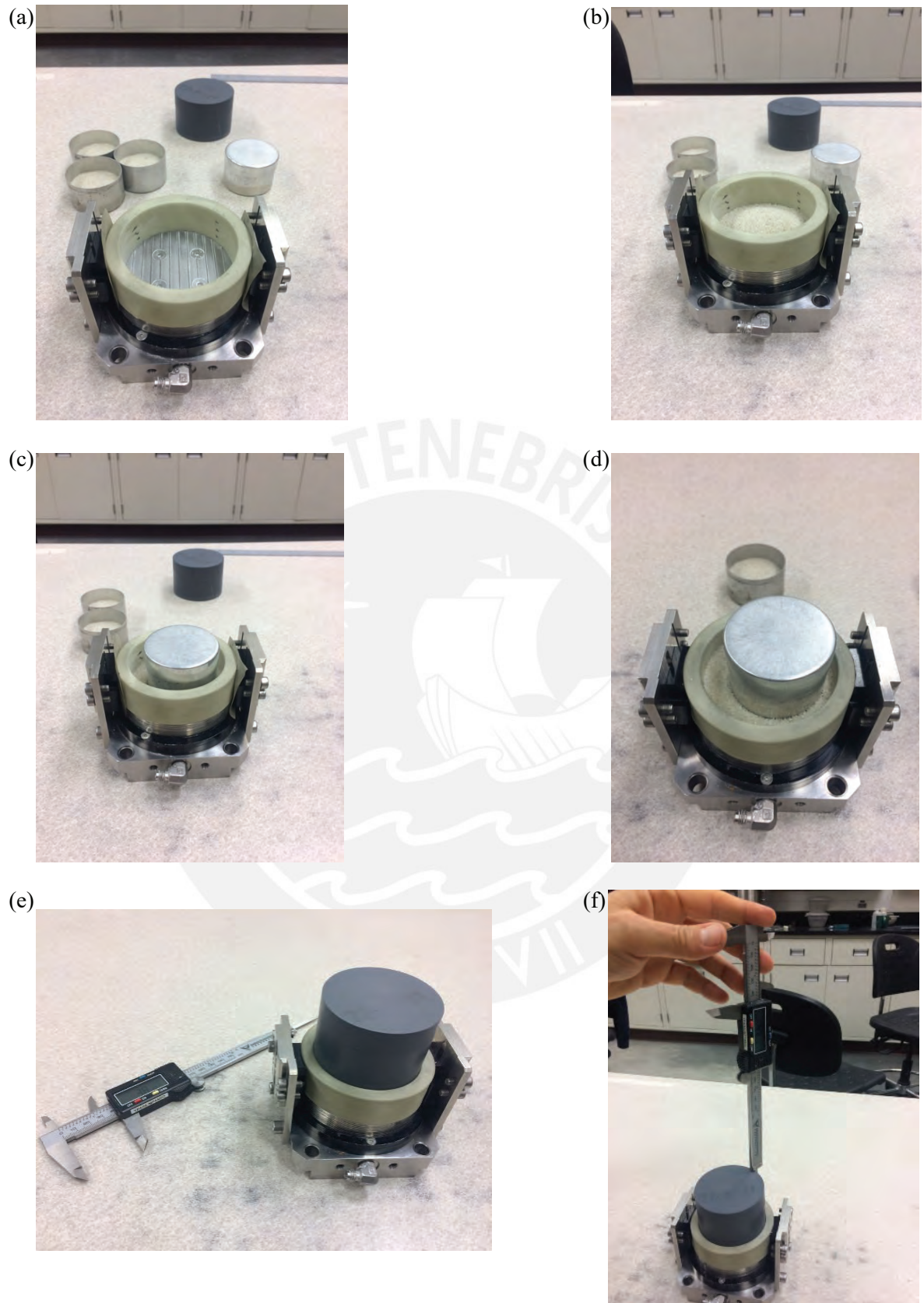


Figure 3-10: Sample preparation procedure for very dense samples: (a) Sample box, tamper and sand split in 3 parts, (b) First layer of sand placed, (c) Compaction of first layer, (d) Compaction of second layer, (e) Finished sample with calibrated cylinder, (f) Measurement of sample height

### 3.5. Testing Procedures

The procedure used to perform dry constant volume cyclic simple shear tests in this study is as follows:

1) *Sample box installation phase*

- The sample is prepared as specified in the sample preparation section, according to the density required in the test to be run.
- The shear box with the prepared sample is installed in the ADVDCSS machine, first placing the sample box in its position, and then tightening four screws that fix the box to the machine, as shown in Figure 3-11

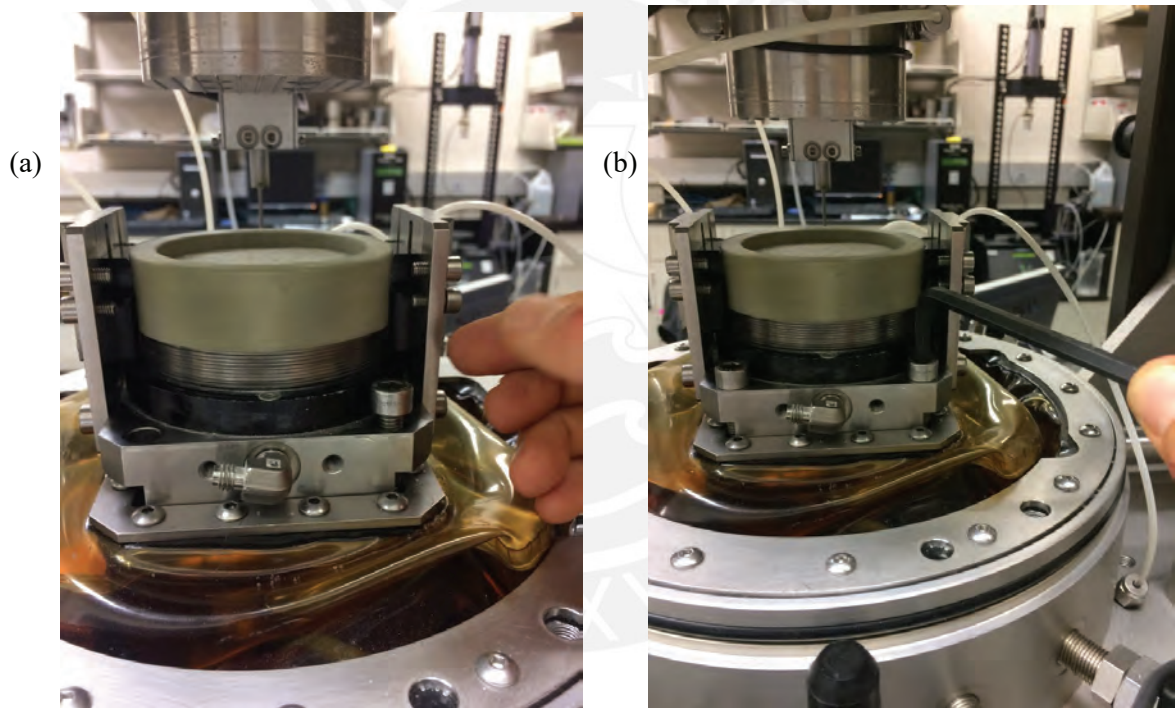


Figure 3-11: Sample box pedestal in ADVDCSS machine: (a) Placing and start of bolt installation, (b) Bolts being tightened with Allen wrench

- The top cap is then lowered to the edge of the rings (Figure 3-12(a)). After alignment is checked, the top cap is lowered further until it touches surface of the sample (Figure 3-12(b)).
- A seating stress between 5 and 10 kPa is applied. Then the top cap is placed on hold (no movement), the ring guides are removed (Figure 3-12(c)), the membrane is set with O-rings over the top cap (Figure 3-12(d)), and seating load is re-applied.

- The axial displacement measured with the LVDT is compared to the expected Axial Displacement based on the measured sample height, and the exact measurement is noted.

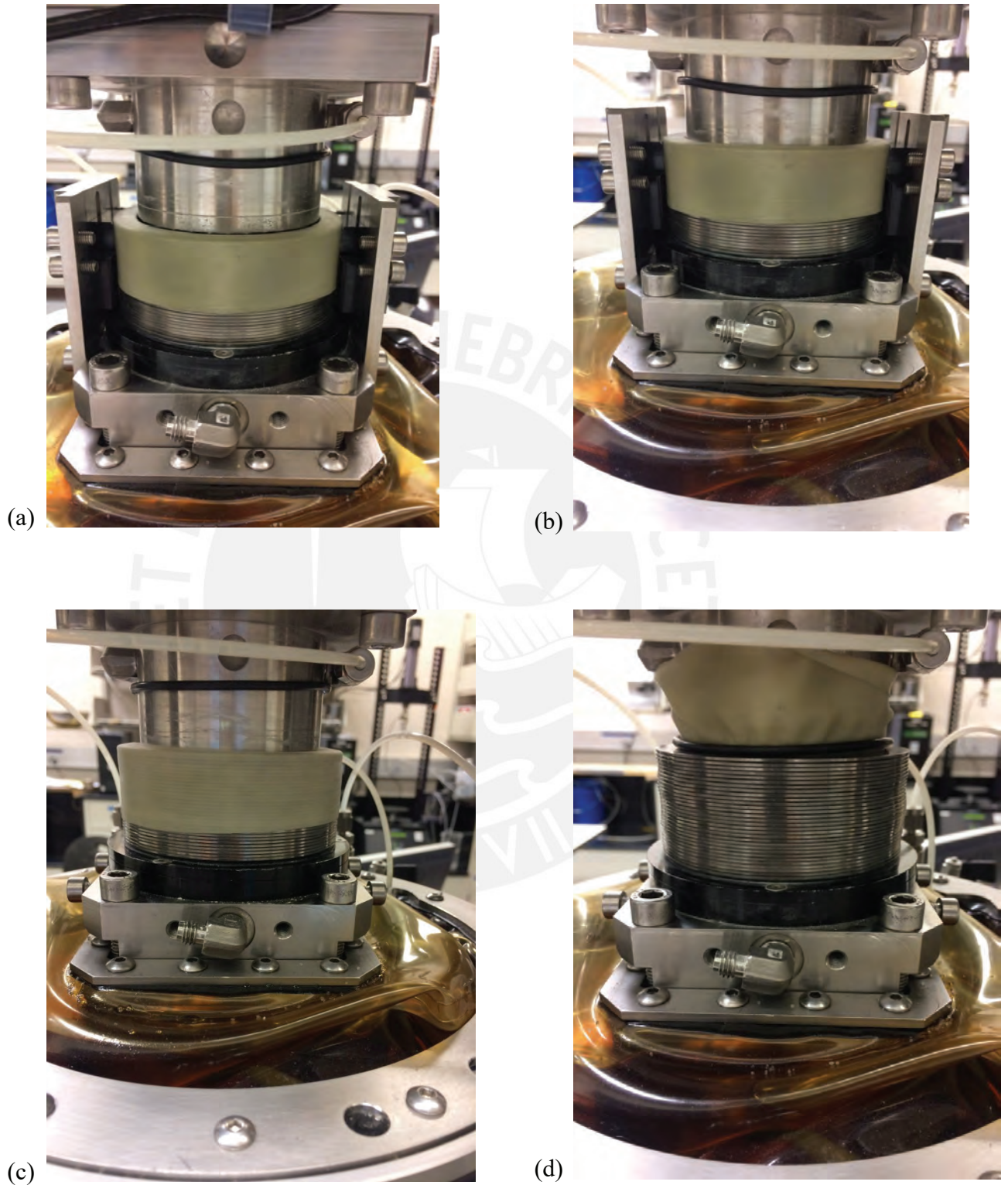


Figure 3-12: Application of seating load on a sand sample: (a) Top cap is lowered to the edge of the rings to check alignment, (b) Top cap is lowered until it touches the surface of the sample, (c) Ring guides are removed, (d) Membrane and O-ring are put in their place for testing.

## 2) *Testing Phase:*

The control program GDS lab is used to program the desired test. The user programs all the parameters to be used in the test. As mentioned before, for this research, the tests are run at constant volume, which is obtained by actively adjusting the force in the top cap to obtain a constant sample height. For monotonic loading, the only testing parameters are normal stress and the rate of strain of the shear load. For cyclic loading, the tests can be either stress-controlled or strain controlled, which give totally different hysteretic curves. In this research, all the tests were run under stress control. In that case the test parameters are the normal stress, the maximum shear stress applied and the frequency of loading. Also, the type of cyclic loading is defined by a previously loaded file that contains the waveform to be used during the test. This file must be created and loaded previously. Dry constant volume tests in general are run in two stages:

- Application of normal stress: The desired normal stress is applied to the sample. After the application of the normal stress, the height of the top cap is noted in order to calculate the volume of the sample after the normal load application, which is then used to calculate the relative density of the sample
- Application of shear load (static/monotonic or dynamic/cyclic): Either monotonic or cyclic loads are applied to the sample until failure occurs. There are several definitions of failure that may be considered in this kind of tests. In monotonic tests, the failure is just defined by a maximum strain. In cyclic stress-controlled tests, failure may be defined using a single or double amplitude strain, or by certain value of the equivalent  $r_u$ . The failure definition utilized in this study is discussed in section 1.4. Figure 3-13 shows a soil sample that had just been tested, and which reached the failure criteria considered.

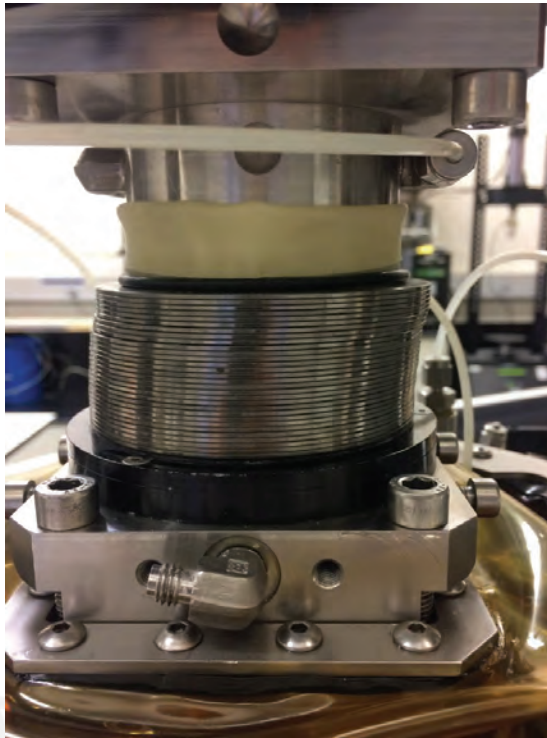


Figure 3-13: Tested sample after failure

### 3.6. Test results and analysis

For all the tests in this study, tests were run well beyond the elected failure criteria of Double Amplitude Strain = 7.5%. All the CSS test results were processed and presented using 4 plots that have matching axes in the vertical and horizontal directions and are plotted in the same scales, which are explained below. Examples of uniform loading cases for different sand densities and two levels of CSR (low and high), as detailed in Table 3-1, are presented in Figures 1-19 to 1-24.

Table 3-1: Example of uniform test results

	Loose	Dense	Very Dense
Low CSR	$\sigma'_{vo} = 100$ kPa CSR = 0.05	$\sigma'_{vo} = 200$ kPa CSR = 0.065	$\sigma'_{vo} = 100$ kPa CSR = 0.05
High CSR	$\sigma'_{vo} = 400$ kPa CSR = 0.09	$\sigma'_{vo} = 200$ kPa CSR = 0.10	$\sigma'_{vo} = 400$ kPa CSR = 0.12

In the mentioned figures, the graph in the upper left (a) shows the Normalized Effective Vertical Stress (NEVS), which is defined as the ratio between the actual vertical stress in the test and the initial vertical stress applied to the sample at the beginning of the dynamic shearing stage of the test, vs the normalized shear stress ( $\tau/\sigma'_{v0}$ ). Initially the samples have an NEVS of 1, and as the cyclic shearing progresses, the NEVS value starts to decrease until approaching a value of zero at failure. The value of NEVS decreases because the applied normal stress decreases during loading to ensure that the testing condition of constant sample height (i.e., constant volume) is maintained. This graph illustrates the progressive decrease of the vertical stress with number of applied cycles. When the sample approaches a NEVS value of 0, the shear strains start to increase dramatically which each additional cycle of load applied to the sample and the hysteresis loops and associated dissipated energy tend to increase in magnitude. The graph in the upper right (b) shows the shear strain vs the normalized shear stress ( $\tau/\sigma'_{v0}$ ), illustrating the progression in size of hysteresis loops and increase of shear strain levels as the applied load cycles increase. The plot in the lower right (d) shows the variation of shear strain with number of simple shear load cycles. This graph effectively illustrates the number of cycles for which the shear strains start to increase dramatically. Closing in the lower left corner (c) shows the complement to NEVS, defined as  $1 - \text{NEVS}$ , versus the number of applied load cycles. It should be noted that some authors in the liquefaction literature approximate  $1 - \text{NEVS}$  from constant volume CSS tests performed on dry samples as an equivalent pore pressure ratio ( $r_u$ ) and approximate the shear strain failure as equivalent to a liquefaction failure that would be observed in an undrained CSS test performed on a saturated sample with the same initial state, under constant total normal stress.

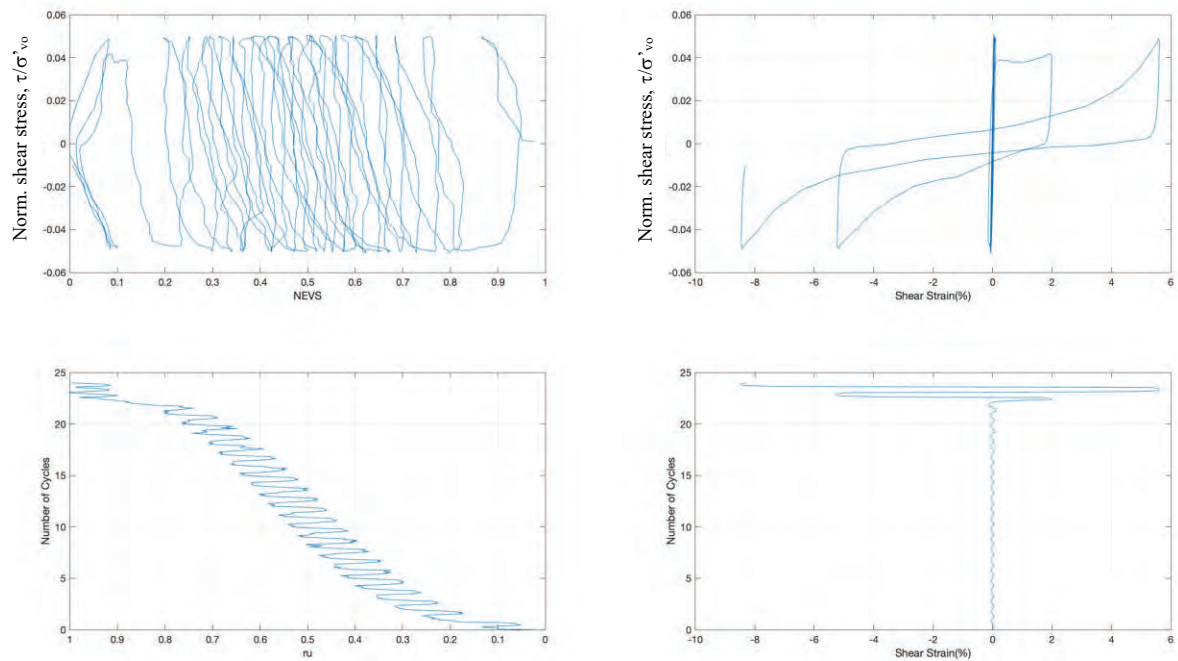


Figure 3-14: Results of Uniform Constant Volume CSS Test in Loose Sand,  $\sigma'_{vo} = 100$  kPa, CSR = 0.05

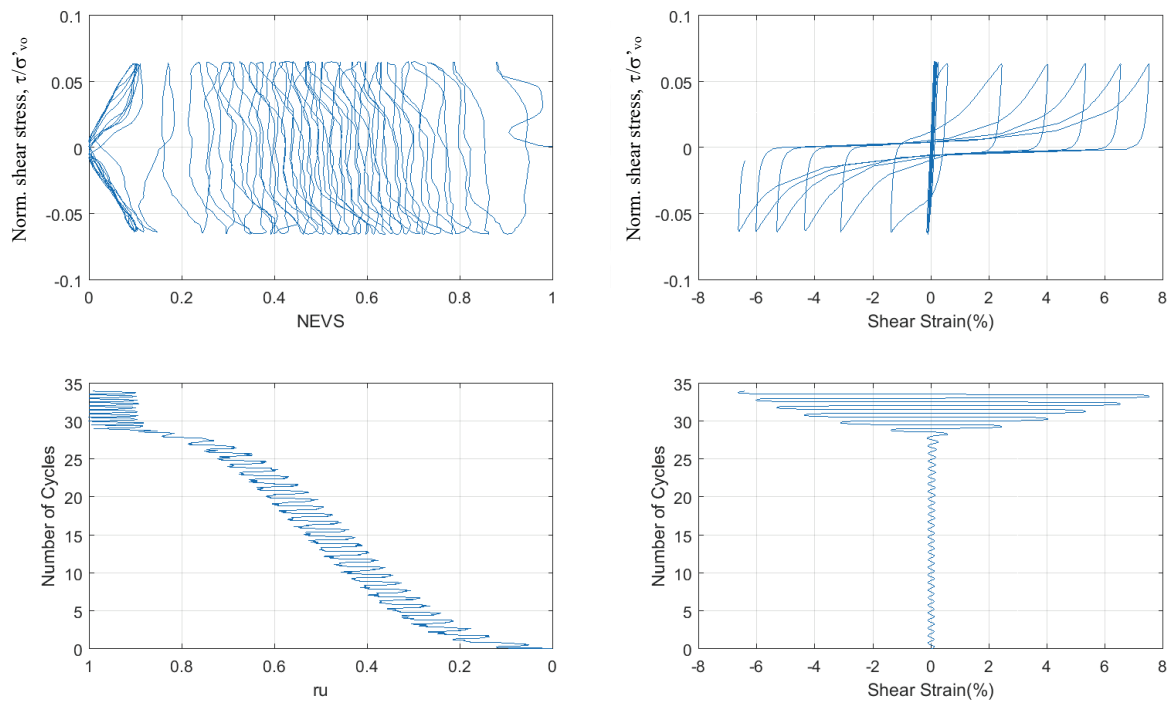


Figure 3-15: Results of Uniform Constant Volume CSS Test in Dense Sand,  $\sigma'_{vo} = 200$  kPa, CSR = 0.065



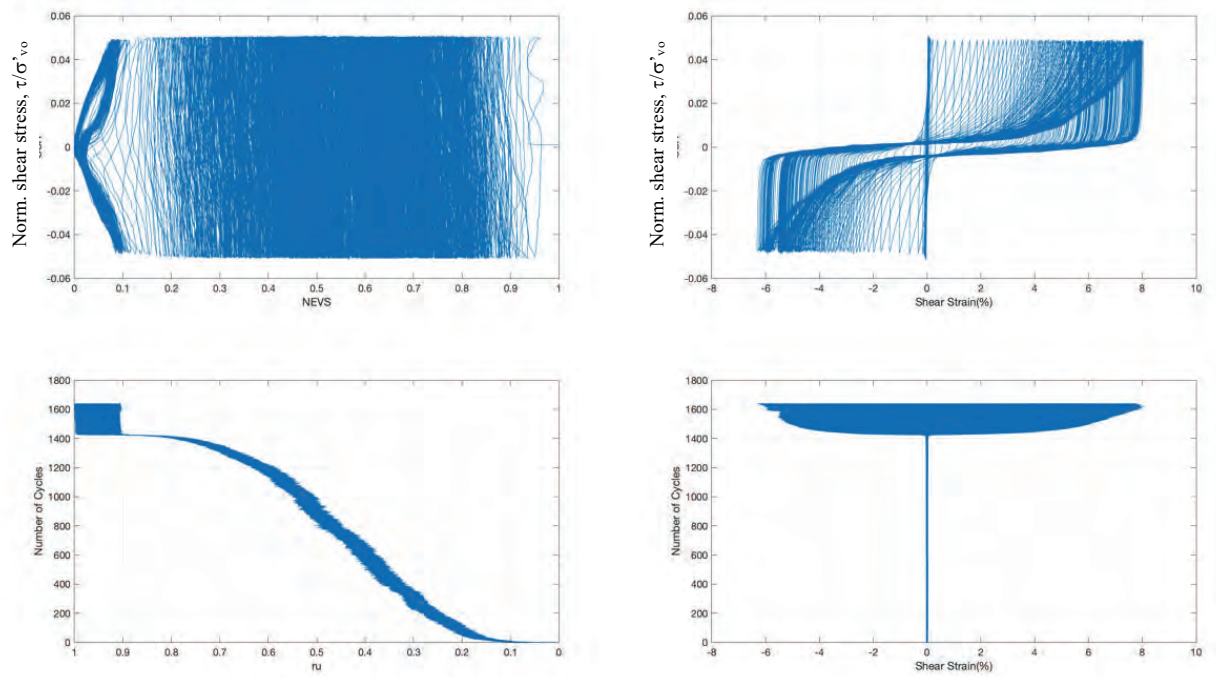


Figure 3-16: Results of Uniform Constant Volume CSS Test in Very Dense Sand,  $\sigma'_{vo} = 100$  kPa, CSR = 0.05

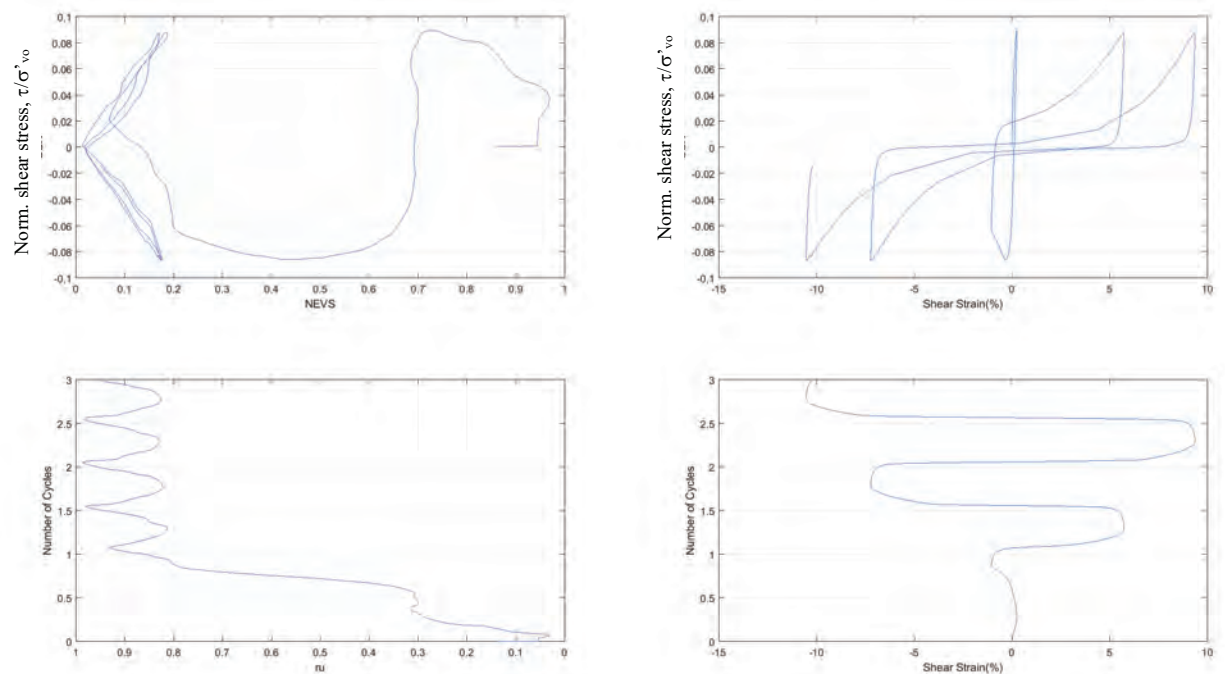


Figure 3-17: Results of Uniform Constant Volume CSS Test in Loose Sand,  $\sigma'_{vo} = 200$  kPa, CSR = 0.09

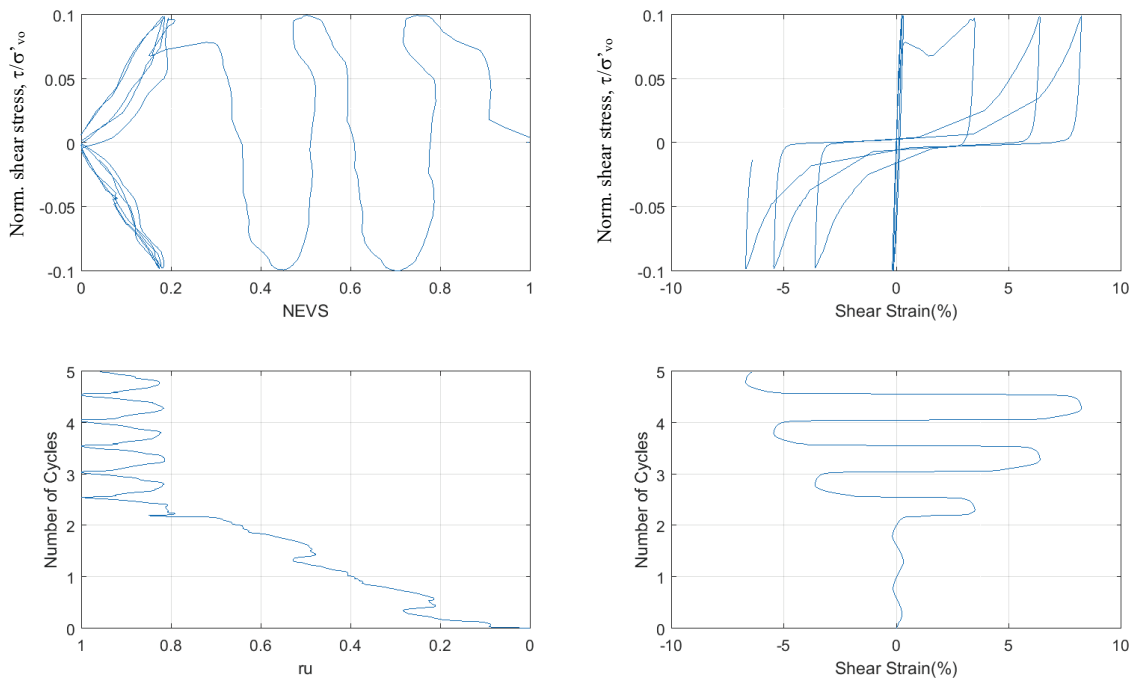


Figure 3-18: Results of Uniform Constant Volume CSS Test in Dense Sand,  $\sigma'_{vo} = 200$  kPa, CSR = 0.1

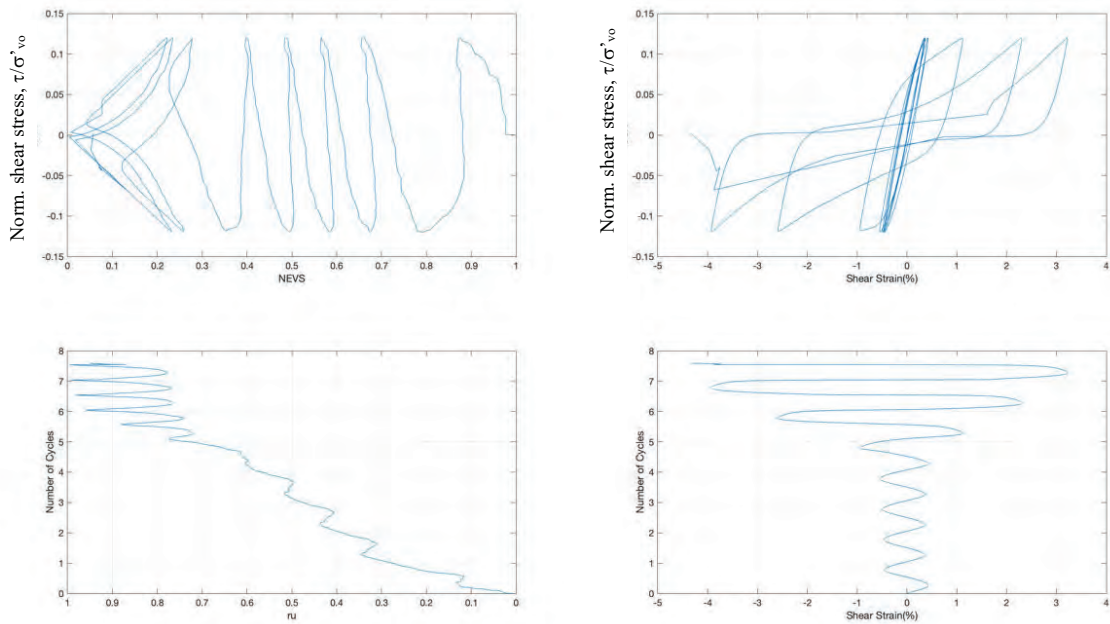


Figure 3-19: Results of Uniform Constant Volume CSS Test in Very Dense Sand,  $\sigma'_{vo} = 400$  kPa, CSR = 0.12

A detailed description of the progression of the sample during the cyclic simple shear tests is presented in section 4.4. The examples of test results presented in Figures 1-19 to 1-24 indicate different behavior during the test depending on the relative density of the sample and the applied Cyclic Stress Ratio. Samples with higher initial relative density need more cycles to reach failure, and therefore dissipated more energy prior to failure. It is important to note that even though tests performed with different initial effective vertical stresses and the same applied CSR behave similarly regarding the number of cycles to failure, the dissipated energy for samples with larger initial effective vertical stresses is significantly more, as the area under the hysteretic curve will be larger (the applied shear stress is larger for the same CSR and larger initial effective vertical stress).

Due to the large number of tests to process, the data processing was performed using a Matlab program, which calculated the number of cycles and the energy dissipated to failure, utilizing several failure criteria, and output that data in a spreadsheet (Excel) file. Details on the calculation of the dissipated energy can be presented in section 4.2 and Figure 4-1. Those results for each test were pasted into a master spreadsheet, where the different failure criteria could be selected, and different test cases could be filtered. In this research, the Double Amplitude Strain of 7.5% was the considered failure criterion, and the energy was calculated to the Zero shear stress before that 7.5% strain.

One convenient way of summarizing the uniform cyclic results is showing the equivalent to the S-N curves (CSR vs number of cycles to failure) for all the tests. Figures 1-25 to 1-30 show those curves for uniform tests at different relative densities and initial effective stress.

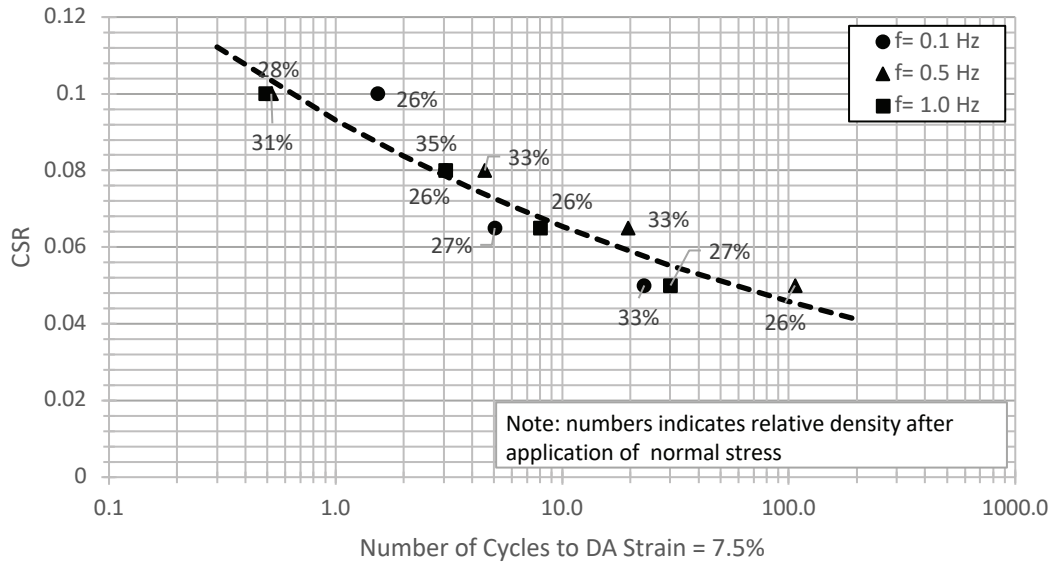


Figure 3-20: Cyclic resistance curve for loose sand with  $\sigma'_{vo} = 100\text{kPa}$

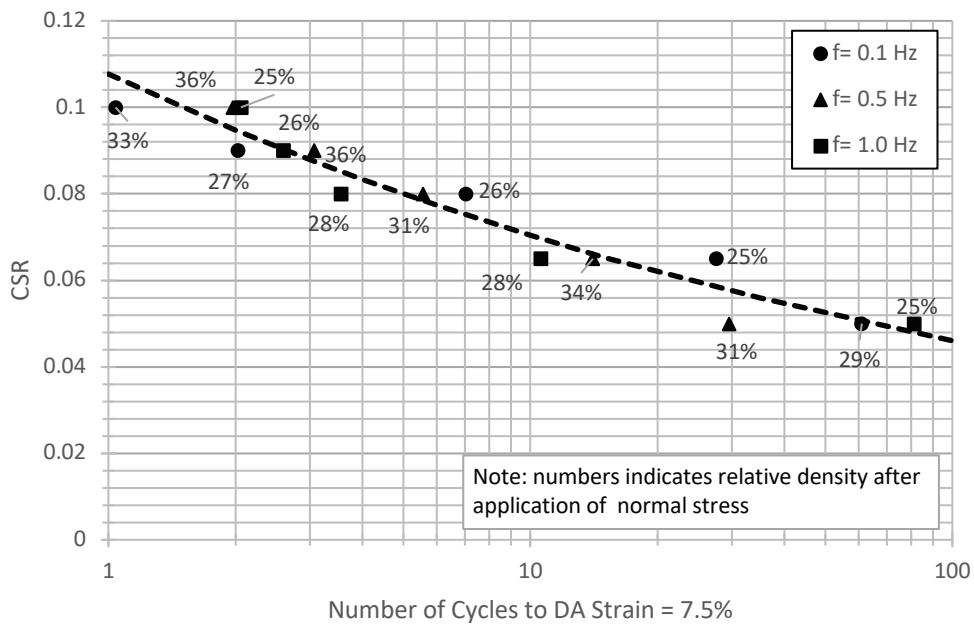


Figure 3-21: Cyclic resistance curve for loose sand with  $\sigma'_{vo} = 200\text{kPa}$

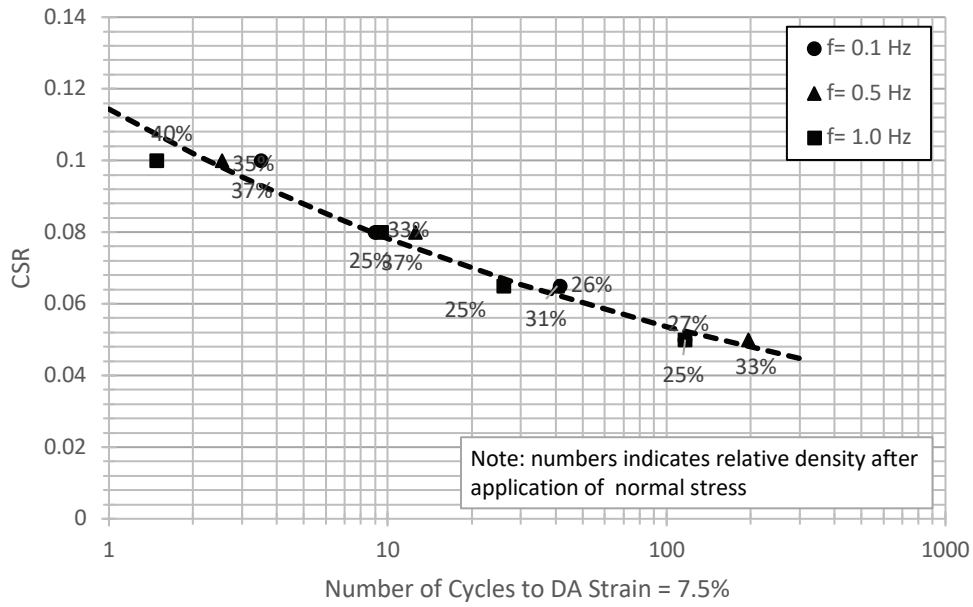


Figure 3-22: Cyclic resistance curve for loose sand with  $\sigma'_{vo} = 400\text{kPa}$

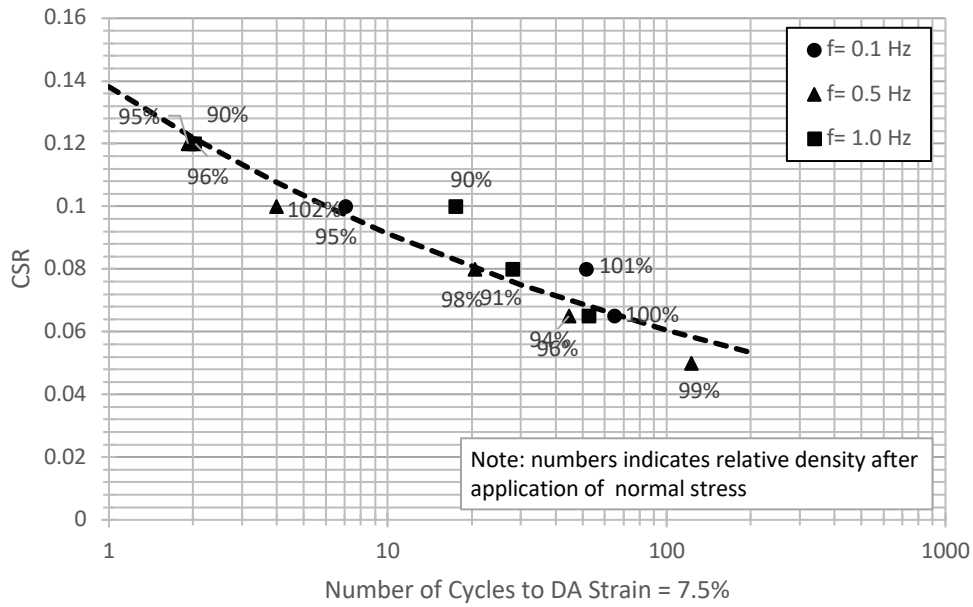


Figure 3-23: Cyclic resistance curve for dense sand with  $\sigma'_{vo} = 100\text{kPa}$

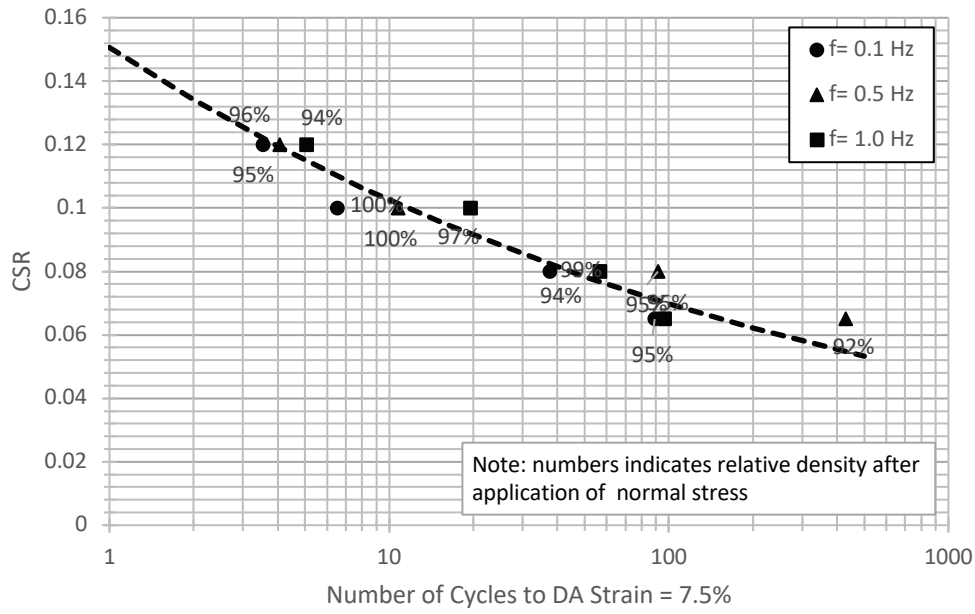


Figure 3-24: Cyclic resistance curve for dense sand with  $\sigma'_{vo} = 200\text{kPa}$

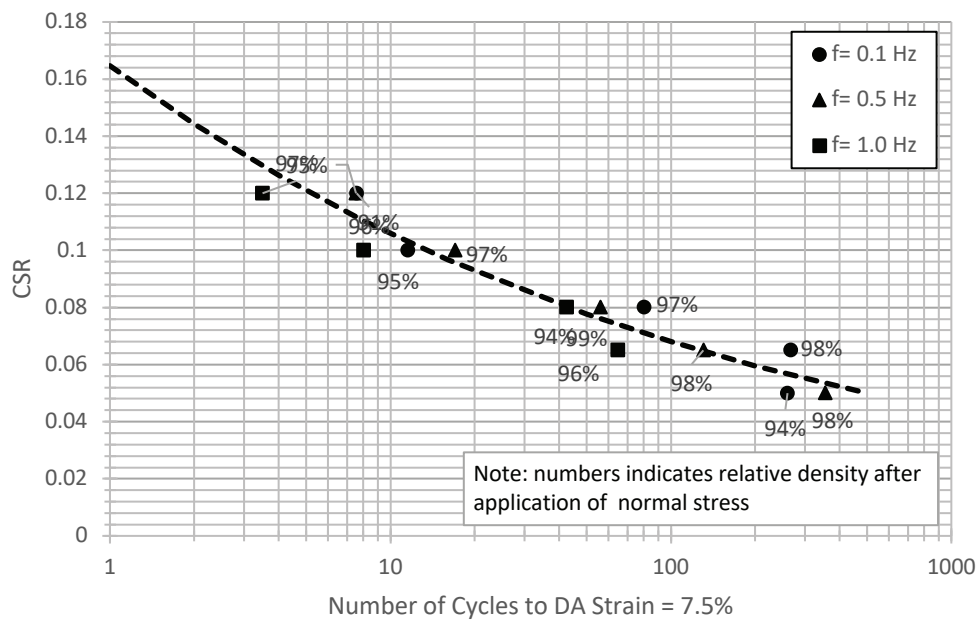


Figure 3-25: Cyclic resistance curve for dense sand with  $\sigma'_{vo} = 400\text{kPa}$

Figure 2-4 and 2-5, in section 2-4 show a summary of the calculated dissipated energies to failure for most of the tests performed in this study and indicate that the cumulative dissipated energy to failure is reasonably constant for a given initial sample state, though the results also show some important scatter and variability that is inherent to these kind of tests in geotechnical engineering. A full description of those figures is also presented in the aforementioned section.

Figure 2-6, also in section 2-4, shows the variation of the cumulative dissipated energy to failure with the initial vertical effective stress and with the relative density of the sample. A detailed description of these graphs is also show in that section.



## 4. *Manuscript #1: Specific Dissipated Energy as a Failure Predictor for Uniform Sands under Constant Volume Cyclic Simple Shear Loading*

The following manuscript was published in the KSCE Journal of Civil Engineering.

### 4.1. Introduction

Most of the early literature involving experimental studies of the cyclic behavior of sands have involved tests with uniform sinusoidal loading signals. However, nowadays with recent advances in testing equipment and control systems, it is more common to find published laboratory tests where the soil samples are subjected to more realistic loading conditions that better represent what soil layers experience during actual earthquakes (e.g. Liang et al., 1995; Tatsuoka & Silver, 1981; Xu et al., 2019). The modern geotechnical testing devices permit additional studies like the one described in this thesis to help improve our understanding of the cyclic behavior of sands under more general loading conditions. As summarized in the literature review of this chapter (section 4.2), many experimental studies on sands have been related to the study of liquefaction of saturated sands. Most of the early studies on sand liquefaction have involved use of cyclic triaxial testing on saturated sand samples under a harmonic deviatoric stress (e.g. Azeiteiro et al., 2017; Evans, 1993; Seed & Lee, 1966; Silver et al., 1976). The early use of uniform sinusoidal load cycles required approximating the complex earthquake field loading conditions to an equivalent number of uniform load cycles (e.g. Annaki & Lee, 1977; Seed et al., 1975). As described later in the literature review section, this equivalency was initially based on achieving similar levels of cumulative damage with the equivalent uniform sinusoidal load to the cumulative damage under the more general loading demand. The more recent liquefaction literature has involved laboratory studies using cyclic simple shear tests and cyclic torsional shear under irregular load cycles. The ability to routinely perform lab tests that use more realistic and general loading types appears to have shifted the focus in liquefaction behavior research from cumulative damage towards cumulative dissipated energy (Green et al., 2000; Green & Terri, 2005b; Kokusho & Tanimoto, 2021).



In addition to liquefaction research, the use of specific dissipated energy may have application as a predictor of failure of sands under other loading types, sample states, or boundary conditions. In this research the focus is not liquefaction of sand, but rather specific dissipated energy of dry sands subjected to constant volume simple shear load cycles of various types.

Specifically, this chapter describes and summarizes the results of a comprehensive experimental program carried out to investigate whether the specific dissipated energy, i.e., the dissipated energy per unit volume of the sample, by the soil sample to reach failure is only dependent on the initial state of the sample and independent of the characteristics of the applied cyclic simple shear loading applied. To test this hypothesis, a total of 269 constant volume cyclic simple shear tests were performed on Ottawa sand samples prepared at 9 different initial states and a wide range of cyclic shear loading types. For all the tests performed the progression towards failure was carefully monitored and the computed accumulation of specific dissipated energy was tracked until failure was reached. This chapter is organized into sections that include background and literature review, description of the experimental program including methodology, presentation and discussion of results, and a final section with a summary and conclusions drawn from this study.

## 4.2. Background and literature review

As mentioned above, the first experimental studies on liquefaction and cyclic behavior of soils involved using testing devices that primarily applied uniform sinusoidal cyclic loading. This situation required estimating an equivalency between non-uniform loading, like the type experienced by soil samples during earthquakes, and uniform sinusoidal loading. For example, the approach based on an equivalent number of uniform cycles was proposed by Seed et al. (1975) and Annaki & Lee (1977). This approach allowed evaluating the effects of different earthquake loadings on a soil tested under a simplified uniform sinusoidal loading and was based on an approach that has long been used to study fatigue of metals. For example, the Palmgren-Miner (P-M) (Miner, 1945; Palmgren, 1924) cumulative damage hypothesis was originally developed for metal fatigue and has been applied extensively in geotechnical earthquake engineering to find this equivalency between irregular and uniform loading (e.g. Annaki & Lee, 1977; Seed et al., 1975; Tatsuoka & Silver, 1981). The P-M model assumes that

the damage leading to failure accumulates linearly with the number of applied cycles of loading. In the P-M model the cumulative damage is computed considering that different levels of damage will be produced in the soil subjected to a non-uniform cyclic loading. The damage produced is computed for a particular load cycle, considering that an irregular loading will contain different levels of load amplitude (e.g., different levels of cyclic stress ratio or CSR), and the soil is assumed to have reached failure when the accumulated damage computed for the different load cycles reaches a value of 100%. An equivalent number of uniform cycles at any stress level would be the value that would cause the same amount of damage to the sample. A detailed description of the P-M hypothesis can be found in Green & Terri (2005). The earlier implementation of cumulative damage based on the P-M hypothesis assumed a linear accumulation of damage. A modified non-linear cumulative damage hypothesis was proposed by Lasley (2015) and is considered a substantial improvement with respect to P-M based approaches as the computed damage is load-dependent. Cumulative damage, linear or nonlinear, remains a popular approach to estimate liquefaction failure for irregular loading demand when using experimental data that is based on application of uniform harmonic loading.

An alternative approach to the use of an equivalency between irregular loading to equivalent uniform cycles is to focus on the accumulated energy dissipated by the soil during any kind of loading demand until it reaches failure. For example, several researchers have proposed the use of energy dissipation to evaluate liquefaction potential (e.g. Azeiteiro et al., 2017; Fardad Amini & Noorzad, 2018; Figueroa et al., 1994; Russell A. Green & Terri, 2005; Ishac & Heidebrecht, 1982; T. Kokusho, 2017; T. Kokusho & Mimori, 2015). The dissipated energy per unit volume of the sample, or specific dissipated energy, can be tracked during a cyclic simple shear test (CSS) by computing the area of the hysteresis loops for each shear stress versus shear strain load cycle. Examples of the dissipated energy per unit of volume for different cycles of a representative constant volume CSS test are shown in Figure 4-1. The cumulative specific dissipated energy experienced by the test sample can then be computed by adding the different hysteresis loops areas in the sequence of load cycles until sample failure is reached. The stress-strain cycles from a representative CSS test shown in Figure 4-1 show small energy dissipation for the initial load cycles, and larger hysteresis loops as the number of load cycles increases resulting in a faster rate of dissipated energy towards the end of the test.

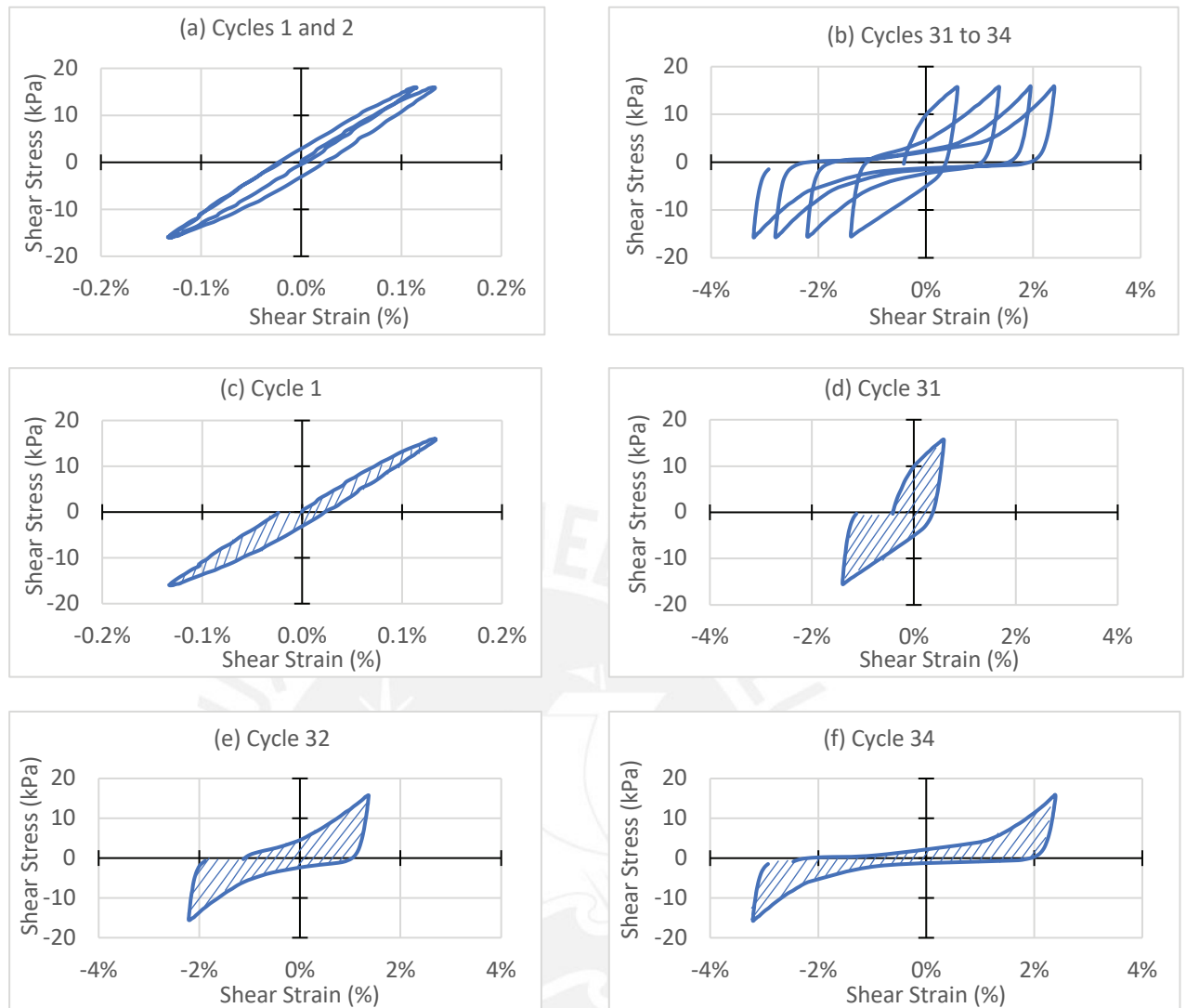


Figure 4-1. Example of Different Stress-Strain Load Cycles from a Representative CSS Test from the Present Study: (a) Stress-Strain Cycles 1 and 2, (b) Stress-Strain Cycles 31 to 34, (c) Hysteresis Loop Used in the Dissipated Energy Calculation for Cycle 1, (d) Hysteresis Loop Used in the Dissipated Energy Calculation for Cycle 31, (e) Hysteresis Loop Used in the Dissipated Energy Calculation for Cycle 32, (f) Hysteresis Loop Used in the Dissipated Energy Calculation for Cycle 34

Figuroa et al. (1994) and Liang et al. (1995) successfully applied the dissipated energy concept to define liquefaction potential, and validated it using undrained hollow cylinder torsional shear tests on saturated sand specimens. According to these authors, the energy per unit volume needed to induce liquefaction is not dependent on the loading form and thus can be used to evaluate the liquefaction potential of sands under general earthquake loads. Green & Terri (2005) and Lasley et al. (2016) have also used the dissipated energy concept to investigate liquefaction of sands under general loading. These authors also proposed adjustments in the approach used to measure the dissipated energy per cycle to help deal with large hysteresis loops that occur near the onset of liquefaction when significant

soil softening has occurred. Kokusho (2013) reported that the cumulative dissipated energy measured on reconstituted sands tested in cyclic triaxial tests under uniform harmonic loading correlated well with pore-pressure buildup, induced strain, and onset of liquefaction. Kokusho & Kaneko (2018) confirmed this finding for similar sand samples tested using torsional simple shear tests not only under uniform harmonic loading but also under a variety of irregular load cycles. The above studies focused on liquefaction behavior of reconstituted sand samples using cyclic simple shear tests and cyclic torsional simple shear, and all support the notion that cumulative dissipated energy predicts cyclic liquefaction reasonably well irrespective of the stress-time history used in the testing. In contrast, Kokusho & Tanimoto (2021) found that the uniqueness of dissipated energy when studying the liquefaction behavior of intact soil samples in Japan, that include the inherent variability found in natural deposits, did not yield a unique correlation between cumulative energy and liquefaction when tested using cyclic triaxial tests. For intact samples and this test type, the authors found that the number of cycles to liquefaction was dependent on the level of CSR used in the test.

In summary, the existing literature involving the application of cumulative dissipated energy for the most part show that cumulative dissipated energy is a promising approach to help predict reasonably well cyclic liquefaction of reconstituted sand samples tested under cyclic simple shear and cyclic torsional shear irrespective of the stress-time history used in the testing. However more experimental studies are required to help assess the level of accuracy of the energy-based approach. The study presented herein hopes to contribute by adding to the limited number of data sets involving uniform and non-uniform load cycles and by presenting information related to the variability of the measured accumulated specific dissipated energy so the engineering community can assess the accuracy of using this parameter as a failure predictor for sands under general cyclic loading.

### 4.3. Experimental program

The experimental program involved 269 cyclic simple shear tests conducted using an Advanced Dynamic Cyclic Simple Shear machine (ADVDCSS) manufactured by GDS Instruments. This system can independently control the vertical axial (normal) and the horizontal (shear) loads or displacements using GDS electromechanical force actuators controlled under closed loop conditions. Figure 4-2 shows

a general view of the ADVDCSS system, which shows the location of the vertical and horizontal actuators and the sample box. All the tests presented in this research work were run under constant volume (i.e., constant height) conditions. The samples were prepared using a cylindrical CSS sample box conformed by a stack of Teflon rings with a diameter of 70 mm and approximate sample height of 20 mm.

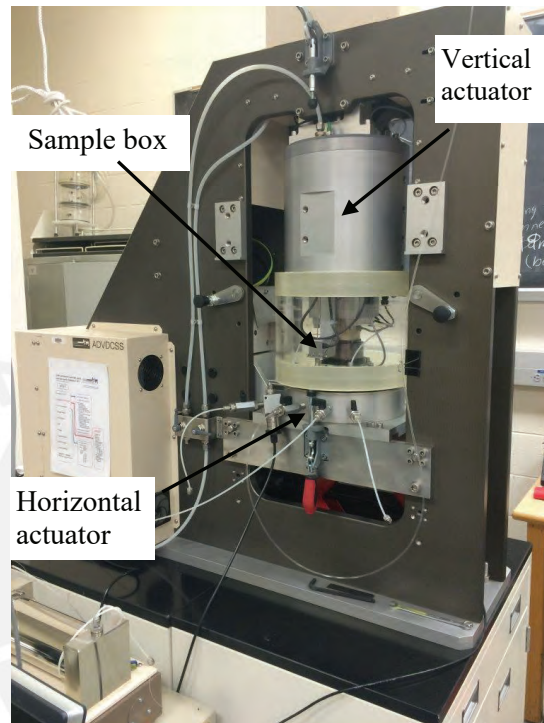


Figure 4-2. General View of ADVDCSS System

#### 4.3.1. Test sand

The test sand used in this experimental program was Ottawa 20/30 silica sand. This is a uniform, poorly graded silica sand with sub-rounded to rounded grains. The mean particle size ( $D_{50}$ ) of this sand is 0.71 mm, and the 20/30 designation is based on having 95 % retained between the ASTM standard sieves #20 and #30. The maximum and minimum void ratios were measured using laboratory procedures in general accordance with ASTM Standard D4253 (ASTM, 2016a) and D4254 (ASTM, 2016b), respectively. The average maximum and minimum void ratio values obtained for the test sand were 0.644 and 0.503, respectively. The CSS tests described later were performed using dry Ottawa sand samples prepared at three different levels of relative density as shown in Table 4-1. This table shows the mean and standard deviation values for the 3 levels of relative density after application of the normal stress used in the CSS testing program.

Table 4-1. Initial states of CSS samples and direct shear monotonic shear strength.

Data Set ID	Number of tests N	Initial State			Shear strength		
		Relative Density		Initial Stress	Peak	Residual	
		State	Mean	St. Dev.	$\sigma_{vo}'$ (kPa)	$(\phi'_p)$ (deg)	$(\phi'_r)$ (deg)
1	31	Loose	27.3%	3.1%	100	29°	29°
2	42		29.0%	4.1%	200		
3	46		29.7%	3.7%	400		
4	7	Dense	63.1%	4.7%	100	34°	32°
5	4		70.3%	5.2%	200		
6	4		69.0%	6.0%	400		
7	35	Very Dense	92.5%	3.1%	100	40°	32°
8	43		92.9%	3.0%	200		
9	46		95.4%	2.2%	400		

The loose samples (average  $D_r = 28.7\%$ ) were prepared by placing approximately 130 g of dry sand inside a 50 mm diameter open pipe that was placed vertically at the center of the CSS sample box. The pipe was then quickly pulled upwards allowing the dry sand to fill the CSS sample box in a loose condition. Next the sample top was carefully leveled, and the initial sample height measured before normal stress application. The procedure used to prepare the dense samples (average  $D_r = 67.5\%$ ) involved using the dry air pluviation through a glass beaker with a 5 mm steel nozzle from a height of 10 mm. The samples prepared using this technique required an approximate weight of 131.7 grams. The height of the samples at the end of the air pluviation was measured and noted. The third set of samples were very dense samples (average  $D_r = 93.6\%$ ) were prepared using dry tamping placed in three equal weight portions. This set of samples involved a predetermined weight of sand of 141 grams that was split into three equal portions, and each layer tamped with a flat tamper weighing 125 grams tamped until each soil layer reached a target elevation mark. In all three sample preparation methods, the sample height was measured after sample preparation (before the application of the normal stress) and after normal stress application. The reported relative densities in Table 4-1 and in the result section correspond to the values corrected for the final sample height after normal stress application.

The shear strength of the Ottawa sand prepared at the three relative density levels described above was measured using a Geocomp ShearTrac II direct shear device. The direct shear tests were performed in general accordance with ASTM Standard D3080 (ASTM, 2011). The measured peak and residual

friction angles are summarized in Table 4-1 for the three levels of relative density considered in this study.

#### 4.3.2. Cyclic simple shear testing program

The cyclic simple shear testing program involved 269 tests conducted with the ADVDCSS GDS system. The cyclic shearing phase for all tests was stress controlled and the applied normal stress was actively controlled to ensure constant sample height conditions, i.e., constant volume. The CSS test program involved 9 possible sample initial states corresponding to 3 initial relative densities (loose, dense, or very dense) and 3 initial normal stresses (100, 200, or 400 kPa) (See Table 4-1). Samples at these 9 possible initial states were subjected to a wide range of cyclic shear loads that are listed into 5 types as described in Table 4-2. The first loading type listed is uniform cyclic loading. As shown in this table the test program involved 18 uniform cyclic shear loading demands that consisted of harmonic shear stresses time histories that correspond to the 6 different levels of cyclic stress ratios (CSR) and 3 frequencies used in this study. The shear stress amplitude is characterized by the CSR which is defined as:

$$\text{as: } CSR = \tau_{cyc} / \sigma'_{vo} \quad (4-1)$$

where,  $\tau_{cyc}$  is the amplitude of the harmonic shear stress loading time history, and  $\sigma'_{vo}$  is the initial normal stress level applied to the test sample before the initiation of the shearing phase.

Table 4-2 also lists four types of non-uniform cyclic loading demands that were used in this study for several of the initial sample states. Non-uniform load pattern Type-1 consisted of alternating sine wave cycles with a constant frequency and two different stress amplitudes (i.e., CSR values) that were alternated in a pattern repeatedly until failure. The Type-1 non-uniform load cycles involved combinations of 4 CSR values and 3 frequencies. The non-uniform load pattern Type-2 consisted in alternating sine wave cycles with a constant shear stress amplitude (i.e., CSR), but changing frequency that was alternated in a pattern repeatedly until failure. Type-2 non-uniform load cycles involved 5 different levels of CSR combined with two frequency values. The non-uniform load pattern Type-3 is similar to Types 1 and 2, but for this loading type the pattern of sine wave cycles varied both the frequency and the shear stress amplitude that was repeated until reaching failure. Type-3 non-uniform loading involved 4 CSR values, and 2 frequencies. Finally, the non-uniform load pattern Type-4

involved applying a sequence of a predetermined number of uniform sine wave cycles at a constant frequency and a low amplitude (CSR) that was then followed by a single sine wave cycle at a high amplitude (CSR) and with the same frequency as in the lower CSR sequence. This pattern of loading was repeated until failure. The large amplitude (CSR) cycle was considered a spike type loading that occurred after the application of the lower CSR sequence. The lower CSR sequences applied in this study involved three number of uniform sine wave cycles (N= 25, 50, or 100) that was then followed by the single large CSR sine wave cycle (i.e., the spike).

Table 4-2. Loading patterns used in this study.

<b>Type of Cyclic Loading</b>	<b>Description</b>	<b>Parameters</b>
<b>Uniform</b>	- CSR and frequency are constant in time. - 18 uniform harmonic load cycles.	- CSR values: 0.05, 0.065, 0.08, 0.09, 0.10, and 0.12. - Frequencies: 0.1, 0.5 and 1 Hz.
<b>Non-uniform Type-1</b> (Alternating sine waves with different CSR and constant frequency)	- Alternating sinusoidal waves with constant frequency, but two different CSR levels that are repeated until failure.	- CSR values: combination of 0.05, 0.065, 0.08, and 0.1. - Frequencies: 0.1; 0.5 and 1 Hz.
<b>Non-uniform Type-2</b> (Alternating sine waves with different frequency and constant CSR)	- Alternating sinusoidal waves with constant CSR level, but two different frequencies that are repeated until failure.	- CSR values: 0.05; 0.065; 0.08; 0.10 and 0.12. - Frequencies: combinations of 0.1 and 0.5 Hz.
<b>Non-uniform Type-3</b> (Alternating sine waves with different frequency and CSR)	- Alternating sinusoidal waves with two different values of CSR and two different frequencies that are repeated until failure.	- CSR values: combination of 0.05; 0.065; 0.08, and 0.1. - Frequencies: combinations of 0.1 and 0.5 Hz.
<b>Non-uniform Type-4</b> Non-uniform CSR (amplitude) - Large Spike	- Load pattern had a constant frequency. - Sequence of low of N uniform sinusoidal cycles at a low CSR value, followed by a single sine wave cycle at a high CSR value. Sequence repeated until failure reached.	- Number of low CSR uniform sine wave cycles varied from 25, 50, or 100 repetitions.

All 9 sets of CSS tests were carried out until failure was reached. For this experimental study failure was defined when the sample reached a 7.5% double-amplitude shear strain, which is a failure criterion commonly used in the cyclic behavior of sands literature (e.g., Finn & Vaid, 1977; S. Lasley, 2015; Vaid & Sivathayalan, 1996; Sivathayalan & Ha, 2011). For each CSS test results were recorded to prepare shear stress-strain plots, variation of shear strain with number of load cycles, and other summary plots (See next section). These results were used to compute the cumulative dissipated energy per unit volume for each CSS test sample until failure was reached. The cumulative dissipated energy per unit



volume was computed to the last zero stress instance in the shear stress-strain cycle just prior to failure defined herein when a 7.5% double amplitude shear strain is reached (S. Lasley, 2015). A summary of relevant test results is provided in the next section.

## 4.4. Results

A set of representative results obtained in this study for a CSS test that used uniform load cycles are shown in Figure 4-3. In this figure the CSS test results are presented using 4 plots that have matching axes in the vertical and horizontal directions and are plotted in the same scales. The graph in the upper left (Figure 4-3(a)) shows the Normalized Effective Vertical Stress (NEVS), which is defined as the ratio between the actual vertical stress in the test and the initial vertical stress applied to the sample at the beginning of the dynamic shearing stage of the test, vs the normalized shear stress ( $\tau / \sigma'_{vo}$ ). Initially the samples have an NEVS of 1, and as the cyclic shearing progresses, the NEVS value starts to decrease until approaching a value of zero at failure. The value of NEVS decreases because the applied normal stress decreases during loading to ensure that the testing condition of constant sample height (i.e., constant volume) is maintained. This graph illustrates the progressive decrease of the vertical stress with number of applied cycles. When the sample approaches a NEVS value of 0, the shear strains start to increase dramatically which each additional cycle of load applied to the sample and the hysteresis loops and associated dissipated energy (like the ones shown in Figure 4-1) tend to increase in magnitude. The graph in the upper right (Figure 4-3(b)) shows the shear strain vs the normalized shear stress ( $\tau / \sigma'_{vo}$ ), illustrating the progression in size of hysteresis loops and increase of shear strain levels as the applied load cycles increase. The plot in the lower right (Figure 4-3(d)) shows the variation of shear strain with number of simple shear load cycles. This graph effectively illustrates the number of cycles for which the shear strains start to increase dramatically. Closing Figure 4-3, in the lower left corner, Figure 4-3(c) shows the complement to NEVS, defined as  $1 - \text{NEVS}$ , versus the number of applied load cycles. It should be noted that some authors in the liquefaction literature approximate  $1 - \text{NEVS}$  from constant volume CSS tests performed on dry samples as an equivalent pore pressure ratio ( $r_u$ ) and approximate the shear strain failure as equivalent to a liquefaction failure that would be observed in an undrained CSS test performed on a saturated sample with the same initial state, under

constant total normal stress. Experimental proof of this equivalency is not conclusive in the literature and there is some debate in the geotechnical community of this often-used equivalency. To avoid entering in this debate, in this research we do not attempt to report this equivalency with undrained CSS tests, and only intended to study and report the failure behavior observed on dry sands tested under constant volume CSS tests.

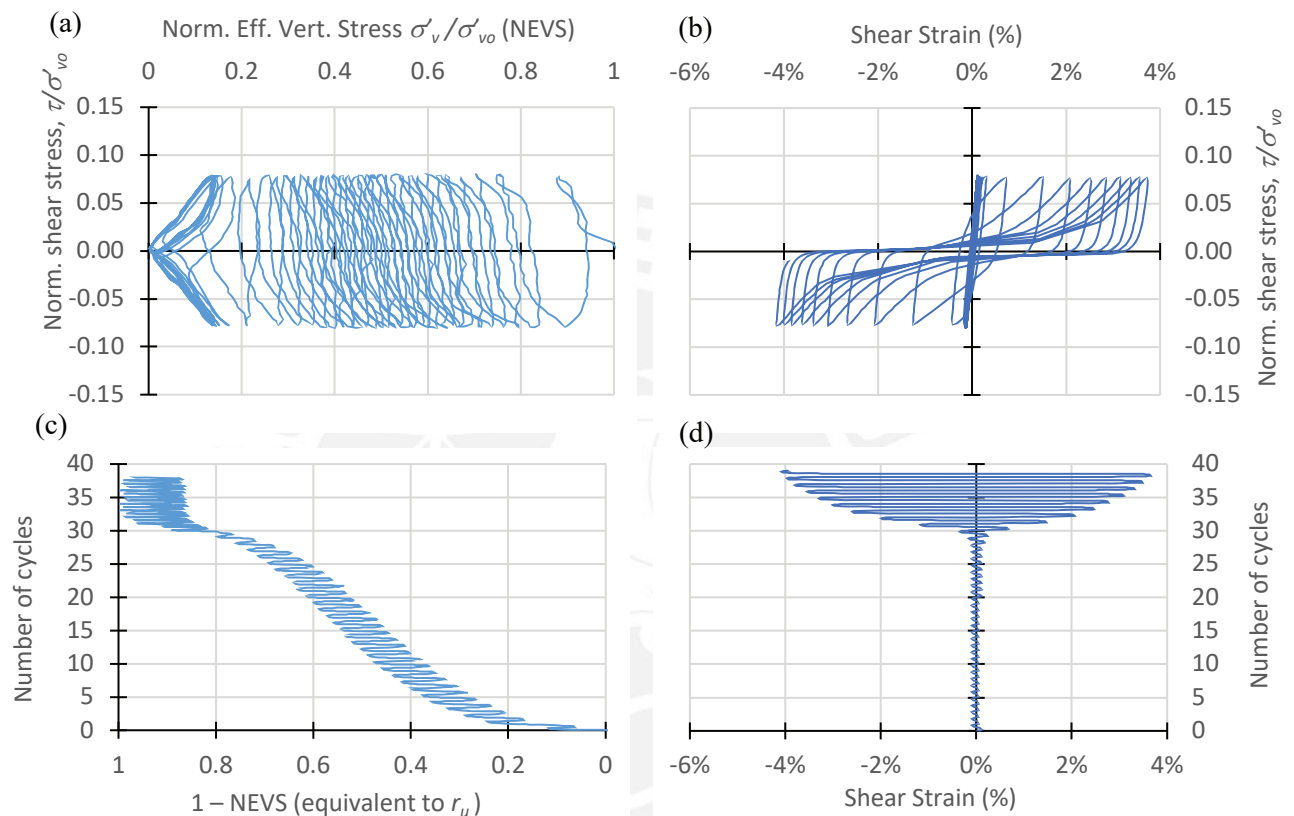


Figure 4-3: Results of Uniform Constant Volume CSS Test in Very Dense Sand,  $\sigma'_{vo} = 200$  kPa,  $CSR = 0.08$ ,  $f = 0.1$  Hz: (a) Norm. Effective Vert. Stress (NEVS) vs Normalized Shear Stress, (b) Shear Strain (%) vs Normalized Shear Stress, (c)  $1 - NEVS$  vs number of cycles, (d) Shear Strain (%) vs Number of Cycles

The representative constant volume CSS test shown in Figure 4-3 was performed on a very dense dry sand at an initial normal stress of 200 kPa, subjected to uniform harmonic cyclic stress cycles with a CSR of 0.08 and a frequency of 0.1 Hz. The progression towards failure for this sample can clearly be seen in this 4-way graph, where the shear strain starts to increase dramatically after an application of about 30 cycles and the sample finally reaches the failure criterion at Cycle 37.

Although not the focus of this research, a close examination of the CSS test results showed that for most tests the first cycles of cyclic shear stress loading caused very small levels of shear strain that were typically less than 0.5%. As the number of cycles progressed the NEVS (normalized effective vertical

stress) value gradually decreased as indicated in the representative CSS results shown in Figure 4-3. For most CSS tests the shear strains rapidly increased beyond the 0.5% value when the NEVS decreased to values between 0.1 and 0.3. The upper NEVS limit of 0.3 was observed for CSS tests involving higher CSR values, while the lower NEVS value of 0.1 was observed for CSS tests subjected to lower values of CSR, independent of the initial effective vertical stress applied to the sample or the sand initial relative density. However, CSS samples with a higher initial vertical stress and/or a higher relative density required the application of larger number of load cycles to reach these larger shear strain values beyond 0.5%. The CSS test results also showed an important difference in stress-strain behavior for loose and very dense sand when approaching the critical NEVS values of close to zero. For loose samples, the final failure, defined when a double amplitude of shear strain of 7.5% was achieved, usually occurred within 1 to 3 cycles after the NEVS value reached zero. In contrast, very dense samples did not achieve the failure criterion when the NEVS value was close to zero, as the observed shear strains increased more slowly compared to the loose samples and required 5 or more load cycles to reach failure.

The cumulative specific dissipated energy during cyclic loading was calculated for all CSS tests until failure by summing the areas inside the different hysteretic loops as described earlier and shown previously in Figure 4-1. These computed cumulative specific dissipated energy values were used to test the hypothesis of this study. The hypothesis was that for a given initial sample state the specific dissipated energy required to reach failure should be reasonably constant and independent of the type of shear stress time history used in the CSS testing. As mentioned before, in this study we used 9 initial sample states defined by the relative density and stress level at the start of the application of the cyclic loading time history. The values of measured cumulative specific dissipated energy obtained for the 9 initial states considered are summarized in Table 4-3. The results are also summarized graphically in Figure 4-4 and Figure 4-5 for the loose and very dense samples, respectively. Each of these two figures show three summary plots that correspond to initial effective vertical stress values of 100, 200, and 400 kPa. The data points presented in the different summary plots reported in Figs. 4 and 5 exclude statistical outliers, which were detected using the interquartile range (IQR) method (e.g., Zwillinger & Kokoska, 1999).

The summary plots in Figure 4-4 and Figure 4-5 show measured values of cumulative specific dissipated energy to failure for different loading times and a given initial sample state. For example, Figure 4-4(a) shows to the left the x-axis values measured for CSS tests performed using uniform load cycles. The symbol of each data point represents the frequency used and, in the corresponding x-axis labels indicate the CSR shear stress amplitude used. In a similar fashion, the data points presented towards the right end of the x-axis correspond to the different types of non-uniform loading cycles that were summarized in Table 4-2. It should be noted that for non-uniform loadings Type-1, Type-3, and Type-4 the labels in the x-axis show more than one CSR value depending on the characteristics of the non-uniform loading. This is not the case for non-uniform loading Type-2 where only a single CSR value is reported as this type of loading kept the CSR constant and varied only the frequency.

The research hypothesis posed in this study was that for a given initial sample state the cumulative specific dissipated energy required to reach failure should be reasonably constant and independent of the type of shear stress time history used in the CSS testing. The results in Table 4-3 and Figure 4-4 and Figure 4-5 show that the cumulative specific dissipated energy required to reach failure is reasonably constant for a given initial sample state. The results show important scatter and variability that is not uncommon in geotechnical engineering. The horizontal dashed lines shown in the summary plots of Figure 4-4 and Figure 4-5 correspond to the computed overall mean for all the cumulative specific dissipated energy values measured for a given initial sample state (i.e., for each of data sets). The main statistics computed for the cumulative specific dissipated energy values measured for the 9 initial states are summarized in Table 4-3. The level of dispersion of the measured cumulative specific dissipated energy values can be assessed from the range, standard deviation, and coefficients of variation (COV) reported in this table. For example, the coefficient of variation, obtained by dividing the sample standard deviation by the sample mean, is often used as a measure of the dispersion of data. The coefficients of variation obtained for the loose, dense, and very dense relative density states ranged from 26% to 44%, 13% to 38%, and 16% to 33%, respectively. Harr (1987) provided approximate descriptors of data variability based on the values of the coefficients of variation. This author considered a “low” variability for data sets with a COV below 10%, for COV values between 15% and 30% the data variability is “moderate”, and for COV values greater than 30%, a “high” variability is assigned.

Based on the simplified descriptors proposed by Harr (1987), and the computed COV values in Table 4-3, the cumulative specific dissipated energy to failure values measured for the samples with loose and very dense states were “medium to high”. In contrast, the variability was found to be between “low to high” for the data sets with a dense initial state. The larger values of COV for the denser states could be associated with the larger number of cycles required to achieve the failure criterion once the NEVS = 0 condition was achieved. The stress-controlled CSS tests also showed larger hysteresis loops as the sample approached failure resulting in a large value of dissipated energy per cycle that can have a great influence in the final value of the cumulative specific dissipated energy for a test. The high influence in the computed cumulative dissipated energy to failure of the selected failure criterion and the large values of dissipated energy in the typically large hysteresis loops of the final load cycles towards failure was also highlighted by Lasley (2015).

Table 4-3. Cumulative Specific Dissipated Energy

Data Set ID	Number of tests N	Initial State			Shear strength		
		Relative Density		Initial Stress	Peak	Residual	
		State	Mean	St. Dev.	$\sigma_{vo}'$ (kPa)	$(\phi'_p)$ (deg)	$(\phi'_r)$ (deg)
1	31	Loose	27.3%	3.1%	100	29°	29°
2	42		29.0%	4.1%	200		
3	46		29.7%	3.7%	400		
4	7	Dense	63.1%	4.7%	100	34°	32°
5	4		70.3%	5.2%	200		
6	4		69.0%	6.0%	400		
7	35	Very Dense	92.5%	3.1%	100	40°	32°
8	43		92.9%	3.0%	200		
9	46		95.4%	2.2%	400		

Despite the observed levels of data variability, the measured cumulative specific dissipated energy to failure values in this experimental study were found to be reasonably constant for a given sample initial state and independent of the type of cyclic stress time history applied to the sample (See Table 4-2 for range of load patterns considered). Furthermore, the levels of variability observed in this study for the measured dissipated energy to failure were found to be comparable to the variability reported by others in the literature for experimental studies involving uniform sands tested under cyclic simple shear loading (e.g., Kokusho & Kaneko, 2018; Lasley, 2015).

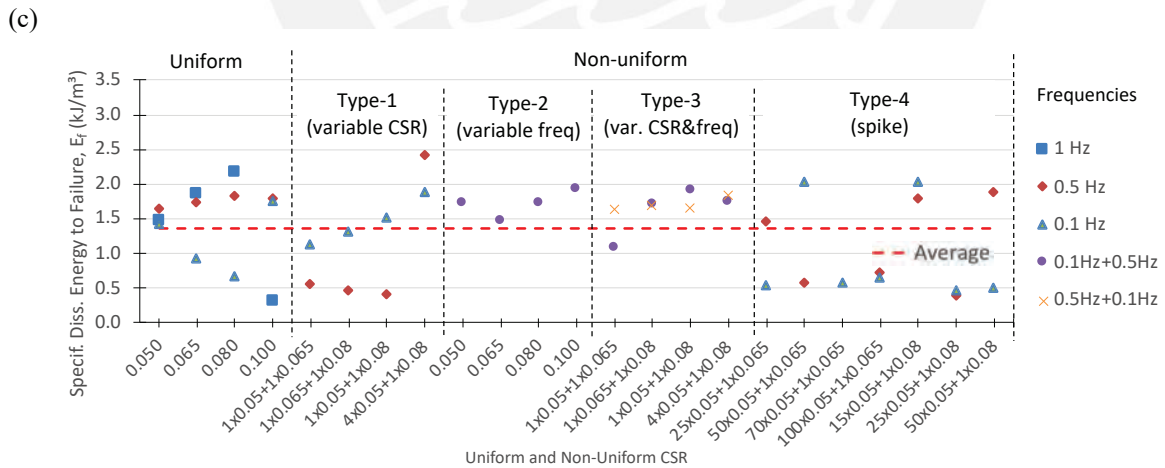
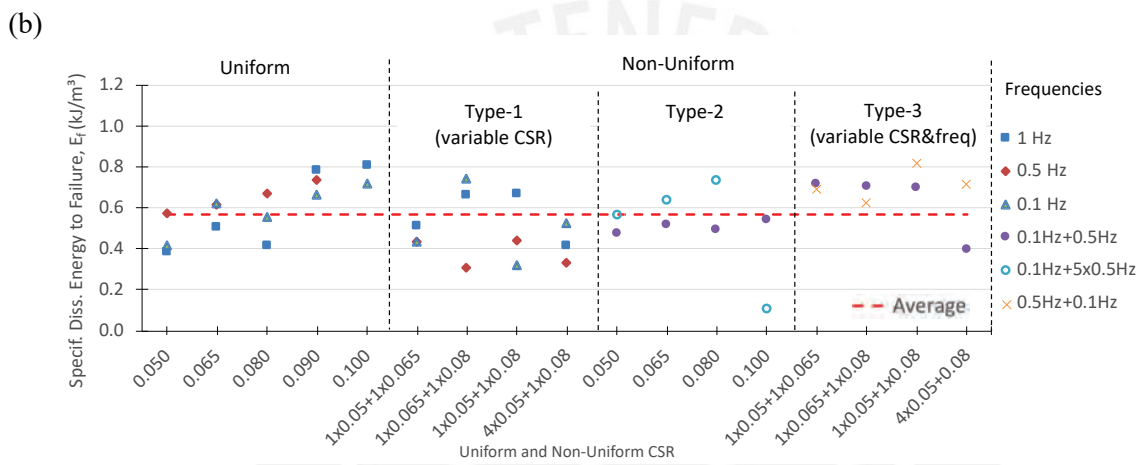
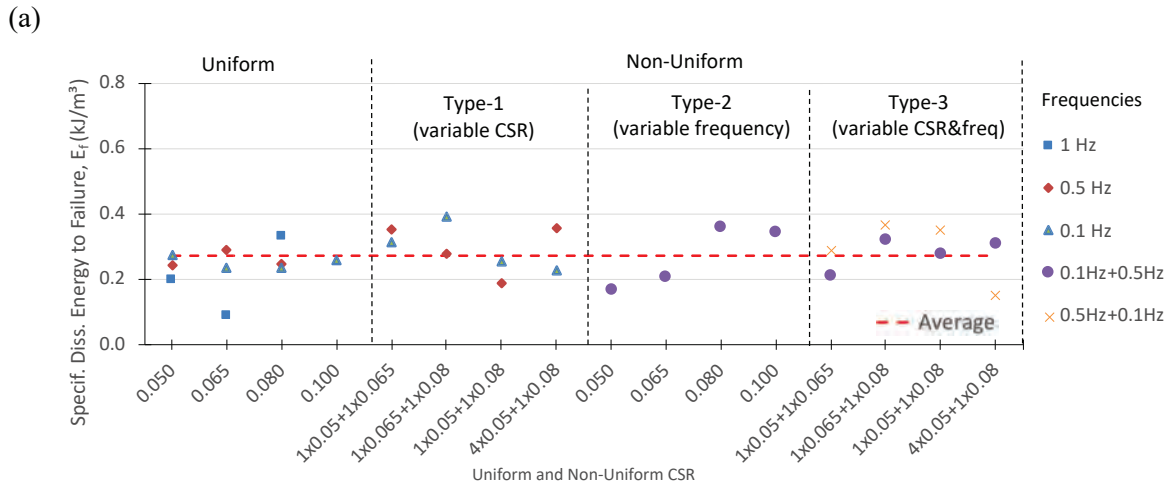


Figure 4-4. Specif. diss. energy to failure - Loose sand. (a)  $\sigma'_{vo} = 100\text{kPa}$ , (b)  $\sigma'_{vo} = 200\text{kPa}$ , and (c)  $\sigma'_{vo} = 400\text{kPa}$ .

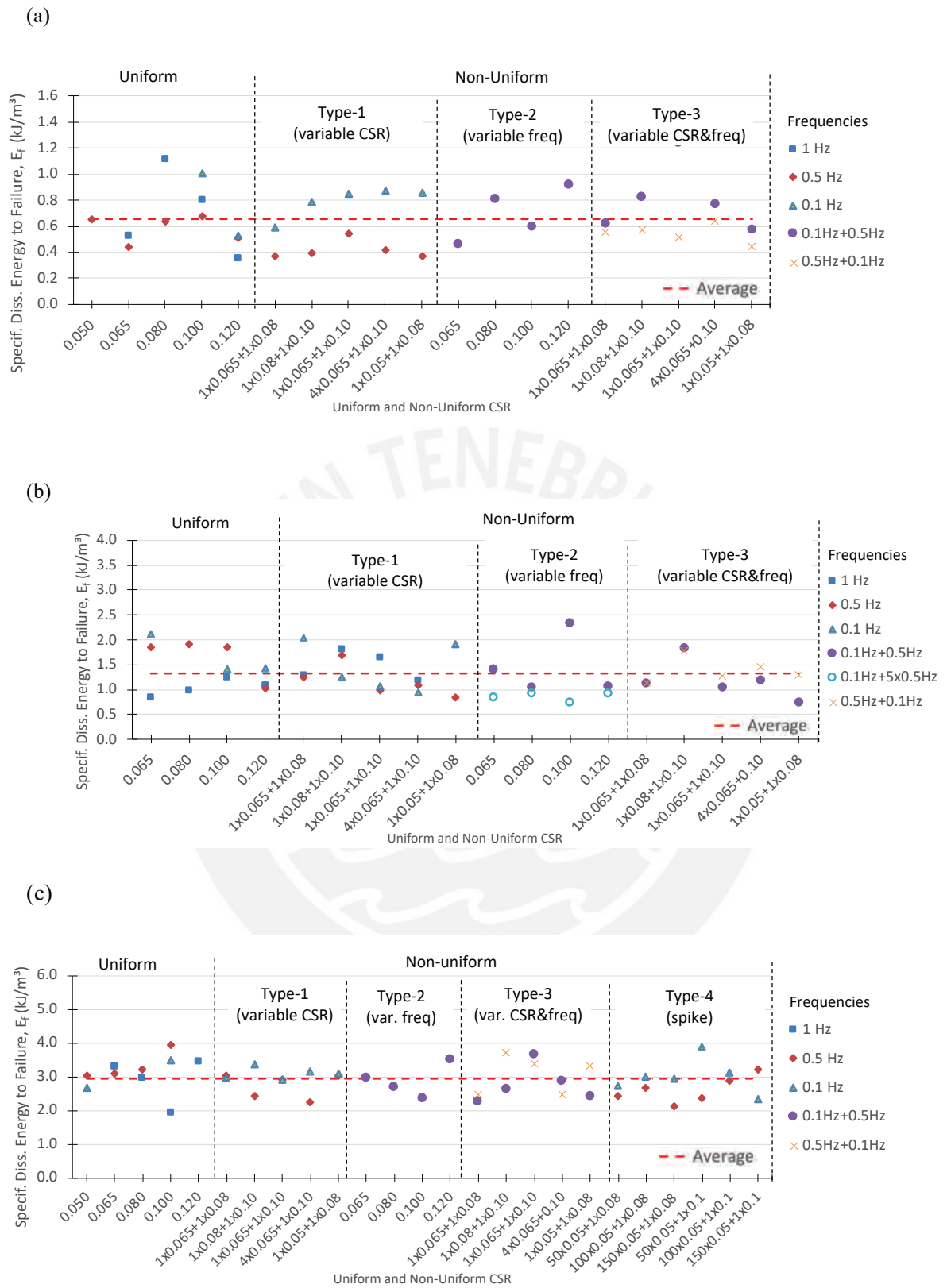
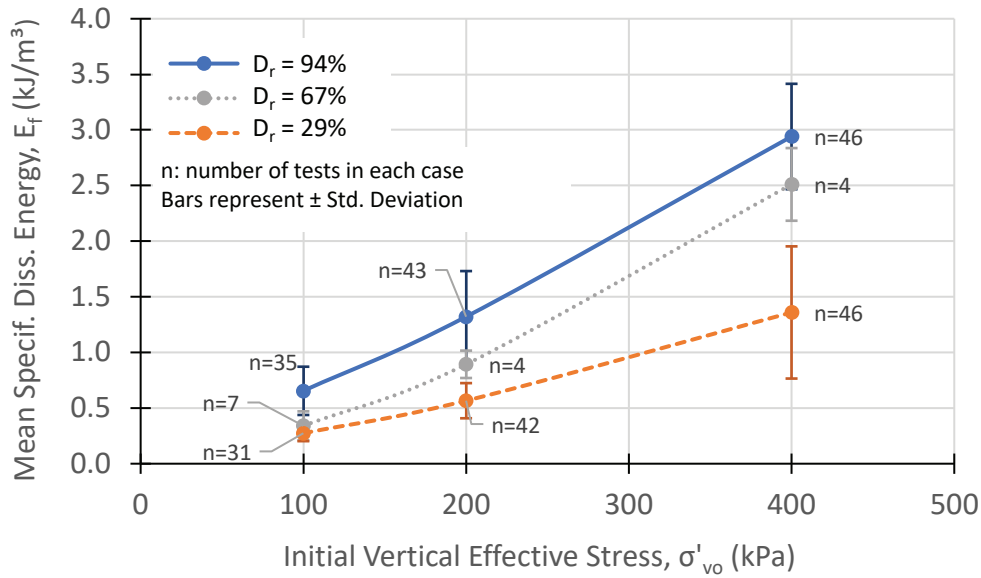


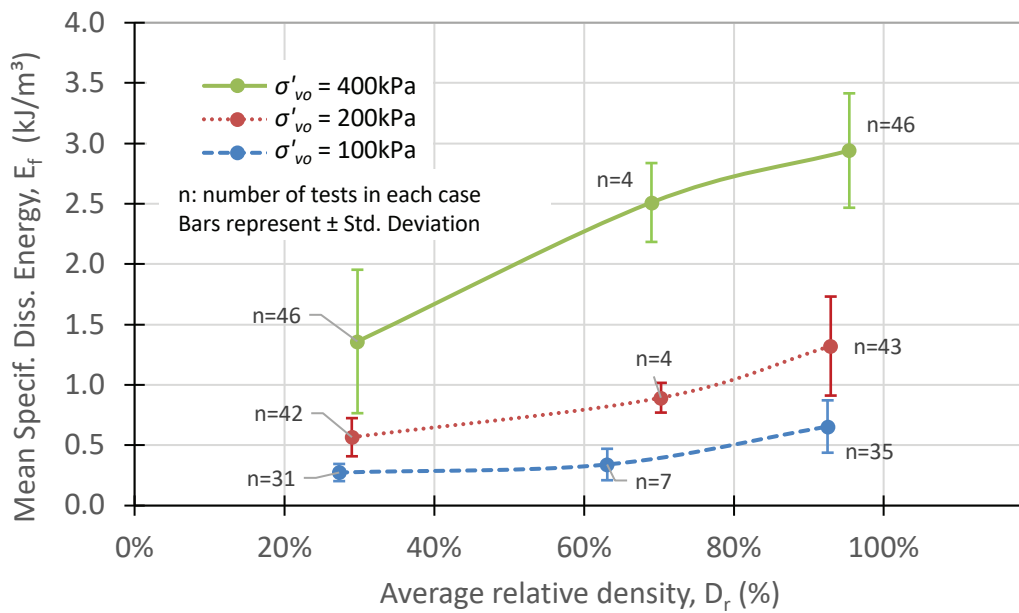
Figure 4-5. Specif. diss. energy to failure – Very dense sand. (a)  $\sigma'_{vo} = 100\text{kPa}$ , (b)  $\sigma'_{vo} = 200\text{kPa}$ , (c)  $\sigma'_{vo} = 400\text{kPa}$ .

The validity of the posed research hypothesis can be further investigated by plotting the mean cumulative specific dissipated energy values measured as a function of the applied initial stress level or the average initial relative density. These plots are shown in Figure 4-6. Figure 4-6 shows the variation of the measured mean cumulative specific dissipated energy to failure as a function of initial effective vertical stress level for the three levels of relative density considered. The data points shown in this plot represent the mean values, and the error bars indicate the standard deviation for each data set. This plot shows that the specific mean cumulative specific dissipated energy for a given initial relative density state increases with increasing initial effective stress level. Figure 4-6 (b) shows the variation of the measured mean cumulative specific dissipated energy to failure as a function of the initial relative density of the samples. This plot shows that the mean cumulative specific dissipated energy to failure for a particular initial effective vertical stress level increases with the increasing initial relative density of the sample. The two plots in Figure 4-6 show the dependency of the mean cumulative specific dissipated energy to failure to the initial state of the sample that is defined by both the initial normal effective stress ( $\sigma'_{vo}$ ) and the initial relative density ( $D_r$ ) of the CSS sample and did not depend on the characteristics of the applied cyclic shear loading applied as it included a wide range of loading types. Furthermore, if we compare the relative increases of mean cumulative specific dissipated energy to failure in both plots, the changes were larger for an increase in the initial effective vertical stress compared to an increase of the initial relative density of the samples. However, this observation is specific to the initial states considered in this experimental study where the range of relative densities considered did not cover the full range of values for the test sand used in the study. Finally, even though Figure 4-6 shows that the mean cumulative specific dissipated energy to failure depends on the initial sample state and not on the characteristics of the applied cyclic shear loading time history the error bars shown in Figure 4-6 reveal an important variability of the mean cumulative specific dissipated energy to failure.





(a)



(b)

Figure 4-6. Variation of the Mean Specific Dissipated Energy to Failure as a Function of (a) Initial Vertical Effective Stress ( $\sigma'_{vo}$ ), and (b) Average Initial Relative Density ( $D_r$ ).

## 5. *Manuscript#2: A simplified method for predicting failure of sands under general cyclic simple shear loading*

The following manuscript was published in ICE Geotechnical Research journal.

### 5.1. Introduction

Accurately predicting the cyclic behavior of sands subjected to either drained or undrained loading conditions remains a challenge in geotechnical engineering. The main challenge is predicting the accumulation of deformations and strains during cyclic loading and the occurrence of failure. This thesis presents a simplified approach to predict the failure of dry sands under constant volume cyclic simple shear independent of the characteristics of the shear stress time history (e.g., method can be applied also to non-uniform or irregular cyclic loading). The method is based on using a multivariable regression obtained using a relatively small number of experimental results performed on the sand of interest prepared at different sample initial states (i.e.,  $D_r$  and  $\sigma'_{v0}$ ) selected based on the project range of interest and subjected simply to only one level of sinusoidal simple shear loading until failure is achieved. The regression is performed on only one test per initial sample state, and it only requires use of a readily accessible, conventional cyclic simple shear device. It is important to point out that proposed methodology will yield a sand-specific regression in order to capture the intrinsic material properties that are unique to each test sand and are independent of the state of the sand. Examples of intrinsic material properties that make the regression specific to each test sand include grain shape, grain size distribution, mineralogy, mineral to mineral friction angle, and specific gravity. To highlight this, the proposed methodology was applied to two different test sands yielding different regressions in order to capture the unique intrinsic characteristics of each soil. The influence of the intrinsic properties in the shear behavior and strength of sands has been reported extensively in the literature (e.g., Been et al., 1991; Cho et al., 2006). Therefore, the regression obtained using the proposed simplified methodology is applicable only to the sand used in the testing program. The proposed simplified method is based on the cumulative energy hypothesis reported in the literature that states that the dissipated energy per

sample volume required to reach failure depends only on the initial state of the sample and is independent of the characteristics of the cyclic loading applied to the sample. Thus, this cumulative energy hypothesis allows using a multivariable regression of the specific energy to failure measured using a small number of data based on easy standardized cyclic simple shear tests that apply uniform sinusoidal cyclic shear loading. Note that since the cumulative energy hypothesis states that only the initial sample state is what determines the required specific energy to failure, only one level of amplitude and one frequency level for the sinusoidal cyclic simple shear test needs to be performed for each sample state. This study will show that a multivariable regression based on a relatively small and simple experimental program consisting of uniform cyclic simple tests on the different initial sample conditions of interest, can predict with reasonable accuracy the failure of the same test sand under more general cyclic shear loading time histories, including complex irregular cyclic shear stress time histories that are similar to the ones generated by an earthquake. It is important to point out that in the literature researchers have proposed regressions for their full experimental dataset to help identify the main variables that influence the results of dissipated energy to failure, ; however, the use of a multivariable regression that is based on using the smallest possible number of test results obtained using only one simple shear cyclic test per sample initial states subjected to uniform sinusoidal load cycles with only one frequency and amplitude level is proposed in this work.

In this research, the multivariable regression is based on data from constant volume (CV) cyclic simple shear (CSS) tests that is shown schematically in Figure 5-1(a). The dissipated energy per unit volume of a sample subjected to a load cycle of a CV-CSS test is equal to the area of the hysteresis loop in the plot of shear stress versus shear strain, as shown in Figure 5-1(b) as the shaded area for the  $i$ th stress-controlled sinusoidal shear stress load cycle of a CSS test. These tests, when run under constant volume conditions and under stress-controlled cycles, show reduced energy dissipation for the initial stress-strain cycles, and increased energy dissipation as the number of load cycles increases. The cumulative specific dissipated energy to failure ( $E_f$ ) is computed by adding the different hysteresis loop areas ( $\Delta W_i$ ) of the successive load cycles until sample failure (as defined in the study that is being conducted) is reached. A detailed description of the procedure used to compute the cumulative specific

dissipated energy to failure ( $E_f$ ) for constant volume CSS tests, under uniform or irregular shear stress time histories, can be found in Zavala et al. (2022).

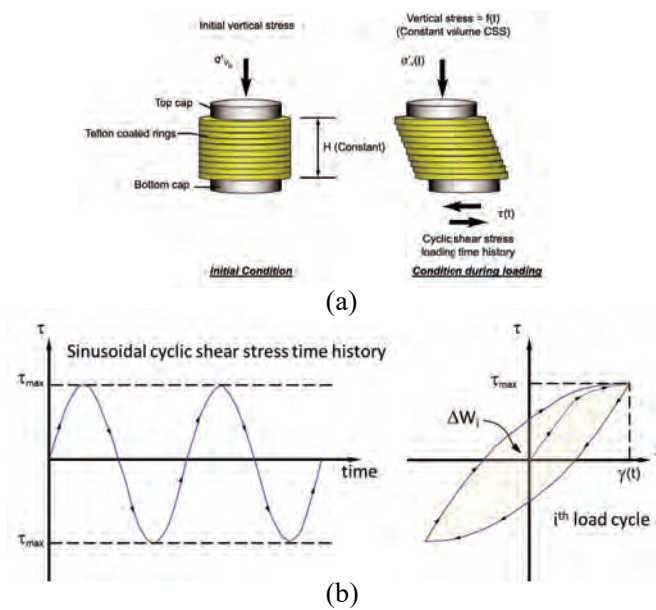


Figure 5-1. (a) Schematic CSS test setup; (b) Sinusoidal load cycles and dissipated energy in the  $i^{th}$  load cycle in a CV stress-controlled CSS test

Several researchers have evaluated the cumulative energy dissipation of sands for different types of cyclic tests (e.g., Azeiteiro et al., 2017; Fardad Amini & Noorzad, 2018; Figueroa et al., 1994; Green & Terri, 2005a; Kokusho, 2017; Kokusho & Kaneko, 2018; Kokusho & Mimori, 2015; S. Lasley, 2015; S. J. Lasley et al., 2017; L. Q. Liang et al., 1995; Polito & Green, 2013). A summary of key findings relevant to this research from these studies is presented below.

Figueroa et al. (1994) and Liang et al. (1995) performed a series of cyclic undrained hollow cylinder torsional shear tests, in Reid Bedford sand samples that were prepared at 3 relative densities and 3 initial effective confining stresses. A total of 36 tests (uniform sinusoidal and random loadings) were run and the dissipated energy to failure was calculated in each case. These studies reported that the cumulative dissipated energy per unit volume required to reach failure was dependent only on the initial sample state defined by the initial relative density and the initial effective confining pressure, and was reported to be independent on the dynamic loading form used in their experiments. This finding supports the cumulative energy hypothesis mentioned earlier that states that the dissipated energy per sample volume required to reach failure depends only on the initial state of the sample and is independent of the

characteristics of the cyclic loading applied to the sample. Furthermore, these two studies developed logarithmic regressions based on all their data, using tests with both uniform and random loadings, to estimate the dissipated energy to failure as a function of the initial state parameters. These studies recommended use of dissipated energy to evaluate liquefaction potential of sands under general earthquake loads.

Polito et al. (2013) performed 28 cyclic triaxial tests using 5 different shapes of periodic deviatoric load time histories and a range of amplitudes defined in terms of cyclic stress ratios (CSR) to identically specimens of Ottawa 20/30 sand, prepared at an initial sample state with a 22% relative density and an initial confining stress of 100 kPa. The authors reported that the dissipated energy required to reach initial liquefaction was independent of the load shape used. Therefore, this is another study that supports the cumulative energy hypothesis mentioned earlier.

Researchers at Virginia Tech (Green and Terri, 2005; Lasley, 2015; Lasley et al., 2016) have also promoted the use of energy-based approaches to investigate behavior of sands under cyclic loading. For example, Green and Terri (2005) presented an energy-based alternative to the Palmgren-Miner fatigue hypothesis to more appropriately account for the non-linear behavior of soils. Lasley (2015) and Lasley et al. (2016) presented correlations to find the number of equivalent uniform cycles to represent general earthquake loading using an energy-based approach. A comprehensive experimental program that included 49 uniform loading and 24 earthquake loading constant volume cyclic simple shear tests performed on Monterrey 0/30 sand samples was reported by Lasley (2015). The initial states for the test samples of this study were compacted to relative densities between 30% and 80% and subjected to three different levels of initial effective vertical stress. The results from this study also support the validity of the cumulative energy hypothesis. Lasley (2015) presents an exponential regression developed using all the test results that correlates the dissipated energy to failure, normalized to the initial effective stress level, to the initial relative density of the sample. This study will be described in more detail later in this chapter, as its results were used to evaluate the simplified methodology proposed herein. The regression reported by Lasley (2015) is based on using the full dataset, in contrast to the approach proposed in this study uses a multivariable regression developed using only a small dataset of

dissipated energy to failure measured from only one simple uniform cyclic simple shear test per sample initial state.

Kokusho and Kaneko (2018) reported results from torsional simple shear tests on Futsu beach sand with 31 tests using uniform harmonic loading and 6 tests using different irregular cyclic loading types. This study reported that cumulative dissipated energy predicted cyclic liquefaction failure reasonably well for a specified initial state and was independent of the loading stress-time history type used.

A recent study by the authors (Zavala et al., 2022) also investigated experimentally the cumulative dissipative energy hypothesis. The authors performed a comprehensive experimental program that tracked dissipated energy from start to failure using 258 CV CSS tests on Ottawa 20/30 sand. The authors considered nine sample initial states and a wide variety of cyclic loading types that included uniform and non-uniform shearing loading. The results of this study supported the validity of the hypothesis that the cumulative specific dissipated energy required to reach failure of a uniform dry sand sample subjected to constant volume stress-controlled CSS testing is reasonably constant and independent of the type of stress-time history used in the testing.

The literature summarized above that have involved detailed experimental studies on uniform sands under different types of cyclic loading (uniform or complex or irregular) support the general validity of the hypothesis of a cumulative specific dissipated energy that is only dependent of the initial state of the sand sample and independent of the characteristics of the cyclic loading applied to the sample. However, it is important to note that most experimental studies show some scatter in the measured dissipated energies to failure, which is common in these kind of tests in granular materials. Regardless of the inherent variability of experimental  $E_f$  values, the literature reports the hypothesis as valid.

This hypothesis is the foundation of the proposed simplified methodology to predict failure of uniform sands under general cyclic loading based on a small dataset that can involve readily available and easy to perform uniform, sinusoidal, cyclic simple shear tests. The proposed methodology is described in the next section and then evaluated and validated using the datasets reported by the authors (Zavala et al., 2022) and by an independent study published by Lasley (2015).

## 5.2. The Proposed Simplified Method

A simplified method that offers a convenient way to estimate the cumulative dissipated energy to failure for a specific granular material subjected to general cyclic loading is proposed herein based on the constant cumulative dissipated energy hypothesis that was described in the previous section. The proposed method involves making predictions using a multivariable regression developed using a small dataset of cyclic simple shear tests performed using the simplest form of cyclic loading of uniform sinusoidal cyclic loading. The method is based on the validity of the constant cumulative dissipated energy hypothesis, and as such only one test per initial sample state (i.e., sample relative density and initial effective vertical stress) is needed. The size of the proposed reduced dataset will depend on the range of sample initial states involved in the project or application of interest.

A flowchart showing the main steps of the proposed simplified method is shown in Figure 5-2. Steps 1 and 2 involve selecting the initial sample states ( $D_r$  and  $\sigma'_{vo}$ ) that will be tested using the simplified CSS testing. The third step in the flowchart involves performing one CV CSS test per sample initial state using uniform harmonic shear loading at only one frequency and amplitude level (or CSR level). Step 4 in the simplified method involves computing the cumulative specific dissipated energy to failure measured in each of the CV CSS tests of Step 3 performed for the different selected initial sample states. The final step involves developing a multivariable regression that relates the cumulative specific dissipated energy to failure to the initial state variables  $D_r$  and  $\sigma'_{vo}$ .

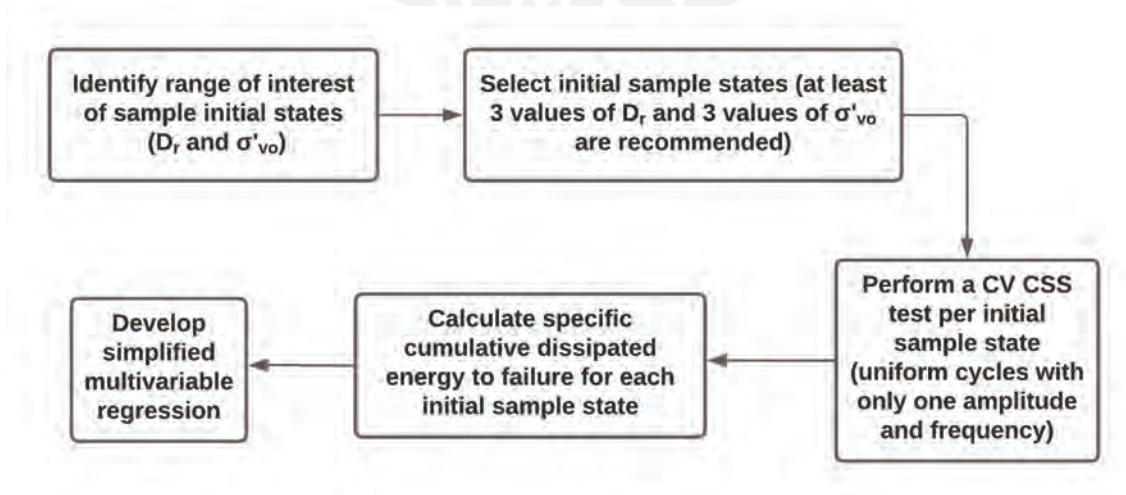


Figure 5-2. Flow chart depicting the proposed simplified method

The multivariable regression involved in Step 5 of Figure 5-2, can be of any form selected by the user. For example, as mentioned in the literature review section, Figueroa et al. (1994) and Liang et al. (1995) used logarithmic multivariable regressions to relate the cumulative dissipated specific energy to failure ( $E_f$ ) to the different sample initial states using the full experimental dataset. In contrast, Lasley (2015) used an exponential type of regression to estimate  $E_f$  based on the sample initial states, and also used the full experimental dataset. In this study several forms of regression equations were investigated, but a logarithmic equation was found to work well and to be convenient. Furthermore, it is recommended to use a dimensionless regression by normalizing the cumulative specific dissipated energy to failure ( $E_f$  in  $\text{kJ/m}^3$  which is equivalent to  $\text{kPa}$ ) and the initial effective vertical stress ( $\sigma'_{v0}$  in  $\text{kPa}$ ) with respect to the atmospheric pressure ( $\sigma_{\text{atm}} = 101.325 \text{ kPa}$ ), as follows:

$$\ln\left(\frac{E_f}{\sigma_{\text{atm}}}\right) = a \times \ln\left(\frac{\sigma'_{v0}}{\sigma_{\text{atm}}}\right) + b \times \ln(D_r) + c \quad (5-1)$$

where  $a$ ,  $b$  and  $c$  are the regression coefficients, and the other variables are as defined before.

The regression coefficients in Equation 1 are obtained using the reduced dataset involving one CV CSS test with uniform sinusoidal loading per initial sample state. The obtained multivariable regression can now be used to predict the cumulative specific dissipated energy to failure for any sample initial state with the range of interest and for general cyclic loading conditions including different periodic loading functions, non-periodic loading, or general irregular cyclic loading such as those generated by earthquakes.

### 5.3. Application of the simplified method to two experimental datasets

This section shows the results of applying the proposed simplified method to data from two comprehensive experimental programs that involved CV CSS tests on uniform dry sands subjected to a wide range of cyclic loading types (e.g., uniform, periodic, non-periodic, and complex irregular earthquake loading). The two datasets are from Zavala et al. (2022), performed by the authors, and from an independent test program by Lasley (2015). The main features of both experimental programs are summarized in Table 5-1



Table 5-1. Main features of test programs by Zavala et al. (2022) and Lasley (2015)

Item	Experimental Datasets	
	Zavala et al. (2022)	Lasley (2015)
DESCRIPTION OF TEST SAND	Ottawa 20/30 sand Shape: subrounded to rounded $G_s = 2.65$ $D_{50} = 0.71$ mm $C_u = 1.2$ $e_{max} = 0.644$ $e_{min} = 0.503$	Monterrey 0/30 sand Shape: subrounded $G_s = 2.66$ $D_{50} = 0.59$ mm $C_u = 1.87$ $e_{max} = 0.845$ $e_{min} = 0.530$
INITIAL STATES	9 initial states $D_r$ from 23% to 100% $\sigma'_{v0} = 100, 200, \text{ and } 400$ kPa	Initial states have a wide range of $D_r$ and 3 values of $\sigma'_{v0}$ $D_r$ from 24% to 83% $\sigma'_{v0} = 60, 100, \text{ and } 250$ kPa
TEST PROGRAM (# of tests, loading Types)	Number of tests: 258 <ul style="list-style-type: none"> <li>• 85 uniform tests <ul style="list-style-type: none"> <li>- CSR: 0.05 to 0.12</li> <li>- <math>f = 0.1, 0.5</math> and 1Hz</li> </ul> </li> <li>• 173 non-uniform tests 4 types of loading</li> <li>• 4 earthquake tests</li> </ul>	Number of tests: 74 <ul style="list-style-type: none"> <li>• 49 Uniform tests <ul style="list-style-type: none"> <li>- CSR: 0.07 to 0.23</li> <li>- <math>f = 0.25</math> Hz</li> </ul> </li> <li>• 25 earthquake tests</li> </ul>

Additional details regarding these two experimental studies, such as sample preparation procedure used, detailed test results (e.g., stress-strain load cycles), complex cyclic shear loading such as earthquake-type loading, and other information can be found in Zavala et al. (2022) and Lasley (2015).

The following subsections presents the multivariable regressions obtained for both datasets using the simplified procedure and the steps in the flowchart of Figure 5-2. The simplified procedure was applied using one CV CSS test with uniform sinusoidal loading per initial sample state within the range of interest for each study. It should be noted that due to the nonlinear nature of the multivariable regression a minimum of nine initial states is recommended in order to reasonably capture the curvature of the regression surface.

### 5.3.1. Application of simplified method to the first experimental dataset

#### 5.3.1.1. Multivariable regression using reduced dataset

Zavala et al. (2022) considered a total of nine initial sample states corresponding to initial vertical effective stresses ( $\sigma'_{v0}$ ) of 100, 200 and 400 kPa, and relative density levels of loose, dense, and very dense (see Table 5-1 for actual  $D_r$  values). Therefore, a total of nine simple CV CSS tests performed using uniform harmonic shear stress cycles at a frequency of 0.1 Hz, at only one level of Cyclic Stress Ratio (CSR) were used to obtain the multivariable regression of the proposed simplified approach.

Obviously, a multivariable regression could have been developed using more tests (or even the full dataset), to include for example more CSR values, frequencies, or tests repetitions that are commonly performed to capture the inherent variability of experimental results related to variations of the sample  $D_r$  and fabric of the sand samples. However, the purpose of this research is to assess the accuracy and usefulness of using a regression obtained based on the smallest amount of data without sacrificing accuracy when predicting failure of the same test sand under other cyclic loading including more complex earthquake-like cyclic loading. The subset of data used to develop the multivariable regression for the experimental study by Zavala et al. (2022) is summarized in Table 5-2.

Table 5-2. Data subset used for the simplified method applied to the Zavala et al. (2022) dataset

Initial State ID	Relative Density (descriptive)	$D_r$ (%)	$\sigma'_{v0}$ (kPa)	CSR	Measured cumulative specific dissipated energy, $E_f$ (kJ/m <sup>3</sup> )
1	Loose	27.0	100	0.065	0.2353
2	Dense	62.6	100	0.065	0.3872
3	Very dense	102.0	100	0.100	1.0060
4	Loose	25.0	200	0.065	0.6219
5	Dense	68.2	200	0.065	0.8898
6	Very dense	100.0	200	0.100	1.4075
7	Loose	26.0	400	0.065	0.9169
8	Dense	72.8	400	0.065	2.9075
9	Very dense	97.0	400	0.100	3.5070

Using the regression form presented in Equation 1, and the reduced set of data in Table 5-2, the following multivariable regression was obtained for the test sand tested by Zavala et al. (2022):

$$\ln\left(\frac{E_f}{\sigma_{atm}}\right) = 1.0991 \times \ln\left(\frac{\sigma'_{v0}}{\sigma_{atm}}\right) + 0.8652 \times \ln(D_r) - 8.8931 \quad (5-2)$$

The above multivariable regression has a coefficient of multiple determination (or  $R^2$ ) of 0.946. A 3D plot representation of this multiple regression is shown in Figure 5-3. In this figure the two horizontal axes correspond to the independent variables (i.e., the sample initial state defined by the normalized initial effective stress and the sample initial relative density), and the vertical axis corresponds to the dependent variable, i.e., the normalized cumulative specific dissipated energy. The regression defined by Equation 5-2 is shown as a 3D mesh surface in the figure. In addition to the 3D

surface that corresponds to the regression, Figure 5-3 also shows the nine experimental data points listed in Table 5-2. A blue line projecting the points across the 3D surface indicates that the point is above the surface, whereas a red dotted line indicates that the point is below the 3D surface. This figure qualitatively shows a good correlation between the 9 data points and the regression in Equation 5-2.

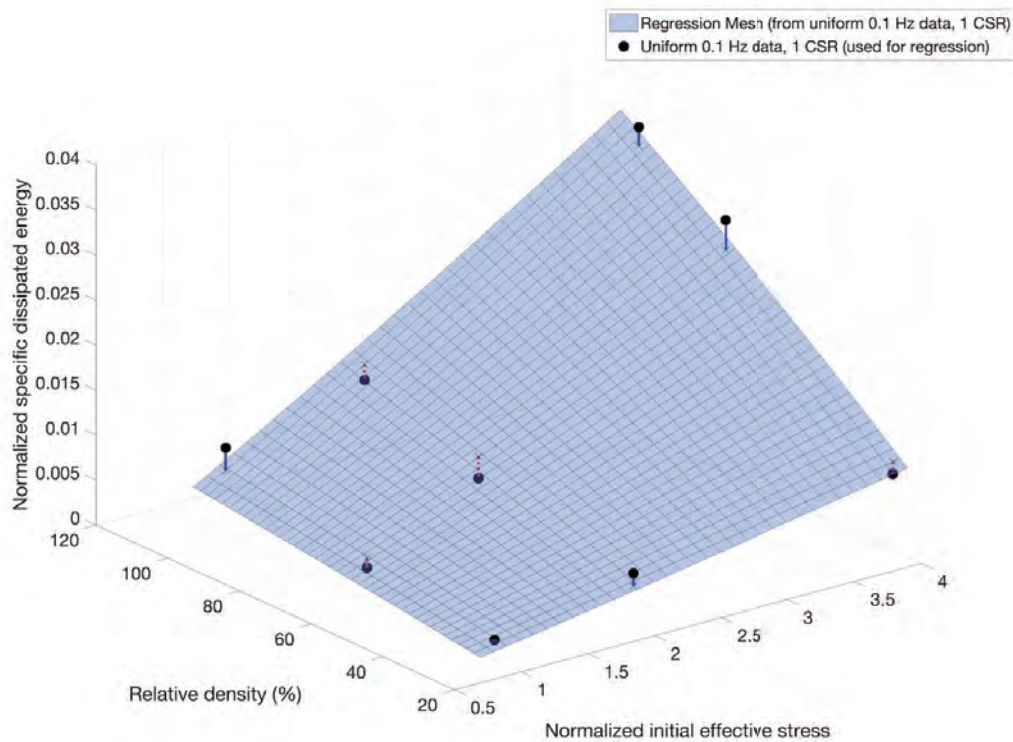


Figure 5-3. 3D mesh plot showing the regression obtained using the selected reduced dataset from Zavala et al. (2022)

### 5.3.1.2. Evaluation of regression using full dataset reported by Zavala et al. (2022)

The regression obtained using the simplified approach, and the results from the selected 9 uniform CV CSS tests in Table 5-2 are evaluated in this section. This was done by comparing the predicted values of cumulative specific dissipated energy to failure using the regression in Equation 5-2, with the energy to failure values measured in experiments from the full dataset reported by Zavala et al. (2022) that were not used to develop the regression.

The full dataset reported by Zavala et al. (2022) involved a wide range of CV CSS tests prepared at the nine initial sample states mentioned earlier and listed in Table 5-2. Zavala et al. (2022) reported results from a large number of CV CSS using the following 5 types of load patterns: i) uniform harmonic cyclic loading (6 levels of CSR and 3 frequencies), ii) alternating sine waves of variable CSR values at

a constant frequency (considered combinations of 4 CSR levels and 3 frequencies), iii) alternating sine waves of different frequency but constant CSR level (combined 0.1 and 0.5 Hz and considered 5 CSR levels), iv) alternating sine waves with different frequency and CSR levels (considered combinations of 4 CSR levels and combined 0.1 and 0.5 Hz), and v) spike loading consisting of a set of low CSR uniform sinusoidal waves followed by a sudden large CSR spike and this sequence was repeated until failure. A detailed description of these experiments and results is outside the scope of the work, but additional information of this study can be found in Zavala et al. (2022).

As mentioned earlier, the results of the Zavala et al. (2022) study supported the general validity of the constant cumulative dissipated energy to failure hypothesis. However, as in other studies experimental results have the usual inherent level of variability. A summary of the experimental values of cumulative specific dissipated energy to failure measured in this study for the nine initial sample states is presented in Table 5-3, and statistical descriptors such as mean, standard deviation, and other parameters are reported based on all the  $E_f$  values measured for each sample initial state considering all tests, and all types of cyclic load time histories reported in this study.

Table 5-3. Summary of cumulative specific dissipated energy to failure in Zavala et al. (2022)

Initial State ID	Number of CSS tests (#)	Initial State Variables				Cumulative Specific Dissipated Energy (kJ/m <sup>3</sup> )					
		Relative Density			Initial Stress	Mean	Std. Dev.	Max	Min	COV	Variability Descriptor <sup>(1)</sup>
		State	Mean	Std. Dev.	$\sigma'_{vo}$ (kPa)						
1	31	Loose	27.3%	3.1%	100	0.2738	0.0711	0.3943	0.0916	26%	Medium
2	42		29.0%	4.1%	200	0.5664	0.1580	0.8188	0.1094	28%	Medium
3	46		29.7%	3.7%	400	1.3596	0.5942	2.4128	0.3127	44%	High
4	7	Dense	63.1%	4.7%	100	0.3403	0.1303	0.4770	0.1410	38%	High
5	4		70.3%	5.2%	200	0.8935	0.1231	1.0321	0.7335	14%	Low
6	4		69.0%	6.0%	400	2.5108	0.3266	2.9075	2.2288	13%	Low
7	35	Very Dense	92.5%	3.1%	100	0.6549	0.2169	1.2414	0.3544	33%	High
8	43		92.9%	3.0%	200	1.3214	0.4101	2.3295	0.7378	31%	High
9	46		95.4%	2.2%	400	2.9412	0.4738	3.9460	1.9418	16%	Medium

Notes: <sup>(1)</sup> Variability descriptor proposed by Harr (1987) based on the coefficient of variation.

Std.Dev. = Standard deviation; Max = Maximum; Min = Minimum; COV = Coefficient of variation.

A comparison of the regression obtained using the simplified method and the reduced set of data (i.e., Equation 5-2) with the full dataset of 258 CV CSS test results reported by Zavala et al. (2022) is shown in Figure 5-3. Like Figure 5-2, in this figure blue lines projecting from the data points across the

3D surface indicate that the points are above the surface, whereas red dotted lines indicate that the points are below the 3D surface. This figure qualitatively shows that even though the dissipated energy to failure in tests with larger relative density and larger initial effective stress has more scatter, the simplified method estimation is close to the average dissipated energy values.

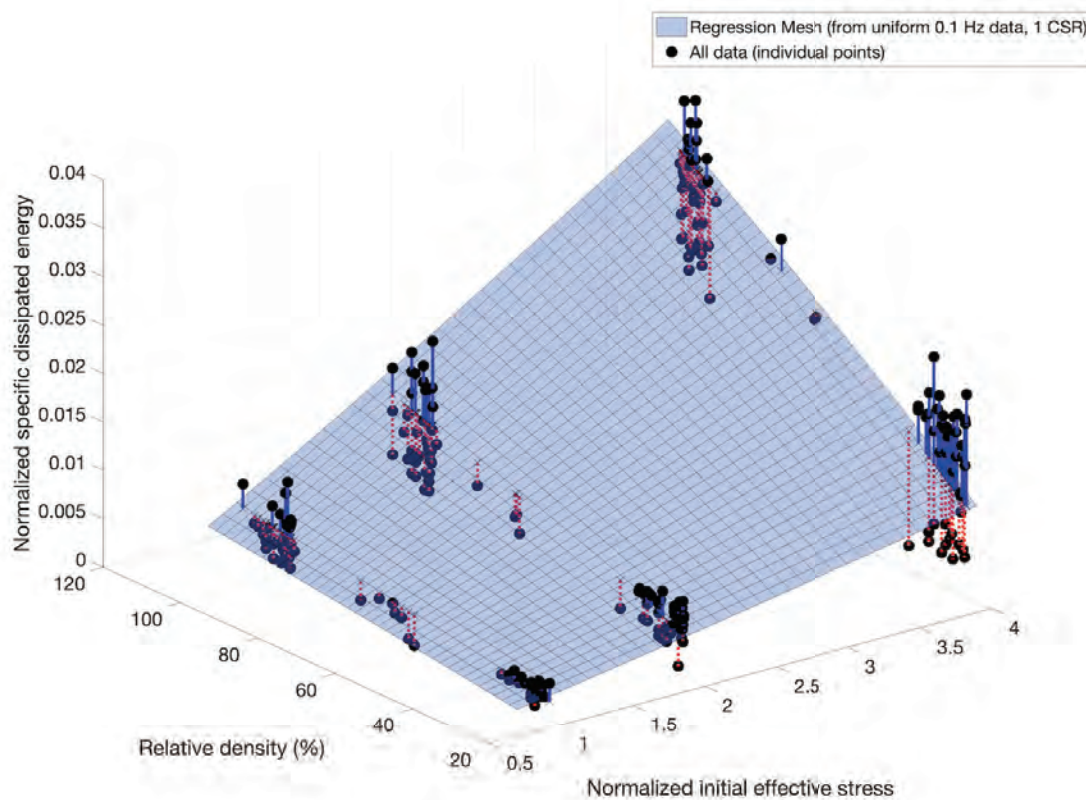


Figure 5-4. Comparison of the multivariable regression using the simplified method with the full dataset of 258 values of normalized cumulative specific dissipated energy reported by Zavala et al. (2022)

As an alternative way to assess the regression presented in Equation (5-2) to predict the cumulative specific dissipated energy to failure from any CV CSS test, even general cyclic loading, a comparison was made between the predicted (i.e., using Equation (5-2) and the measured cumulative specific dissipated energy to failure as shown in Figure 5-5. This plot also shows the 1:1 equality line that would correspond to a perfect prediction and two lines corresponding to predictions that are  $\pm 25\%$  with respect to the measured values; 54% of the predictions fall within this  $\pm 25\%$  range. The percentage of predictions that fell within the larger range of  $\pm 40\%$ , with respect to the 1:1 line, was found to be 77%.

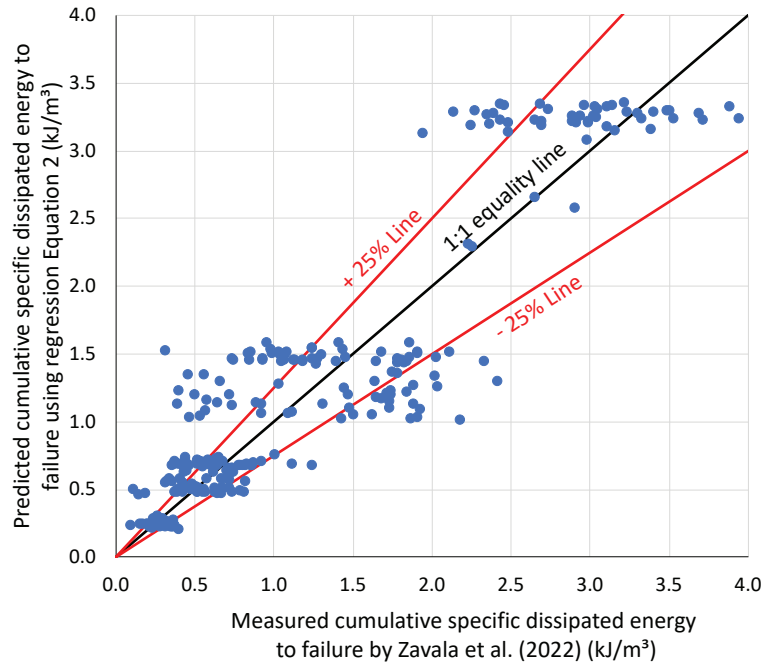


Figure 5-5. Comparison plot of predicted versus measured normalized cumulative specific dissipated energy to failure using Equation 2 regression (simplified method) for Zavala et al. (2022) (n = 258)

An additional evaluation of the simplified method was made by comparing the accuracy of Equation 5-2 with the level of accuracy of predictions of  $E_f$  values using a multivariable regression developed using the whole dataset reported by Zavala et al. (2022). As mentioned earlier, different regression equation types were considered, but for the sake of brevity only the results for the logarithmic-type regression are reported. Using the whole dataset reported by Zavala et al. (2022) the following multivariable regression was obtained:

$$\ln\left(\frac{E_f}{\sigma_{atm}}\right) = 1.105 \times \ln\left(\frac{\sigma'_{vo}}{\sigma_{atm}}\right) + 0.7123 \times \ln(D_r) - 8.3532 \quad (5-3)$$

where the variables are as defined before.

The value of the coefficient of multiple determination (or R-squared) for the regression presented in Equation 3, that used all 258 CV CSS test results from this study, was 0.802. In general, the higher the

R-squared, the better the model fits the data. The computed relatively high value of R-squared suggests that the proposed model fits the experimental data reasonably well.

Figure 5-6 shows a comparison plot of the predicted (i.e., using Equation 5-3) and the measured cumulative specific dissipated energy to failure. It also shows the 1:1 equality line that would correspond to a perfect prediction, and two lines corresponding to predictions that are  $\pm 25\%$  with respect to the measured values; 57% of the predictions fell within this  $\pm 25\%$  range. The percentage of predictions that fell within the larger range of  $\pm 40\%$ , with respect to the 1:1 line, was found to be 83%.

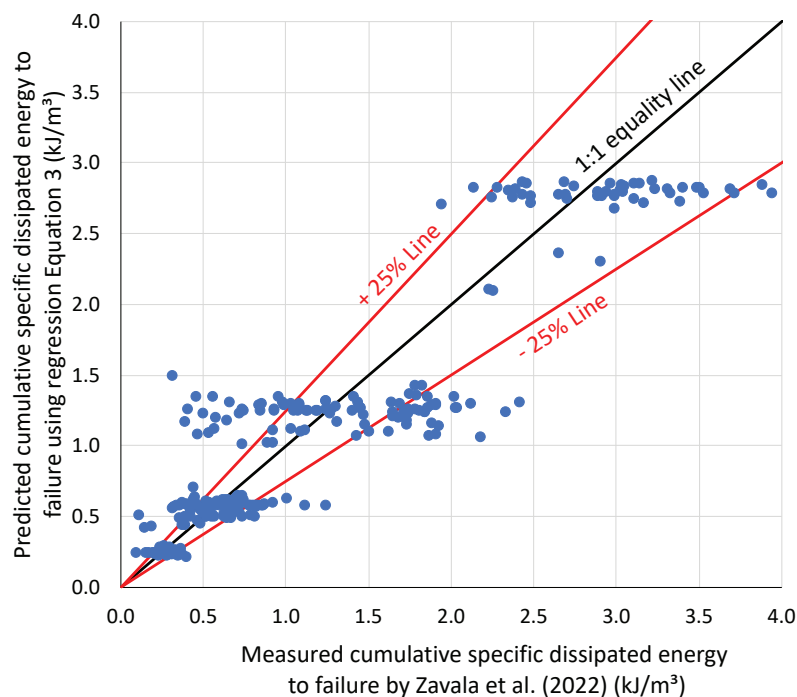


Figure 5-6. Comparison plot of predicted versus measured cumulative specific dissipated energy to failure using Equation 3 regression (whole dataset) for Zavala et al. (2022) (n = 258)

An additional comparison of the two regressions, i.e., Equation 5-2 (simplified method using 9 tests) and Equation 5-3 (using the whole dataset, n=258) can be made by comparing the root mean square error (RMSE) and the Mean Absolute Error (MAE) of the measured vs the predicted data. The RMSE is the standard deviation of the residuals (prediction errors) and is a standard way to measure the error of a model in predicting quantitative data. The MAE is the average of the errors between predicted and measured data and is other way of measuring the accuracy of prediction models. The value of the RMSE between the measured dissipated energy and the predicted dissipated energy (using the simplified

method, i.e., Equation 5-2), is  $0.414 \text{ kJ/m}^3$  and its value between measured and estimated dissipated energy using the whole dataset regression (i.e., Equation 3-3) is  $0.389 \text{ kJ/m}^3$ . Likewise, the value of the MAE between the measured and predicted dissipated energy using Equation 5-2 is  $0.314 \text{ kJ/m}^3$  and its value between measured and estimated dissipated energy using Equation 5-3 is  $0.289 \text{ kJ/m}^3$ . These close RMSE and MAE values suggest that the correlation between measured and estimated data using both equations have a similar level of accuracy. A graphical comparison of the predictions made using Equation 5-2 (proposed simplified method) and Equation 5-3 (whole dataset regression) is shown in Figure 5-7. This plot shows that the two correlations have similar predictions as they are very close to the 1:1 equality line shown in this figure.

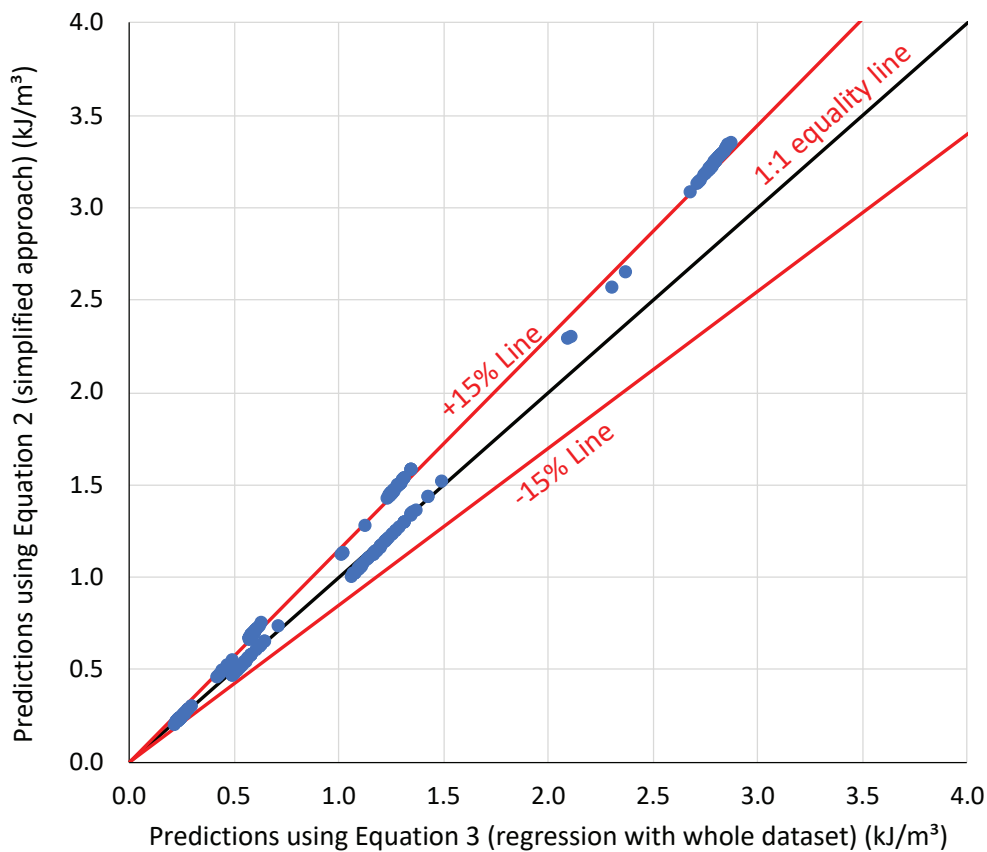


Figure 5-7. Comparison of estimated cumulative specific dissipated energies to failure using the simplified method regression (Equation 3-2) and the whole dataset regression (Equation 3-3)



### 5.3.1.3. Evaluation of regression using a CV-CSS test under earthquake-like cyclic loading

In addition to the 258 tests reported by Zavala et al. (2022) the authors also performed several unpublished CV CSS tests subjected to complex shear stress time history like the one shown in Figure 5-8. For the sake of brevity, only one test with general irregular shear loading is presented and discussed. The shear stress time history applied to the sample was obtained using 1D seismic site analyses with the program SHAKE91 (Idriss and Sun, 1992) to replicate the cyclic stresses a sand sample would experience during an earthquake. The time history shown in Figure 5-8 has a duration of 44 seconds, a predominant frequency of 0.8 Hz, and a peak normalized shear stress of 0.156.

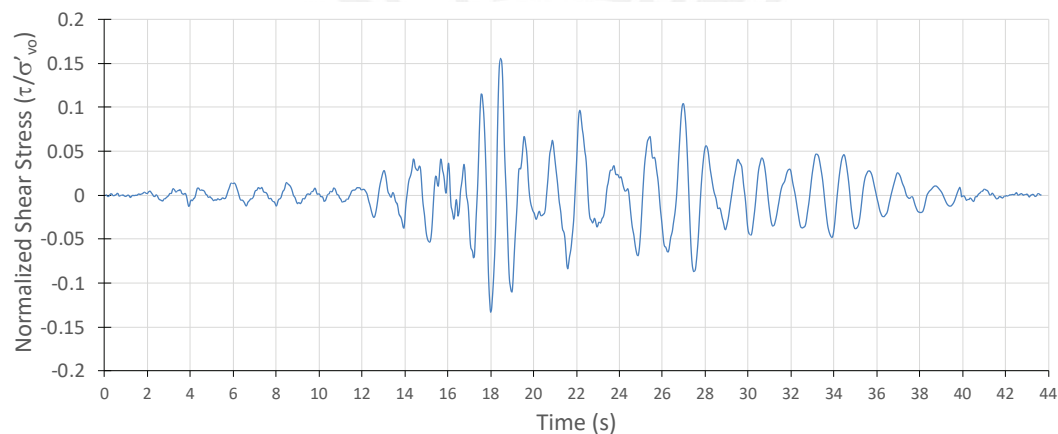


Figure 5-8. Shear stress time history used in a CV CSS test under earthquake-like loading

The CV CSS test had an Ottawa sand sample with an initial state defined by a very dense sand state ( $Dr = 91.3\%$ ) and an initial effective vertical stress of 200 kPa. The peak shear stress of the applied signal was 31.1 kPa that occurred at the signal time of 18.5 s. The sample was tested using the same device and procedure described in Zavala et al. (2022). The results for this CV CSS test under earthquake-like loading are summarized in Figure 5-9. The summary of results is presented using four plots with matching axes. For this specific test, the figure shows that the shear strains are very low when the applied normalized shear stress (NSS) low and below 0.05, which occurs during the first 17 seconds of the excitation signal. For this test, NSS values are the value of the applied shear stress normalized with respect to 200 kPa. Larger shear strains start to develop in the sample when the NSS values reach about 0.10, but are still not significant in magnitude. As shown in Figure 5-9, the shear

strains increase dramatically when the peak NSS of 0.156 is reached at a time of about 18.5 seconds. The strains continue to accumulate past the load cycle with the peak shear stress until failure is reached. As described in Zavala et al. (2022) failure was defined when the sample reached a double amplitude strain of 7.5 percent. For this test failure occurred at a time of 20.6 seconds.

The cumulative specific dissipated energy to failure measured in this test was  $1.326 \text{ kJ/m}^3$ . Using the simplified methodology, based on the regression in Equation 3-2, the estimated dissipated energy to failure for a sample with an initial state of  $D_r = 91.3\%$  and an initial effective vertical stress of 200 kPa is  $1.460 \text{ kJ/m}^3$ . This difference between the predicted and measured  $E_f$  values corresponds to an error of 10.1%, which is a reasonably good prediction for this type of parameter.

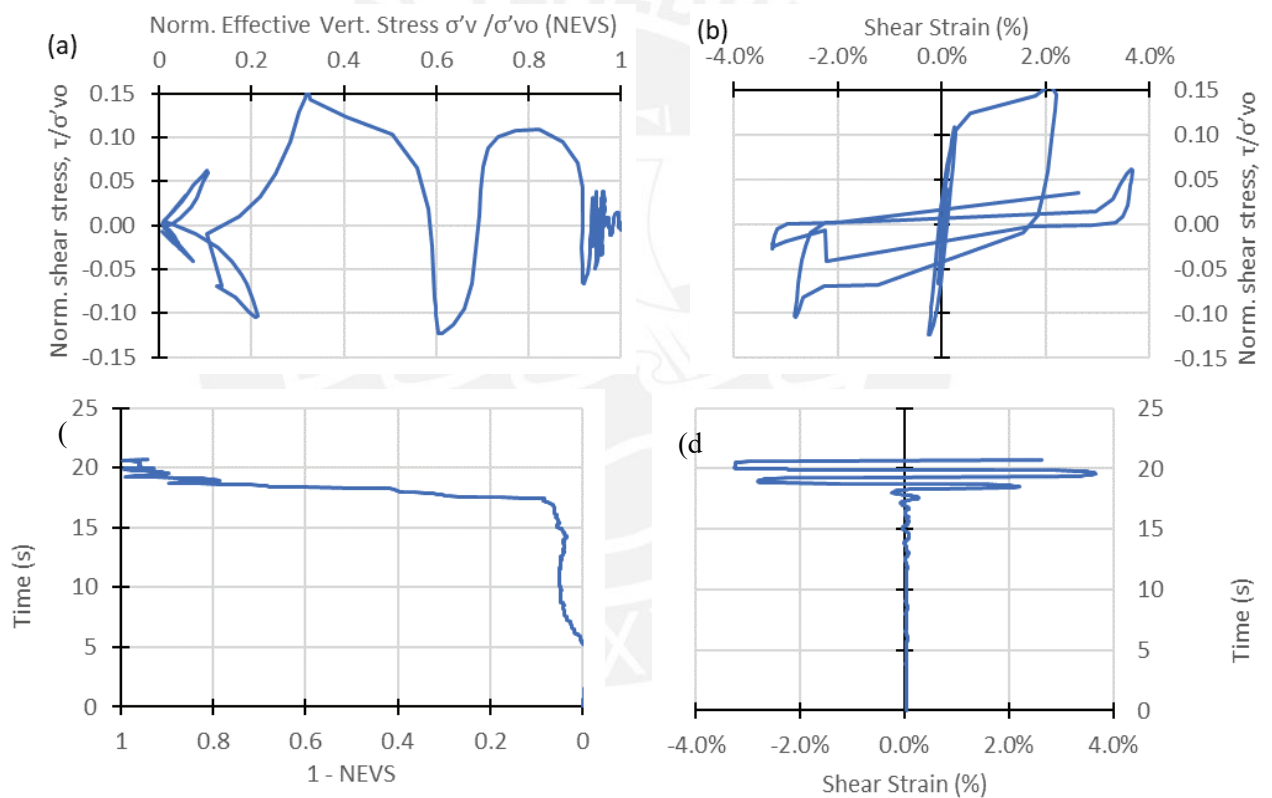


Figure 5-9. Results of a CV CSS Test under irregular loading of Figure 5-8 on an Ottawa sand sample at a very dense sand state an initial  $\sigma'_{vo} = 200 \text{ kPa}$

### 5.3.2. Application of simplified method to the Lasley (2015) experimental dataset

The proposed simplified method was further evaluated using the independent experimental dataset published by Lasley (2015). This author conducted 49 CV cyclic simple shear tests on Monterey 0/30 sand samples using uniform cyclic loading and 24 tests using earthquake-like loading. The main features of this experimental study were summarized in Table 5-1.

#### 5.3.2.1. Multivariable regression using reduced dataset

According to the methodology explained above, nine representative tests were selected, which include the three initial vertical stresses considered (60, 100 and 250 kPa), and relative densities between 25.9% and 70.6%. The data points used to this regression were selected in order to cover the range of initial conditions corresponding to most of the full dataset and are shown in Table 5-4.

Table 5-4. Data subset used for the simplified method applied to the Lasley (2015) dataset

Initial State ID	Relative Density (%)	$\sigma'_{v0}$ (kPa)	CSR	Measured dissipated energy (kJ/m <sup>3</sup> )
1	27.3	60	0.08	0.49
2	35.5	60	0.10	0.50
3	41.1	60	0.22	0.94
4	25.9	100	0.10	0.41
5	49.7	100	0.17	1.70
6	83	100	0.21	6.60
7	33.3	250	0.12	2.40
8	63.7	250	0.19	7.00
9	70.6	250	0.23	20.0

The obtained regression formula obtained using this simplified dataset follows:

$$\ln\left(\frac{E_f}{\sigma_{atm}}\right) = 1.0434 \times \ln\left(\frac{\sigma'_{vo}}{\sigma_{atm}}\right) + 2.2336 \times \ln(D_r) - 12.5528 \quad (5-4)$$

Figure 5-10 shows the 3D mesh plot of the regression corresponding to Equation 5-4, and the 9 points that represent the selected initial conditions (horizontal axes) and the measured normalized cumulative specific dissipated energy to failure (vertical axis) for the reduced dataset. The 3D mesh shows a relatively good correlation with the selected data points, except for the point corresponding to

the highest relative density and initial effective stress. Even though this point was one of the nine data points chosen to develop the regression, inherent variability of this type of test may cause values of dissipated energy to not match the prediction very well. The value of the coefficient of multiple determination (or  $R^2$ ) of the regression presented in Equation 5-4 is 0.958.

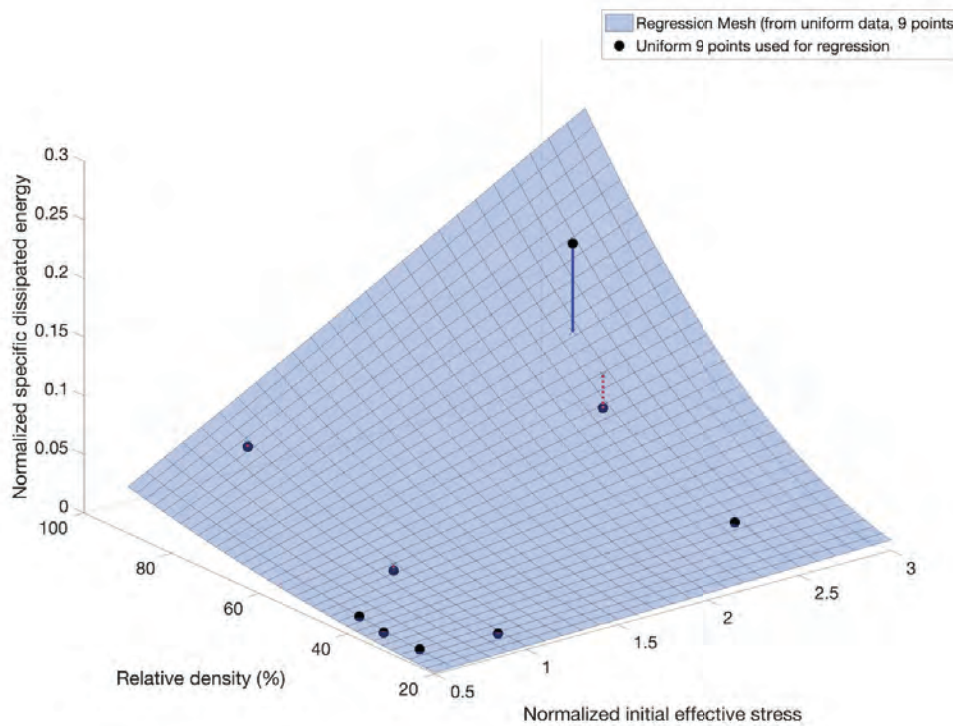


Figure 5-10. 3D mesh plot showing the regression obtained using the selected reduced dataset from Lasley (2015)

### 5.3.2.2. Evaluation of regression full dataset reported by Lasley (2015)

The regression obtained with the simplified set of data (Equation 5-4) is plotted against all the dataset in Figure 5-11. This figure shows a 3D mesh plot of that regression and the measured normalized cumulative specific dissipated energy to failure for the full dataset. The graph qualitatively shows a reasonably good correlation, except for the data point corresponding to the highest relative density and initial effective stress, which was also mentioned above.

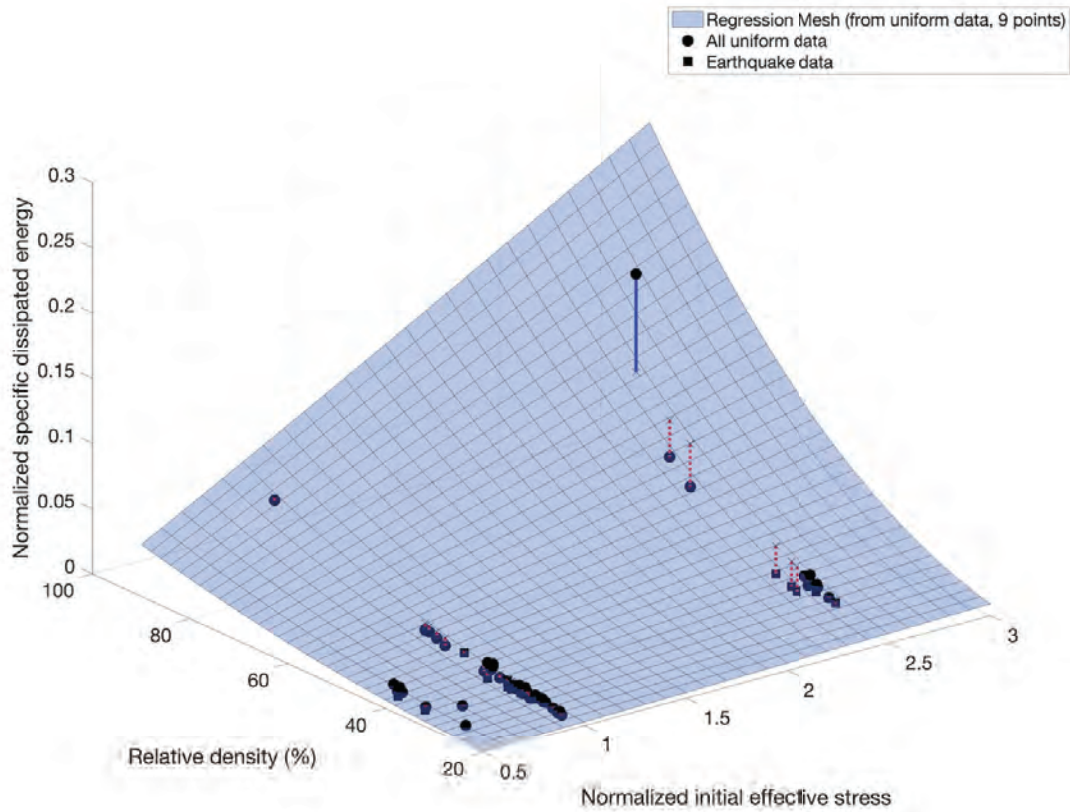


Figure 5-11. Comparison of the multivariable regression using the simplified method with the full dataset of 74 values of normalized cumulative specific dissipated energy reported by Lasley (2015)

In order to further assess the ability of the regression presented in Equation 5-4 to predict the dissipated energy to failure in a CSS test, a comparison was made between the predicted and measured normalized cumulative specific dissipated energy to failure. The former was calculated using the regression obtained through the simplified set of data, and the latter was measured for each of the tests in the full dataset from Lasley (2015). This comparison is shown in Figure 5-12, which indicates that in most cases the dissipated energy prediction is close to the measured dissipated energy for the same initial testing conditions.

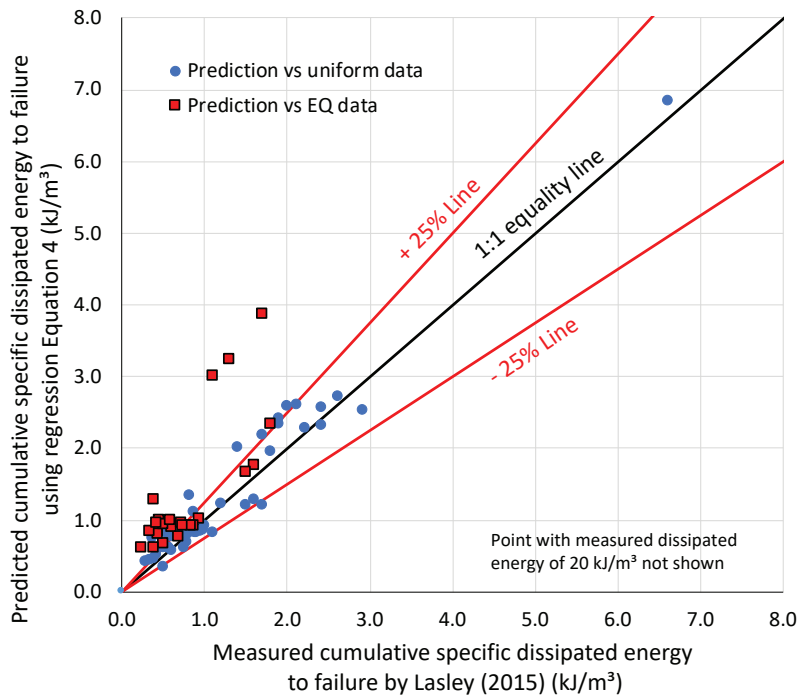


Figure 5-12. Comparison of normalized cumulative specific dissipated energy to failure calculated with the regression obtained using the reduced set of data, and points of normalized specific dissipated energy of all tests reported by Lasley (2015)

As mentioned before, the root mean square error (RMSE) and the mean absolute error (MAE) are standard ways to measure the error of a model in predicting quantitative data. The value of the RMSE between the measured and predicted dissipated energy using Equation 3-4 for the all the dataset is  $1.235 \text{ kJ/m}^3$ , and the MAE value for the same is  $0.632 \text{ kJ/m}^3$ . To further evaluate the predictions obtained using the simplified method and compare them with those made with a full dataset regression, such regression was made using Lasley (2015) whole dataset, though is not presented for the sake of brevity. The value of the RMSE between the measured and predicted dissipated energy using such regression for the all the dataset is  $1.422 \text{ kJ/m}^3$ , and the MEA value for the same is  $0.442 \text{ kJ/m}^3$ .

### 5.3.3. Summary of comparison between simplified method and whole dataset predictions

Table 5-5 summarizes the root mean square error (RMSE) and the mean absolute error (MAE) obtained with the predictions using the simplified method and a whole dataset regression, for both datasets.

Table 5-5. Values of Root Mean Square Error (RMSE) and Mean Absolute Error (MAE)

<b>Dataset</b>	<b>Prediction method</b>	<b>RMSE (kJ/m<sup>3</sup>)</b>	<b>MAE (kJ/m<sup>3</sup>)</b>
Zavala et al. (2022)	Whole dataset regression	0.389	0.289
	Simplified Method	0.414	0.314
Lasley (2015)	Whole dataset regression	1.422	0.442
	Simplified Method	1.235	0.632

Table 5-5 shows that for both datasets, the values of RMSE and MAE for the dissipated energy predictions are similar when using the simplified method as compared to the whole dataset regression and supports the idea of using a reduced dataset to create a regression to predict the cumulative specific dissipated energy to failure for sands subjected to cyclic shear loading.

## 6. *Summary, conclusions and recommendations for future work*

### 6.1. Summary of findings

This thesis sought to explore different aspects of the behavior of sands when subjected to cyclic loading. The first objective was to evaluate the research hypothesis that the cumulative specific dissipated energy required to reach failure measured in CSS tests should be reasonably constant for a given initial sample state defined by the initial relative density and stress level and independent of the type of stress-time history applied to the test sample. The objective was to develop a simplified approach or methodology to predict failure of sands when subjected to general cyclic loading, utilizing only simple harmonic tests. To achieve these objectives, a test program was developed. Over 250 constant volume cyclic simple shear (CSS) tests were conducted under uniform and non-uniform shearing loading applied to dry Ottawa sand samples prepared at nine initial stress states that corresponded to three relative density levels (loose, dense, and very dense), and three initial vertical effective stresses levels (100, 200, and 400 kPa). The test program involved uniform and non-uniform cyclic shear time histories with different frequencies, amplitudes, and mixed patterns. Dissipated energy to failure (defined as the sample reaching a double amplitude shear strain of 7.5%) was calculated in all cases, and the results were analyzed. The experimental program showed that the measured cumulative dissipated energy to failure was reasonably constant for the same initial sample conditions, but with some variability inherent to geotechnical laboratory testing. Also, a simplified method to predict the dissipated energy to failure of a sample subjected to general loading, based on a multivariable regression performed on a simplified set of laboratory results, was presented, and was next validated with two independent data sets. In both cases the method was found to yield reasonable predictions of failure of sands when subjected to complex and irregular shear loading.



## 6.2. Manuscript #1 conclusions

A test program was designed and performed to evaluate the research hypothesis that the cumulative specific dissipated energy required to reach failure measured in CSS tests should be reasonably constant for a given initial sample state defined by the initial relative density and stress level and independent of the type of stress-time history applied to the test sample. A total of 269 constant volume cyclic simple shear (CSS) tests were conducted under uniform and non-uniform shearing loading applied to dry Ottawa sand samples prepared at nine initial stress states that corresponded to three relative density levels (loose, dense, and very dense), and three initial vertical effective stresses levels (100, 200, and 400 kPa). The test program involved uniform and non-uniform cyclic shear time histories with different frequencies, amplitudes, and patterns as described in Table 4-2. The experimental program presented showed that the measured cumulative dissipated specific energy to failure, defined when the double amplitude shear strain reaches 7.5%, for the different sample initial states was reasonably constant and independent of the type of loading applied to the sample. However, the test results showed coefficients of variation ranging between 13 to 44% indicating significant variability of the measured values of cumulative dissipated specific energy to failure. The higher values of COV were observed for the CSS tests involving very high-density samples where it was observed that more load cycles were required at NEVS=0 state in order to achieve the specified failure criterion. This larger number of load cycles also had large hysteresis loops thus having a large influence in the final value of the measured cumulative specific dissipated energy. The level of variability observed in the measured dissipated energy to failure was to be comparable to the variability reported by others in the literature for experimental studies involving uniform sands tested under cyclic simple shear loading.

Despite the significant levels of data variability observed, the measured values of cumulative specific dissipated energy to failure were found to be reasonably constant for a given sample initial state and independent of the type of cyclic stress time history applied to the sample. The mean cumulative specific dissipated energy was found to increase with increasing initial stress level and relative density. The findings support the notion that specific dissipated energy can be used as a reasonable failure

predictor for uniform dry sands based on their initial state and are independent of the type of cyclic simple shear loading waveform using in the testing.

In conclusion, this experimental study helped evaluate and validate the research hypothesis that for a given initial sample state the cumulative specific dissipated energy required to reach failure of a uniform, dry, sand sample tested under stress-controlled, constant volume CSS testing should be reasonably constant and independent of the type of stress-time history used in the testing. However, the measured values of cumulative specific dissipated energy required to reach failure were found to have some important variability that may be related to inherent variability of geotechnical parameters even under relatively well controlled conditions available in laboratory studies like the present one.

### 6.3. Manuscript #2 conclusions

This paper described a simplified approach proposed to predict the failure of dry sands subjected to general shear stress time histories such as the ones experienced during earthquakes. The proposed simplified method is based on the cumulative energy hypothesis reported in the literature that states that the dissipated energy per sample volume required to reach failure depends only on the initial state of the sample and is independent of the characteristics of the cyclic loading applied to the sample. Therefore, the proposed method allows the prediction of failure of sands under general cyclic loading, without the need for advanced and costly cyclic testing and can be based on a multivariable regression developed using results from a relatively small number of standard and readily accessible cyclic simple shear tests involving uniform sinusoidal loading. The proposed simplified methodology is sand specific as the failure of granular soils is controlled by their intrinsic properties (e.g., particle shape, grain size distribution, mineralogy, etc); therefore, the obtained regressions are valid for each specific sand used to develop them. The small dataset required for the regression involves only one test per sample initial state (e.g.,  $D_r$  and  $\sigma'_{v0}$ ) that should be selected based on the project range of interest. The test required for each sample initial state involves a routine CV CSS test with only one level of sinusoidal simple shear loading tested until failure. The proposed simplified method was evaluated using two comprehensive experimental studies involving two different types of sands. The first dataset is from an

experimental program by the authors reported in Zavala et al. (2022) that involved 20/30 Ottawa sand subjected to different cyclic loading types that included simple sinusoidal cyclic shear and also complex cyclic shear time histories. This paper also compared the simplified approach using an unpublished CV CSS performed on the same Ottawa sand but under general earthquake-type loading. Additionally, the proposed approach was also evaluated using an independently published dataset by Lasley (2015) that used Monterey 0/30 sand. The predictions using the simplified approach, which is based on a small dataset of simple CV CSS tests, were found to yield predictions with a similar level of accuracy to the predictions using regressions based on the full dataset. Therefore, for the different sources of experimental data considered herein, the simplified approach was found to yield reasonably good predictions of the failure of the two test sands when subjected to complex and irregular shear stress loading.

The proposed simplified approach can help predict the failure of sands under general cyclic loading by tracking the dissipated energy of the sand sample during the test. This might be useful because it predicts the failure of sands under general cyclic loading without the need for specialized testing equipment usually required to apply this kind of loading scheme to a sand sample. This approach also has the potential to be extended to the prediction of failure of sands in the field when the expected applied energy to the soil can be estimated.

The main conclusions and recommendations drawn from this study are:

- A reduced dataset of simple cyclic simple shear tests, based on one CV CSS test per sample initial state within a range of interest, can be used to produce a regression equation that can predict reasonably well the dissipated energy to failure in the same test sand under general or complex cyclic loading. In the analysis made with the two datasets considered, the values of the root mean square error (RMSE) and mean absolute error (MAE) between predicted and measured dissipated energy, using the simplified method, were found to be very similar to the ones obtained using a whole dataset regression equation. The close values of RMSE and MAE suggest that the proposed simplified methodology has a similar level of accuracy to the more costly and time-consuming full dataset regression.

- The simplified method was assessed and validated. Thus, it is possible to predict reasonably well the failure of a specific sand when subjected to general or complex simple shear loading by tracking the dissipated energy during the test and using the proposed simplified approach that is based on the cumulative energy hypothesis reported in the literature.
- The comparison of the predicted cumulative energy to failure versus the measured experimental values in general support the cumulative energy hypothesis reported in the literature, but also show that the dissipated energy values required to reach failure for a given sample initial state have important scatter that could be related to the inherent scatter of experimental test results in sands due to small differences in sample density and fabric.
- The regression obtained using the simplified set of cyclic simple shear tests predicts fairly well the dissipated energy to failure of a large set of cyclic simple shear under a wide range of loading conditions, including those subjected to an earthquake-type CSS test.
- It is recommended that the simplified method uses a set of CV CSS tests based on at least nine sample initial states (defined by the relative density and initial vertical stress) based on the range of interest of the project. Specifically, the recommendation is that the 9 points should be based on the 3 x 3 matrix formed by the minimum, average, and maximum values of the relative density and the initial effective stress ( $\sigma'_{vo}$ ) of interest.
- This simplified method is particularly useful when access to advanced CSS testing devices is not available.

## 6.4. Recommendations for further studies

Recommendations for extending this research are the following:

- Perform the evaluation of the cumulative dissipated energy hypothesis using a similar test program with different types of sands. The same evaluation performed in this research using different types of uniform and non-uniform cyclic loadings should be performed with other types

of sands, which will help understand if the validity of the hypothesis is affected by the type of sand used.

- Perform the same evaluation using different shear modes, i.e., different types of lab tests such as cyclic triaxial and torsional tests. The shear mode that is applied to the soil influence its response to cyclic loading. Therefore, it is important to validate the hypothesis using different shear modes.
- Validate the findings of this research for other testing conditions such as truly undrained CSS tests, and for non-uniform samples such as undisturbed, intact samples from the field. This research was done using dry constant volume tests, which according to some researchers can be considered equivalent to truly undrained tests. However, as the studies in this aspect are not conclusive, it is recommended to do the evaluation using truly undrained test, though testing under those conditions is complex and takes much more time.
- Test the simplified method to predict failure of sands with other types of sands. In this research the simplified method was tested with two types of sands. However, it will be very useful to test it with sand of different granulometric distribution and roundness.
- Utilize the different regressions that can be obtained for different types of sands, and explore the possibility of finding a relationship of the coefficients with the sand properties. The simplified method presented in chapter 3 is sand specific. Therefore, the regression needs to be developed for each different sand, which involves performing a limited number of cyclic simple shear tests. It would be useful to develop correlations to calculate the regression parameters based on index properties of the sands. Obtaining this kind of correlation might be very difficult because there is no inherent relationship between the parameters that need to be correlated, and a very large amount of data might be .
- Extend the assessment done in this study to field conditions. This study was performed in laboratory samples, but field conditions can be much different because of a variety of factors, such as heterogeneity of the soil and drainage conditions, so it would be important to extend the assessment to include those conditions.

## References

- Annaki, M., & Lee, K. L. (1977). Equivalent Uniform Cycle Concept for Soil Dynamics. *Journal of the Geotechnical Engineering Division*, 103(GT6), 549–564.
- ASTM. (2011). D3080/D3080M-11. Standard test method for direct shear test of soils under consolidated drained conditions. *ASTM International*.
- ASTM. (2016a). D4254-16 Standard test methods for minimum index density and unit weight of soils and calculation of relative density. In *ASTM Standards*.
- ASTM. (2016b). Standard test method for maximum index density and unit weight of soils using a vibratory table. *ASTM International, West Conshohocken, PA*.
- Azeiteiro, R. J. N., Coelho, P. A. L. F., Taborda, D. M. G., & Grazina, J. C. D. (2017). Energy-based evaluation of liquefaction potential under non-uniform cyclic loading. *Soil Dynamics and Earthquake Engineering*, 92. <https://doi.org/10.1016/j.soildyn.2016.11.005>
- Been, K., Hachey, J., & Jefferies, M. G. (1991). The critical state of sands. *Geotechnique*. <https://doi.org/10.1680/geot.1991.41.3.365>
- Casagrande, A. (1936). Characteristics of cohesionless soils affecting the stability of earth fills. *Journal of Boston Society of Civil Engineers*, 23, 257–276.
- Cho, G.-C., Dodds, J., & Santamarina, J. C. (2006). Particle Shape Effects on Packing Density, Stiffness, and Strength: Natural and Crushed Sands. *Journal of Geotechnical and Geoenvironmental Engineering*. [https://doi.org/10.1061/\(asce\)1090-0241\(2006\)132:5\(591\)](https://doi.org/10.1061/(asce)1090-0241(2006)132:5(591))
- DeAlba, P., Chan, C., & Seed, H. B. (1975). *Determination of soil liquefaction characteristics by large-scale laboratory tests*. Earthquake Engineering Research Center, University of California, Berkeley.
- Dobry, R., Ladd, R. ., Yokel, F. Y., Chung, R. M., & Powell, D. (1982). Prediction of pore water pressure buildup and liquefaction of sands during earthquakes by the cyclic strain method. In *NBS building science series* (Issue 138). U.S. Dept. of Commerce For sale by the Supt. of Docs., U.S. G.P.O.
- Evans, M. D. (1993). Liquefaction and dynamic properties of gravelly soils. *Built Environment*. <https://doi.org/10.2495/AIR990911>
- Fardad Amini, P., & Noorzad, R. (2018). Energy-based evaluation of liquefaction of fiber-reinforced sand using cyclic triaxial testing. *Soil Dynamics and Earthquake Engineering*, 104(October 2017), 45–53. <https://doi.org/10.1016/j.soildyn.2017.09.026>
- Figuroa, J. L., Saada, A. S., Liang, L. Q., & Dahisaria, N. M. (1994). Evaluation of Soil Liquefaction by Energy Principles. *Journal of Geotechnical Engineering-Asce*, 120(9), 1554–1569. [https://doi.org/Doi.10.1061/\(Asce\)0733-9410\(1994\)120:9\(1554\)](https://doi.org/Doi.10.1061/(Asce)0733-9410(1994)120:9(1554))
- Finn, W. D. L. (1985). Aspects of constant volume cyclic simple shear. *Advances in the Art of Testing Soils under Cyclic Conditions - Proceedings of a Session Sponsored by the Geotechnical Engineering Division, ASCE Detroit Convention*, 74–98.
- Finn, W. D. L., & Vaid, Y. P. (1977). Liquefaction potential from drained constant volume cyclic simple shear tests. *6th World Conference on Earthquake Engineering*, 3, 2157–2162.
- Finn, W. D. L., Vaid, Y. P., & Bhatia, S. K. (1979). Constant volume cyclic simple shear testing. *Second International Conference on Microzonation for Safer Construction - Research and Application*, 839–851.
- Green, R. A., Mitchell, J. K., & Polito, C. P. (2000). An Energy-Based Excess Pore Pressure Generation Model for Cohesionless Soils. *Proceeding of the John Booker Memorial Symposium*, 1–9.
- Green, R. A., & Terri, G. A. (2005a). Computation of number of equivalent cycles for liquefaction evaluations. *Geotechnical Special Publication*, 131(143), 544–566.

[https://doi.org/10.1061/40797\(172\)31](https://doi.org/10.1061/40797(172)31)

- Green, R. A., & Terri, G. A. (2005b). Number of equivalent cycles concept for liquefaction evaluations - Revisited. *Journal of Geotechnical and Geoenvironmental Engineering*, 131(4), 477–488. [https://doi.org/10.1061/\(ASCE\)1090-0241\(2005\)131:4\(477\)](https://doi.org/10.1061/(ASCE)1090-0241(2005)131:4(477))
- Harr, M. E. (1987). *Reliability-Based Design in Civil Engineering*. McGraw-Hill.
- Ishac, M. F., & Heidebrecht, A. C. (1982). Energy dissipation and seismic liquefaction in sands. *Earthquake Engineering & Structural Dynamics*. <https://doi.org/10.1002/eqe.4290100105>
- Ishihara, K. (1985). *Stability of natural deposits during earthquakes. 1*, 321–276. [https://doi.org/10.1007/978-3-319-73568-9\\_174](https://doi.org/10.1007/978-3-319-73568-9_174)
- Ishihara, K. (1993). Liquefaction and Flow Failure during Earthquakes. *Geotechnique*, 43(3), 351–415.
- Ishihara, K. (1996). Soil behaviour in earthquake geotechnics. In *The Oxford engineering science series* (Issue 46). Clarendon Press.
- Ishihara, K., & Nagase, H. (1988). Multi-directional irregular loading tests on sand. *Soil Dynamics and Earthquake Engineering*, 7(4), 201–212. [https://doi.org/http://dx.doi.org/10.1016/S0267-7261\(88\)80004-6](https://doi.org/http://dx.doi.org/10.1016/S0267-7261(88)80004-6)
- Ishihara, K., & Yasuda, S. (1975). Sand liquefaction in hollow cylinder torsion under irregular excitation. *Soils and Foundations*, 15(1).
- Jefferies, M., & Been, K. (2016). *Soil liquefaction : a critical state approach* (2nd ed.). CRC Press. <https://doi.org/10.1201/b19114>
- Kokusho, T. (2013). Liquefaction potential evaluations: Energy-based method versus stress-based method. *Canadian Geotechnical Journal*. <https://doi.org/10.1139/cgj-2012-0456>
- Kokusho, T. (2017). Liquefaction potential evaluations by energy-based method and stress-based method for various ground motions: Supplement. *Soil Dynamics and Earthquake Engineering*, 95(January), 40–47. <https://doi.org/10.1016/j.soildyn.2017.01.033>
- Kokusho, T., & Kaneko, Y. (2018). Energy evaluation for liquefaction-induced strain of loose sands by harmonic and irregular loading tests. *Soil Dynamics and Earthquake Engineering*, 114(July), 362–377. <https://doi.org/10.1016/j.soildyn.2018.07.012>
- Kokusho, T., & Mimori, Y. (2015). Liquefaction potential evaluations by energy-based method and stress-based method for various ground motions. *Soil Dynamics and Earthquake Engineering*, 75, 130–146. <https://doi.org/10.1016/j.soildyn.2015.04.002>
- Kokusho, T., & Tanimoto, S. (2021). Energy Capacity versus Liquefaction Strength Investigated by Cyclic Triaxial Tests on Intact Soils. *Journal of Geotechnical and Geoenvironmental Engineering*, 147(4), 04021006. [https://doi.org/10.1061/\(asce\)gt.1943-5606.0002484](https://doi.org/10.1061/(asce)gt.1943-5606.0002484)
- Lasley, S. (2015). *Application of fatigue theories to seismic compression estimation and the evaluation of liquefaction potential*. Virginia Tech.
- Lasley, S. J. ., Green, R. A., & Rodriguez-Marek, A. (2016). New stress reduction coefficient relationship for liquefaction triggering analyses. *Journal of Geotechnical and Geoenvironmental Engineering*, 142(11). [https://doi.org/10.1061/\(ASCE\)GT.1943-5606.0001530](https://doi.org/10.1061/(ASCE)GT.1943-5606.0001530)
- Lasley, S. J., Green, R. A., Chen, Q. S., & Rodriguez-Marek, A. (2016). Approach for Estimating Seismic Compression Using Site Response Analyses. *Journal of Geotechnical and Geoenvironmental Engineering*, 142(6). [https://doi.org/Artn 0401601510.1061/\(ASCE\)Gt.1943-5606.0001478](https://doi.org/Artn 0401601510.1061/(ASCE)Gt.1943-5606.0001478)
- Lasley, S. J., Green, R. A., & Rodriguez-Marek, A. (2017). Number of Equivalent Stress Cycles for Liquefaction Evaluations in Active Tectonic and Stable Continental Regimes. *Journal of Geotechnical and Geoenvironmental Engineering*. [https://doi.org/10.1061/\(asce\)gt.1943-5606.0001629](https://doi.org/10.1061/(asce)gt.1943-5606.0001629)
- Liang, L., Figueroa, J. L., & Saada, A. S. (1995). Liquefaction under random loading: Unit energy approach. *Journal of Geotechnical Engineering*, 121(11), 776–781. [https://doi.org/10.1061/\(ASCE\)0733-9410\(1995\)121:11\(776\)](https://doi.org/10.1061/(ASCE)0733-9410(1995)121:11(776))

- Liang, L. Q., Figueroa, J. L., & Saada, A. S. (1995). Liquefaction under Random Loading - Unit Energy Approach. *Journal of Geotechnical Engineering-Asce*, 121(11), 776–781. [https://doi.org/10.1061/\(Asce\)0733-9410\(1995\)121:11\(776\)](https://doi.org/10.1061/(Asce)0733-9410(1995)121:11(776))
- Miner, M. A. (1945). Cumulative Damage in Fatigue. *Journal of Applied Mechanics*, 12(3), A159–A164.
- National Academies of Sciences, Engineering, and M. (2021). State of the Art and Practice in the Assessment of Earthquake-Induced Soil Liquefaction and Its Consequences. In *State of the Art and Practice in the Assessment of Earthquake-Induced Soil Liquefaction and Its Consequences*. The National Academies Press. <https://doi.org/10.17226/23474>
- Nemat-Nasser, S., & Shokooh, A. (1979). A unified approach to densification and liquefaction of cohesionless sand in cyclic shearing. *Canadian Geotechnical Journal*, 16(4), 659–678. <https://doi.org/10.1139/t79-076>
- Palmgren, A. (1924). Die lebensdauer von kugellagern (Life length of rollerbearings, in German). *Zeitschrift Des Vereins Deutscher Ingenieure*, 68(14), 339–341.
- Pickering, D. (1973). Drained Liquefaction Testing in Simple Shear. *Journal of the Soil Mechanics and Foundation Division*, 99(12), 1179–1184.
- Polito, C., & Green, R. (2013). Effect of load shape on relationship between dissipated energy and residual excess pore pressure generation in cyclic triaxial tests. *Canadian Geotechnical ...*, 50(11), 1118–1128. <https://doi.org/10.1139/cgj-2012-0379>
- Polito, C., Green, R. A., Dillon, E., & Sohn, C. (2013). Effect of load shape on relationship between dissipated energy and residual excess pore pressure generation in cyclic triaxial tests. *Canadian Geotechnical Journal*. <https://doi.org/10.1139/cgj-2012-0379>
- Seed, H. B., Idriss, I. M., Makdisi, F., & Banerjee, N. (1975). *Representation of Irregular Time Histories by Equivalent Uniform Stress in Liquefaction Analysis*. Earthquake Engineering Research Center, University of California, Berkeley.
- Seed, H. B., & Lee, K. L. (1966). Liquefaction of Saturated Sands During Cyclic Loading. *Journal of the Soil Mechanics and Foundation Division*, 92(6), 105–134.
- Silver, M. L., Chan, C. K., Ladd, R. S., Lee, K. L., Tiedemann, D. A., Townsend, F. C., Valera, J. E., & Wilson, J. H. (1976). Cyclic Triaxial Strength of Standard Test Sand. *ASCE J Geotech Eng Div*, 102(5), 511–523. [https://doi.org/10.1016/0148-9062\(76\)91550-3](https://doi.org/10.1016/0148-9062(76)91550-3)
- Tatsuoka, F., & Silver, M. (1981). Undrained Stress-Strain Behavior of Sand Under Irregular Loading. *Soils and Foundations*, 21(1), 51–66.
- Vaid, Y. P., & Sivathayalan, S. (1996). Static and cyclic liquefaction potential of Fraser Delta sand in simple shear and triaxial tests. *Canadian Geotechnical Journal*, 33(2), 281–289. <https://doi.org/DOI 10.1139/t96-007>
- Wu, J. (2002). *Liquefaction triggering and post-liquefaction deformation of Monterey 0/30 sand under UNI-directional cyclic simple shear loading*. University of California, Berkeley.
- Wu, J., Kammerer, A., Riemer, M., Seed, R., & Pestana, J. (2004). *Laboratory study of liquefaction triggering criteria*. 2580.
- Xu, D. sheng, Liu, H. bei, Rui, R., & Gao, Y. (2019). Cyclic and postcyclic simple shear behavior of binary sand-gravel mixtures with various gravel contents. *Soil Dynamics and Earthquake Engineering*, 123(August 2019), 230–241. <https://doi.org/10.1016/j.soildyn.2019.04.030>
- Zavala, G. J., Pando, M. A., Park, Y., & Aguilar, R. (2022). Specific Dissipated Energy as a Failure Predictor for Uniform Sands under Constant Volume Cyclic Simple Shear Loading. *KSCE Journal of Civil Engineering*, 26(2), 703–714. <https://doi.org/10.1007/s12205-021-1205-4>
- Zwillinger, D., & Kokoska, S. (1999). CRC Standard Probability and Statistics Tables and Formulae. In *CRC Standard Probability and Statistics Tables and Formulae*. <https://doi.org/10.1201/9781420050264>



*Appendix: Influence of irregular loading and frequency on the cumulative damage and dissipated energy of dry loose sand under cyclic simple shear*

Conference paper presented at the 19th International Conference on Soil Mechanics and Geotechnical Engineering, Seoul 2017

# Influence of irregular loading and frequency on the cumulative damage and dissipated energy of dry loose sand under cyclic simple shear

Influence du chargement irrégulier et de la fréquence sur les dommages cumulés et l'énergie dissipée d'un sable meuble sec sous cisaillement simple cyclique

**Guillermo J. Zavala**

Department of Engineering, Pontificia Universidad Católica del Perú, Peru, [gjavala@pucp.edu.pe](mailto:gjavala@pucp.edu.pe)

**Miguel A. Pando**

Department of Civil and Environmental Engineering, University of North Carolina at Charlotte, USA, [mpando@uncc.edu](mailto:mpando@uncc.edu)

**Youngjin Park**

Department of Civil and Environmental Engineering, University of North Carolina at Charlotte, USA, [y.park@uncc.edu](mailto:y.park@uncc.edu)

**Rafael Aguilar**

Department of Engineering, Pontificia Universidad Católica del Perú, Peru, [raguilar@pucp.pe](mailto:raguilar@pucp.pe)

**ABSTRACT:** This paper presents an experimental study involving cyclic simple shear (CSS) tests performed on dry loose Ottawa sand at an initial normal stress of 200 kPa and sheared under a constant volume condition. Horizontal shear loading involved 3 frequencies, and both uniform sinusoidal and irregular loading. The CSS tests involving uniform sinusoidal loading showed that for the 3 frequencies considered, the cycles to failure plots did not vary significantly with frequency. The study of the influence of irregular loading on the developed cumulative damage and dissipated energy was carried out by comparing these quantities with measured values in CSS tests on similar samples tested under uniform loading. The results show that the predictions of equivalent uniform cycles, done using the P-M cumulative damage hypothesis, are quite variable and that the accumulation of damage from irregular loading in most cases was observed to develop faster than predicted using equivalent uniform cycles. In contrast, the dissipated energy per unit volume until failure measured in all CSS tests (uniform and irregular loading, and 3 frequencies), was found to be relatively constant, and supports the use of energy-based approaches to study cyclic behavior of loose dry sands.

**RÉSUMÉ:** Cet article présente une étude expérimentale portant sur des essais de cisaillement simple cyclique (CSS) effectués sur du sable meuble sec d'Ottawa avec une contrainte normale initiale de 200 kPa et un cisaillement sous condition de volume constant. Trois fréquences ont été utilisées pour la charge de cisaillement horizontal, testée à la fois de manière uniforme sinusoïdale et irrégulière. Les tests de CSS impliquant une charge sinusoïdale uniforme ont montré que pour les trois fréquences considérées, l'évolution du nombre de cycles jusqu'à la rupture ne variait pas significativement avec la fréquence. L'influence de la charge irrégulière sur le développement des dommages cumulés et l'énergie dissipée a été réalisée en comparant ces quantités avec les valeurs mesurées dans les essais de CSS sur des échantillons similaires testés sous charge uniforme. Les résultats montrent que les prédictions de cycles uniformes équivalents—effectuées en utilisant l'hypothèse P-M de dommages cumulatifs—sont très variables. Par ailleurs, l'accumulation de dommages causés par une charge irrégulière a été observée dans la plupart des cas plus rapidement que prévu en utilisant des cycles uniformes équivalents. En revanche, tous les tests de CSS (charge uniforme et irrégulière et trois fréquences) montrent que l'énergie dissipée par unité de volume jusqu'à la rupture est relativement constante, ce qui conforte l'utilisation d'approches basées sur l'énergie pour étudier le comportement cyclique des sables meubles secs.

**KEYWORDS:** irregular loading, cyclic simple shear, cumulative damage, dissipated energy, liquefaction, ADVDCSS.

## 1 INTRODUCTION

In recent years, most of the laboratory studies on cyclic behavior of sands have involved uniform sinusoidal loading signals applied with geotechnical test devices such as the cyclic simple shear or the cyclic triaxial. However, it is well known that during earthquakes the sand layers experience complex stress histories that involve varying amplitudes and frequencies. Early generations of geotechnical testing devices were primarily geared to apply uniform sinusoidal load, or displacement, controlled cycles and this may have motivated early research, carried out in the 1970s, that looked for ways to convert random loading signals into equivalent uniform signals with a selected amplitude and frequency. This also led to the determination of an equivalent number of uniform cycles that could be used to represent the effects of certain earthquake loading in soils. Nowadays with recent advances in testing equipment it is possible to apply complex loading to soil samples, including non-uniform shear stresses with variable amplitude and

frequency. Taking advantage of these advances this paper presents results of an experimental program carried out to investigate the influence of frequency and irregular loading on the cumulative damage and dissipated energy during cyclic simple shear (CSS) of dry loose sands.

## 2 BACKGROUND AND LITERATURE REVIEW

The following section provides some background on CSS testing on dry sands carried out at constant volume. These tests are commonly reported as being equivalent to undrained CSS carried out on saturated sands at the same initial relative density and effective stress level. The literature review subsection describes the cumulative damage concept and the approach based on this quantity that is often used to compute number of equivalent uniform cycles for an irregular load. Additionally this subsection provides a brief review of dissipated energy of dry sands tested under uniform CSS tests.

2.1. Background - Constant volume CSS testing:

Constant volume CSS testing on dry sands has been used by several researchers to study liquefaction and cyclic behavior of sands (e.g., Finn et al. 1979, Lasley et al. 2016). This testing approach involves maintaining the height of a dry CSS specimen constant by using an active control of the applied vertical normal stress during the cyclic simple shearing. At any instance during the CSS test the difference between this variable applied vertical normal stress, required to maintain constant the sample height, and the initial applied vertical normal stress has been approximated by many researchers as equivalent to the excess pore water pressure that would have been developed in an undrained CSS test carried out on saturated sand samples prepared to the same initial relative density and with the same initial effective stress state. A comparison of pseudo-drained and truly undrained CSS tests was performed by Pickering (1973) using Ottawa sand samples at an average initial void ratio of about 0.65 and at a shear loading frequency of 2 Hz. The results reported in this study suggest these two test approaches are similar but the pseudo-drained tests were on the conservative side in terms of number of cycles required to reach failure. The equivalency between the constant volume CSS test on a dry sand sample and a truly undrained CSS test on a saturated sand was further reported by W.D.L. Finn (Pickering’s advisor) and co-workers at the University of British Columbia (Finn 1985, Finn and Vaid 1977, Finn et al. 1979). Figure 1, from Finn & Vaid (1977), shows the number of cycles to liquefaction from dry constant volume CSS are lower compared to the number of cycles recorded from undrained CSS on saturated samples of uniform medium dense sands. This figure, often cited in references that have used dry, constant volume CSS, suggests that constant volume CSS on dry samples is on the conservative side compared to equivalent undrained CSS on saturated samples. This experimental evidence although useful, seems to be scarce (and in Fig. 1 involves different sands), and warrants further evaluation of the validity of this equivalency of these two CSS tests types. However, this was outside the scope of this paper.

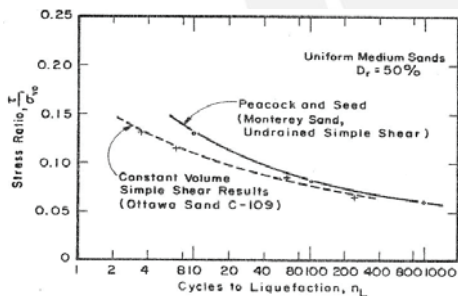


Figure 1: Comparison of Dry, Constant Volume CSS ( $\sigma'_{no}=196$  kPa) and Undrained, Saturated, CSS test results for liquefaction resistance of sand (from Finn & Vaid, 1977) [fair use]

2.2. Literature review

2.2.1. Cumulative damage hypothesis and equivalent number of uniform cycles

Converting or finding equivalence between a non-uniform load, like an earthquake, and a uniform sinusoidal load applied for an equivalent number of cycles has been studied since the 1970s (e.g., Seed et al. 1975, Annaki and Lee 1977). Researchers have been looking at this problem in an effort to be able to perform an adequate comparison between field soil behavior under complex irregular earthquake loading and laboratory soil behavior, originally, and still typically, tested under uniform cyclic stresses. The approach of converting a random signal to an equivalent uniform signal has several advantages, such as

being able to analyze the effect of different earthquake on a soil by using a single set of data. Converting random stresses to an equivalent damaging stress has long been used to study metal fatigue. For example the Palmgren-Miner (P-M) (Miner 1945, Palmgren 1924) cumulative damage hypothesis, commonly used to study metal fatigue, has been applied to find this equivalency between irregular and uniform loading. This model assumes that the damage leading to failure accumulates linearly with the number of cycles of loading. Cumulative damage (D) was defined by Miner as the ratio of the absorbed work ( $w_i$ ) after  $n_i$  cycles and the total absorbed work at failure (W). He also alternatively defined damage (D) as the ratio of the number of cycles ( $n_i$ ) in the load history having an amplitude  $S_i$  and the total number of cycles ( $N_i$ ) of this same amplitude  $S_i$  required to cause failure. Both these definitions of D, are as follows:

$$D = \sum_{i=1}^m \frac{w_i}{W} = \sum_{i=1}^m \frac{n_i}{N_i} \quad (1)$$

In the above expression, D= 0 corresponds to the initial state of the sample before cyclic loads have been applied, D=1 corresponds to the damage state of the sample at failure, and D values between 0 and 1 correspond to the damage state of a sample that has been subjected to a certain loading but has not yet failed. An equivalent number of uniform cycles at any stress level ( $S_i$ ) would be the value that causes the same amount of damage. A detailed description of the P-M hypothesis can be found in Green and Terri (2005).

One of the first applications of the P-M hypothesis to attempt to represent irregular earthquake time histories as equivalent stress series for liquefaction evaluations was done by Seed et al. (1975). This study used data from DeAlba et al. (1975), who performed large scale liquefaction tests using a shaking table involving saturated sand under a constant normal stress. The authors developed S-N curves, which plot number of cycles to cause initial liquefaction versus cyclic stress ratio ( $CSR = \tau_{max}/\sigma'_{no}$ ) used in the tests, for Monterey #0 Sand at four different relative densities.

Annaki and Lee (1977) performed an experimental program to check the validity of Seed’s implementation of the P-M hypothesis using triaxial tests under uniform and irregular deviatoric load cycles. The authors stated that their data generally confirm the validity of the equivalent uniform cycles, or the cumulative damage method of dealing with irregular loading effects on soil, and support the analysis presented by Seed et al. (1975).

Tatsuoka and Silver (1981) formulated a relationship between double amplitude (DA) shear strain, stress ratio for uniform loading, number of loading cycles and relative density, finding that the equations they developed were a better representation of their test results than the linear relationship proposed by Seed et al. (1975) when plotted in a log-log scale.

Recently Lasley et al. (2016) proposed the use of a modified Richart-Newmark non-linear cumulative damage hypothesis that they report as a substantial improvement with respect to P-M based approaches as the computed damage is load-dependent. This paper did not look at this new approach.

2.2.2. Dissipated energy approach

Another approach commonly used to study the cyclic behavior of sands under uniform and irregular loading is the energy dissipated by the soil during the loading event until failure. Several researchers have used energy dissipation to evaluate liquefaction potential (e.g., Davis and Berrill 1982, Figueroa et al. 1994, Green and Terri 2005). In CSS tests the dissipated energy per unit volume is computed by the cumulative area of the hysteresis loops in the shear stress-strain curves. The dissipated energy has been found to explain densification of drained tests and liquefaction of sands under undrained loading. Figueroa et al. (1994) and Liang et al. (1995) used the energy

concept to define liquefaction potential, and validated it using undrained hollow cylinder torsional shear tests on saturated sand specimens. According to these authors, the energy per unit volume needed to induce liquefaction is not dependent on the loading form and can thus be used to evaluate the liquefaction potential under general earthquake loads.

Green and Terri (2005) and Lasley et al. (2016) emphasized the fact that the P-M hypothesis applies to high-cycle fatigue conditions (low amplitude, large number of cycles), which is usually the case in metal fatigue applications, but is not directly applicable to low-cycle fatigue conditions (large amplitude and low number of cycles). These authors also point out that damage predictions using the P-M hypothesis are load-path independent. Thus propose an alternative implementation to the P-M hypothesis using energy principles that can be used to calculate an equivalent number of cycles at a uniform stress and to predict liquefaction.

### 3 EXPERIMENTAL PROGRAM

The test program reported in this paper involved samples prepared with Ottawa 20/30 silica sand. This sand is a poorly graded subrounded to rounded sand, with a  $D_{50} = 0.71\text{mm}$ , and 95% of the material retained between the standard sieves #20 and #30. The maximum and minimum void ratios were measured to be 0.644 and 0.302, respectively. Tests were conducted using an Advanced Dynamic Cyclic Simple Shear machine (ADVDCSS) manufactured by GDS Instruments, that is capable of running CSS tests with non-uniform loading. The samples were prepared dry on a loose state with relative density values ranging between 25% and 36%. The cylindrical CSS sample had a diameter of approximately 70 mm and an approximate height of 20 mm. Loose samples were prepared using a short pipe of 50mm of diameter that was placed in the sample box and filled with a predetermined weight of sand (130g). The pipe was quickly pulled up leaving the sample in a loose state. Next the sample was carefully leveled and the initial sample height measured before normal stress application.

The samples were sheared under stress control on constant volume conditions (constant height). CSS test results reported in this paper were all conducted with an initial normal stress of 200 kPa and subjected to sinusoidal horizontal shear loading that had either uniform or non-uniform amplitudes and frequencies of 0.1, 0.5, or 1.0 Hz. The uniform tests involved Cyclic Stress Ratios (CSRs) of 0.05, 0.065, 0.08, 0.09 and 0.10. Non-uniform CSS tests were carried out at 0.1, 0.5, and 1 Hz and denoted with test ID of "A", "B", and "C", respectively. The four variable amplitude wave forms involved a sequence of CSRs which are listed in Table 1 and were repeated until sample failure was reached.

Table 1: Non-uniform load types

Type	Description of shear load sequence
1	sine wave CSR = 0.05 followed by sine wave CSR = 0.065
2	sine wave CSR = 0.05 followed by sine wave CSR = 0.08
3	sine wave CSR = 0.065 followed by sine wave CSR = 0.08
4	4 sine waves CSR = 0.05 followed by a sine wave CSR = 0.08

The test program involved 27 tests, 15 uniform tests and 12 non-uniform tests (listed in Table 2). For this experimental program failure was defined when the sample reached 7.5% double-amplitude shear strain which is a failure criterion commonly used in the literature (e.g., Lasley 2015, Sivathayalan and Ha 2011, Vaid and Sivathayalan 1996).

Table 2: Non-uniform tests performed for this study

Case	1A	2A	3A	4A	1B	2B	3B	4B	1C	2C	3C	4C
Type (Table 1)	1	2	3	4	1	2	3	4	1	2	3	4
Frequency (Hz)	0.1	0.1	0.1	0.1	0.5	0.5	0.5	0.5	1	1	1	1

## 4 RESULTS

### 4.1. Uniform cycles – effect of frequency on cycles to failure

The results of the uniform tests are shown in Figure 2, along with a trendline. The results indicate that the frequency does not have significant effect on the results. The modest variability in the cycles to failure are attributable to the intrinsic variability of the tests and the samples. Furthermore this range of cycles to failure is within the variability observed from tests series carried out at a constant frequency. Thus it is concluded that frequency, between 0.1 to 1.0 Hz, did not have significant influence in the number of cycles to failure from constant volume CSS on loose dry Ottawa sand samples at  $\sigma'_{no} = 200$  kPa.

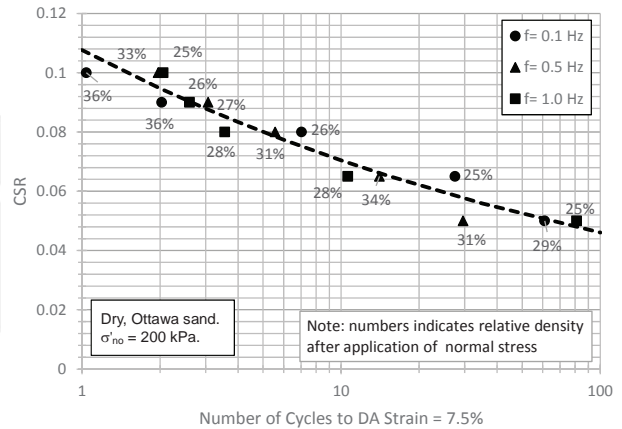


Figure 2: Influence of frequency on cycles to failure (DA Strain=7.5%) from constant volume, uniform CSS at  $\sigma'_n = 200$  kPa.

### 4.2. Cumulative damage - number of cycles to failure

The predicted number of equivalent uniform cycles to failure computed using a simplified cumulative damage analysis based on the P-M hypothesis is presented in Figure 3.

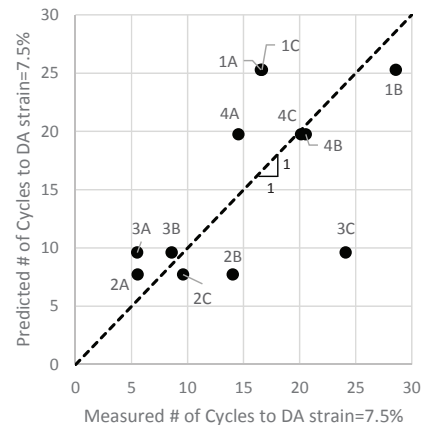


Figure 3: Measured vs predicted number of cycles to failure (DA strain=7.5%) using cumulative damage hypothesis for non uniform data

This figure highlights some of the shortcomings of cumulative damage analyses based on the load-path independent P-M hypothesis.

### 4.3. Dissipated energy to failure

The measured dissipated energies per unit volume at failure, without the correction for softening in the final load cycles proposed by Green and Terri (2005), are summarized in Figure 4 for all the CSS tests considered in this paper. The dashed line in this figure represents the overall mean of all energy values measured.

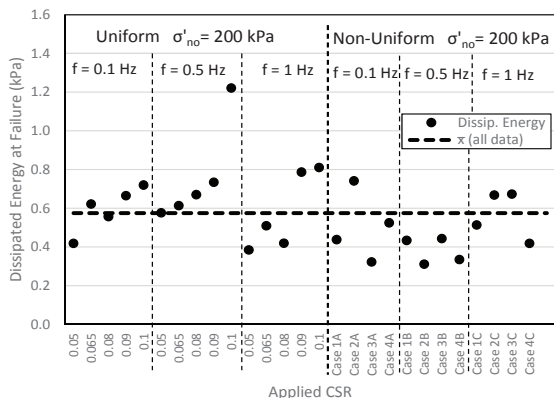


Figure 4: Summary of dissipated energy per unit volume to reach failure (DA shear strain = 7.5%) from all tests

It is important to point out that the dissipated energy per unit volume was computed to the last zero stress instance in the shear stress-strain cycle just prior to failure defined herein when a 7.5% double amplitude shear strain is reached (Lasley, 2015). A summary of the computed averages for each loading frequency considered are summarized in Table 3.

Table 3: Average Dissipated Energy per unit volume (Uniform and non-uniform tests)

Frequency	Mean (kPa)	St. Dev. (kPa)	COV
0.1 Hz	0.5566	0.1438	26%
0.5 Hz	0.5935	0.2770	47%
1.0 Hz	0.5762	0.1628	28%
<b>All</b>	<b>0.5754</b>	<b>0.1959</b>	<b>34%</b>

From the results presented in Figure 4 and in Table 3 we can see that the energy per unit volume dissipated by all samples until failure is reached was fairly uniform, regardless of the loading type, CSR level, or frequency. Variability of results is reasonably small and likely related to inherent sample variability, even though special care was taken in making samples as repeatable as possible. It is also worth noting that even with completely different number of cycles to failure, the dissipated energy to failure remained at very similar levels.

### 5 Summary and Conclusions

Twenty seven constant volume CSS tests were conducted at uniform and non-uniform shearing loading applied to samples of loose, dry Ottawa sand at an initial normal stress of 200 kPa. All CSS tests were conducted until failure, defined as a double amplitude shear strain of 7.5%. The tests results were used to assess the influence of irregular loading and frequency on the cumulative damage and dissipated energy per unit volume of dry loose sand. The main conclusions drawn are:

- CSS tests with uniform load cycles showed that the curve of number of cycles to failure versus CSR was not significantly influenced by frequency, at least for the 3 frequencies considered of 0.1, 0.5, and 1 Hz.
- The predictions of number of cycles to failure using a P-M based cumulative damage model for the irregular cycles were

found to be imprecise. This is related to shortcomings of the P-M hypothesis that as pointed out by Green and Terri (2005) was originally meant to be used for high-cycle fatigue as in metals and is load path independent which for cyclic loading of dry sands is not realistic.

- The measured dissipated energy per unit volume to reach failure was found to be fairly uniform for the 27 CSS tests considered in this paper. Even though some variability was observed, dissipated energy values were quite uniform despite the different loading conditions considered and the great range of number of cycles to failure observed within the test program. Despite the modest variability observed in the measured dissipated energy per unit volume it is believed to be within variability reported by others in the literature and thus supports the approach of using dissipated energy to study cyclic behavior of sands and liquefaction.

### 6 Acknowledgements

The authors would like to thank the Pontificia Universidad Católica del Perú for the funding provided to the first author to spend a sabbatical year at UNC Charlotte.

### 7 References

Annaki M. and Lee K.L. 1977. Equivalent Uniform Cycle Concept for Soil Dynamics. *J. of Geot. Eng. Division* 103(GT6), 549-564.

Davis, R.O. and Berrill, J.B. 1982. Energy Dissipation and Seismic Liquefaction of Sands. *Earthquake Engineering & Structural Dynamics* 10(1), 59-68.

DeAlba P., Chan C. and Seed, H.B. 1975. Determination of soil liquefaction characteristics by large-scale laboratory tests. EERC Report 75-14.

Figueroa J.L., Saada, A.S., Liang L.Q. and Dahisaria, N.M. 1994. Evaluation of Soil Liquefaction by Energy Principles. *J. of Geotechnical Engineering* 120(9), 1554-1569.

Finn W.D.L. 1985. Aspects of constant volume cyclic simple shear. *ASCE Advances in the art of testing soils under cyclic conditions*, Proc. Geotechnical Engineering Div., ASCE Detroit Convention.

Finn W.D.L. and Vaid Y.P. 1977. Liquefaction potential from drained constant volume cyclic simple shear tests. *6<sup>th</sup> World Conference on Earthquake Engineering*, New Delhi, India. Vol 3, 2157-2162.

Finn W.D.L., Vaid Y.P. and Bhatia, S.K. 1979. Constant volume cyclic simple shear testing. *2<sup>nd</sup> Int. Conf. on Microzonation for Safer Construction*, San Francisco, CA. Vol 2, 839-851

Green R.A. and Terri G.A. 2005. Number of equivalent cycles concept for liquefaction evaluations - Revisited. *JGGE* 131(4), 477-488.

Lasley S.J. 2015. Application of fatigue theories to seismic compression estimation and the evaluation of liquefaction potential (Doctoral dissertation), Virginia Tech, Blacksburg, VA.

Lasley S.J., Green R.A. and Rodriguez-Marek A. 2016. Number of Equivalent Stress Cycles for Liquefaction Evaluations in Active Tectonic and Stable Continental Regimes. *J. of Geotechnical and Geoenvironmental Engineering* (Online pre-release).

Liang L.Q., Figueroa J.L. and Saada A.S. 1995. Liquefaction under Random Loading - Unit Energy Approach. *J. of GE*, 121(11), 776-781.

Miner, M.A. 1945. Cumulative Damage in Fatigue. *Journal of Applied Mechanics* 12(3), A159-A164.

Palmgren A. 1924. Life length of roller bearings (in German). *Zeitschrift des Vereins Deutscher Ingenieure* 68(14), 339-341.

Pickering, D. 1973. Drained Liquefaction Testing in Simple Shear. *J. of the Soil Mechanics & Foundation Division* 99(12), 1179-1184.

Seed H.B., Idriss I.M., Makdisi F. and Banerjee N. 1975. Representation of Irregular Time Histories by Equivalent Uniform Stress in Liquefaction Analysis. EERC Report 75-29.

Tatsuoka F. and Silver M. 1981. Undrained stress-strain behavior of sand under irregular loading. *Soils and Foundations* 21(1), 51-66.